Water-soluble Porphyrin-based Nanorings

A Thesis submitted for the Honour School of Chemistry

Part II 2025

Ross Clark

Jesus College

Summary

This work describes the synthesis of sulfonic acid dendrimer (**SAD**) **Zn *c*-P6•T6** (**Figure 1**), the first porphyrin nanoring soluble in water at low pH. Additionally, it describes the synthesis of carboxylic acid dendrimer (**CAD**) **NH *c*-P6** and attempts of post-porphyrin side chain modification upon it.[1] Deriving from the established synthetic work within the Anderson group, preceding organic soluble nanoring sulfonate phenyl ester (**SPE**) **Zn *c*-P6•T6** could be synthesized *via* template-directed synthesis.[2] The 24-fold sulfonate phenyl esters of **SPE Zn *c*-P6•T6** could then be deprotected *via* basic hydrolysis, revealing the sulfonate group and activating water solubility. Basic hydrolysis also allows for control of the **SPE Zn *c*-P6•T6** ring, which was lacking under tert-butyl-ester dendrimer (**TBuED**) **NH *c*-P6•T6** variant specifically, demetalation, detemplation, and deprotection can now occur under orthogonal conditions.

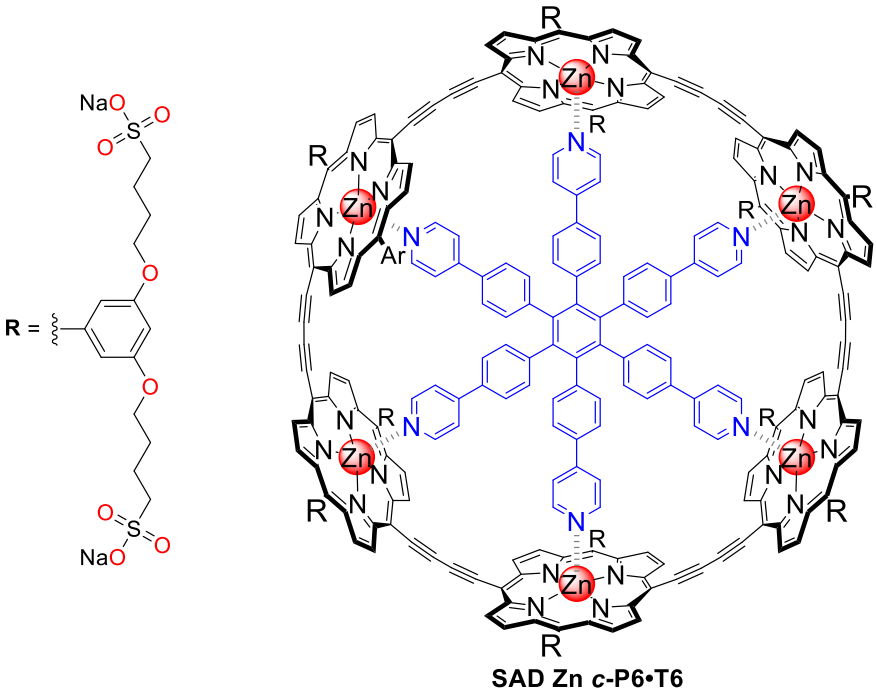

Figure 1: **SAD Zn *c*-P6•T6**, a new butadiyne-linked water-soluble porphyrin nanoring.

The initial efforts focused on the modification of **CAD NH porphyrin** to exchange the carboxylic acid groups with sulfonic acid *via* amide coupling. The effect of increased solubility in low pH conferred by the sulfonic acids, whilst allowing for incorporation on the established work of Jack

Pickering's porphyrin synthesis,[1] proved inaccessible. The lack of driving force on the 8-fold amide coupling resulted in a wide distribution of products with low yields on the fully substituted amide system. The focus then shifted to forming an activated ester from pentaflourophenol, which proved unfruitful as only minor conversion occurred. Final attempts of side chain modification involved attempting carboxylate nucleophilic attack on a primary iodo group to attach an alkyl sulfonic acid, which proved to be unsuccessful due to low full conversion. These negative results caused the abandonment of **CAD** side chain modification in favour of a return to side chain design.

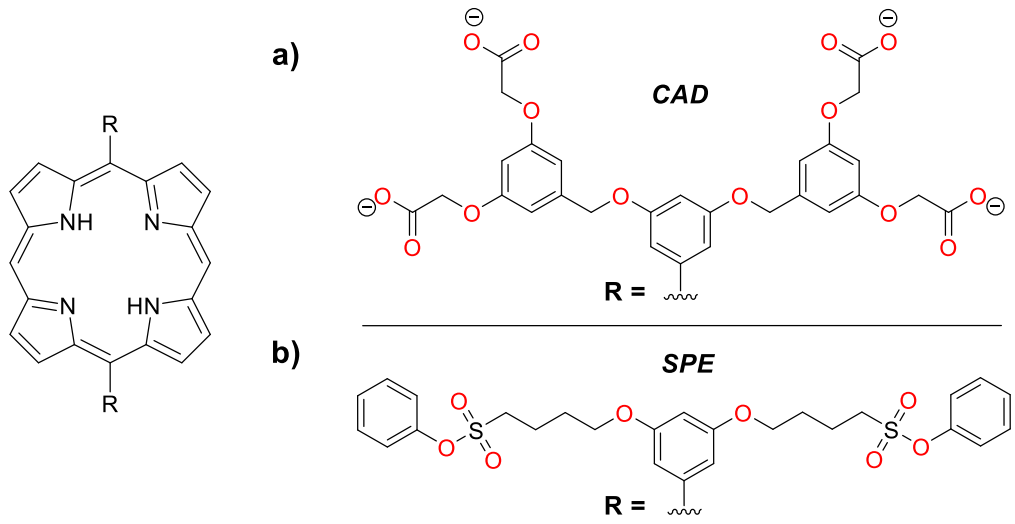

Figure 2: a) **CAD** side chain system, which proved impossible to convert. b) **SPE** side chain designed to replace it.

Learning from the failed attempts of **CAD** modification, a series of new side chains were developed leading to the phenyl butanesulfonate groups. The **SPE** side chain proved extremely similar, in polarity and solubility, to the successful **TBuED** side chain. This allowed for the design of **SPE** porphyrin and the corresponding nanoring. Thus, a pH flexible water-soluble porphyrin nanoring has been achieved providing a true basis for further study of its potential biochemical properties.

References

1. J. Pickering, Synthesis and Applications of a Water-Soluble Porphyrin Nanoring, MChem diss, Oxford University, **2024**.

2. Hoffmann, M., Kärnbratt, J., Chang, M.-H., Herz, L. M, Albinsson, B. and Anderson, H. L, *Angew Chem Int Ed*, **2008**, 47, 4993-4996.

Acknowledgements

I would like to thank Harry Anderson for the opportunity to undertake my Part 2 project in his laboratory group. His support during this year has been instrumental in enabling the success of this project and greatly improving my understanding of chemistry. Further thanks must be made to the entire HLA group for their support throughout this entire project without which I would have probably gone insane from the endless consuming nature of amide coupling.

Particularly, I would like to thank my supervisors Dr A Rubio and Michael Foster for the seemingly endless patience they had with me throughout my 8 months with them, which greatly improved my organic chemistry. Without their aid throughout my thesis, I can confidently say I wouldn't have been able to achieve what I did. Additionally, thanks must go to Sara Borghi both for chemistry advice and for helping keep my spirits up throughout my thesis as my fume cupboard neighbour. I would also like to thank Sam Leggatt, who has been an amazing fellow Part II and whom I have nothing but positive things to say about. I wish him the best in his PhD within the group.

Outside the world of Chemistry, I would like to thank my partner, Max Sogan, who has supported me throughout every frustration during my time at Oxford University, giving me patience and amazing happiness during my time here. I could not have asked for a better person to spend this time with.

Finally, I would like to thank my family, especially my mum Sarah Clark. Through every trouble and struggle they have supported me, doing all they can to help my path forward. From dyslexia to exam anxieties, they have put just as much effort into my success as I have. I would not change it for the world.

List of Abbreviations

Ac	Acetyl	*l*-PN	Linear porphyrin N-mer
Ar	Aryl	m/z	Mass to charge ratio
a.u.	Arbitrary units	MALDI-TOF	Matrix Assisted Laser Desorption Ionisation-Time of Flight
CAD	Carboxylic Acid Dendrimer		
c-PN	Cyclic porphyrin N-mer		
DCC	N.N' Dicyclohexylcarbodiimide	NBS	N-Bromosuccinimide
DCM	Dichloromethane	Neo-P	Neopentyl alcohol
DCTB	{(2E)-2-Methyl-3-[4-(2-methyl-2-propanyl)phenyl]-2 propen-1-yliswnw}malononitrile	NMR	Nuclear Magnetic Resonance
		Pet Ether	Petroleum Ether (40-60°C)
DDQ	2,3-Dichloro-5,6-dicyano-*p*-benzoquinone	SAD	Sulfonic Acid Dendrimer
		SEC	Size Exclusion Chromatography
DIPA	Diisopropylamine		
DIPEA	Diisopropylethylamine	SPE	Sulfonate Phenyl Ester
DMF	Dimethyl formamide	TBAF	Tetra-n-butylammonium flouride
DMSO	Dimethyl sulfoxide		
DPM	Di-(2-pyrrolyl)-methane	TBuED	Tert-Butyl Ester Dendrimer
EI	Electrospray ionisation		
Eqv	Equivalent(s)	TBuE	Tert-Butyl Ester
GPC	Gel Permeation Chromatography	TCE	Trichloroethyl
HPLC	High Performance Liquid Chromatography	THS	Trihexylsilyl
		TN	Template for cyclic N-mer
HATU	Hexaflourophosphate Azabenzotriazole Tetramethyl Uronium	*t*-Bu	Tertiary butyl
		UV/Vis	Ultraviolet-Visible
HBTU	Hexaflourophosphate Benzotriazole Tetramethyl Uronium		
HOMO	Highest Occupied Molecular Orbital		
IUPAC	International Union of Pure and Applied Chemistry		
LUMO	Lowest Occupied Molecular Orbital		

Contents

1 Introduction

1.1 Porphyrin: Structure and Properties.

Porphyrins are naturally occurring molecules, macrocycles containing four pyrrole units interconnected by methine bridges.[1] This resulting cyclic structure contains 26 delocalised π electrons, 18 of which form a circuit giving rise to Hückel aromaticity, shown in **Figure 1**, resulting in a planar geometry.[2] At the centre of the macrocycle lies a cavity which acts as the coordination site of metals in metalloporphyrins.[3] Substituents on the macrocycle are commonly labelled by two methodologies, the IUPAC numbering system and *meso-β* labelling,[4, 5] which are shown in **Figure 1**.

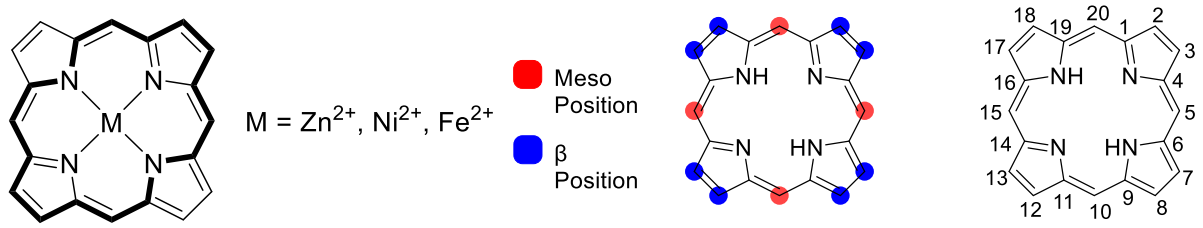

Figure 1: Left, 18 π electron aromatic circuit inside the porphyrin with a metal guest species.[2] Middle, *meso-β* labelling of porphyrin.[5] Right, IUPAC numbering system on porphyrin.[4]

The extensive conjugation of π orbitals within a porphyrin result in a small HOMO-LUMO gap,[6] which gives rise to two intensive absorption transitions in the visible region of the electromagnetic spectrum,[7] at 400 nm (Soret or B band) and 550 nm (Q band) approximately. These transitions can be explained *via* the "Gouterman's four-orbital model" (**Figure 2**).[8] This model elaborates that through the configurational interaction, the transition of two π orbitals to their degenerate energy π* orbitals (a_{1u} and a_{2u} to e_g) emerges the S_0, S_1 and S_2 states. The configurational interaction can be destructive and constructive giving rise to a stronger Soret band and a weaker Q band. Therefore, porphyrins are typically intensely coloured, as suggested by their name deriving from the Greek "porphura", meaning purple.

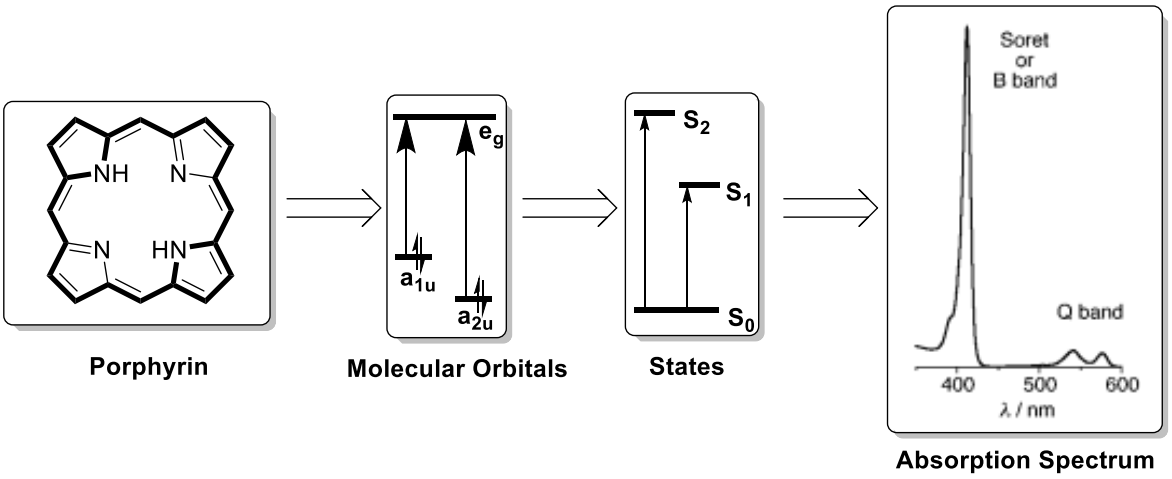

Figure 2: "Gouterman four-orbital model" of a typical porphyrin and how the model results the absorption spectrum.[8] Reprinted with permission from Ref. 8.

These colourful transitions can be further affected by the occupation of the central cavity by a metal species.[9] From this metallic customisation emerges a common porphyrin motif encountered within natural molecules, such as haemoglobin,[10] chlorophyl,[11] and cytochromes.[12] Chlorophyl's magnesium coordination effect is mainly used in nature to maintain chlorophyl's structure, which maintains the two intensive absorptions in the visible light region of the electromagnetic spectrum for best use in the photosystems of plants (**Figure 3**).[13,14] Haemoglobin, in contrast, utilises its metal cation as a coordination site for the binding of O_2, shown in **Figure 4**, to facilitate transport through the blood system.[15] This coordination binding of metal cations has found extensive use in supramolecular chemistry, and in our case provides the basis of the template-directed synthesis of porphyrin nanorings.[16]

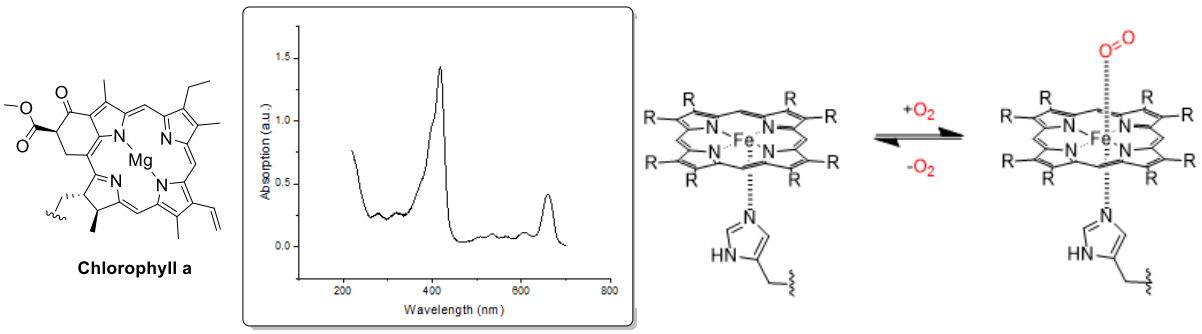

Figure 3: Left, Chlorophyll A[11] and its corresponding absorption spectra in methanol.[17] Right, Haem group binding of molecular oxygen for transport in cells.[1]

1.2 Template-directed Synthesis

Template-directed synthesis has found a home in almost all macrocycle-based organic laboratory work.[18-20] Jeremy K.M. Sanders explains that "The [chemical] template provides instructions for the formation of a single product from a substrate or substrates which otherwise have the potential to assemble and react in a variety of ways.".[21] This useful property emerges from the non-covalent molecular interactions between template and substrate.[18] A good example of this is heteroatom coordination. These interactions assemble the substrate around specific locations of the template, preorganising the system in favour of a desired product created by new covalent bond formation. When the template-directed reaction completes, the weaker, non-covalent interactions allow for the displacement of the template retrieving the desired product.[18]

Charles J. Pedersen's crown ethers represent one of the earliest examples of template-directed synthesis (**Scheme 1**).[22] Utilising a coordinating K^+ cation, electronegative O species and their optimum distances, a cyclic structure emerges. The terminal alkoxide is thus placed adjacent to the terminal chlorine. The resulting nucleophilic attack is greatly favoured closing the resulting macrocycle at a fast rate, which results in the cyclic species being favoured over linear oligomer.

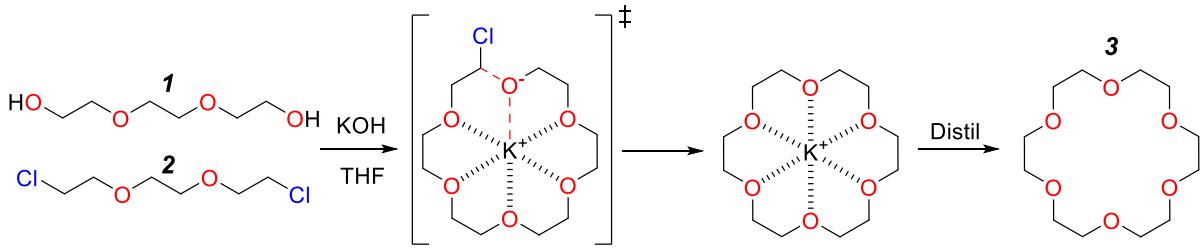

Scheme 1: 18-crown-6 ether synthesis *via* modified Williamson ether synthesis.[22]

In the 21st century, template-directed synthesis found extensive use as the driving force for the assembly of complicated organic frameworks. Hunter *et al.* demonstrated the use of a porphyrin derivative and a 1,4-diazabicyclo[2.2.2]octane (DABCO) template to construct triazole oligomers (**Scheme 2**).[23] By first binding the triazole monomer *via* esterification to a carboxylic acid at the opposing *meso* positions of a zinc porphyrin, Hunter was able to utilise the strong coordination between tertiary amines and the zinc centre to align the azide groups of the monomers to their

terminal alkynes ready for copper(I) mediated linkage.[24] This preorganisation of the substrate vastly reduced the number of oligomers (**Figure 4**), demonstrating the clear advantages of template-directed synthesis, especially in polymerisation reactions.

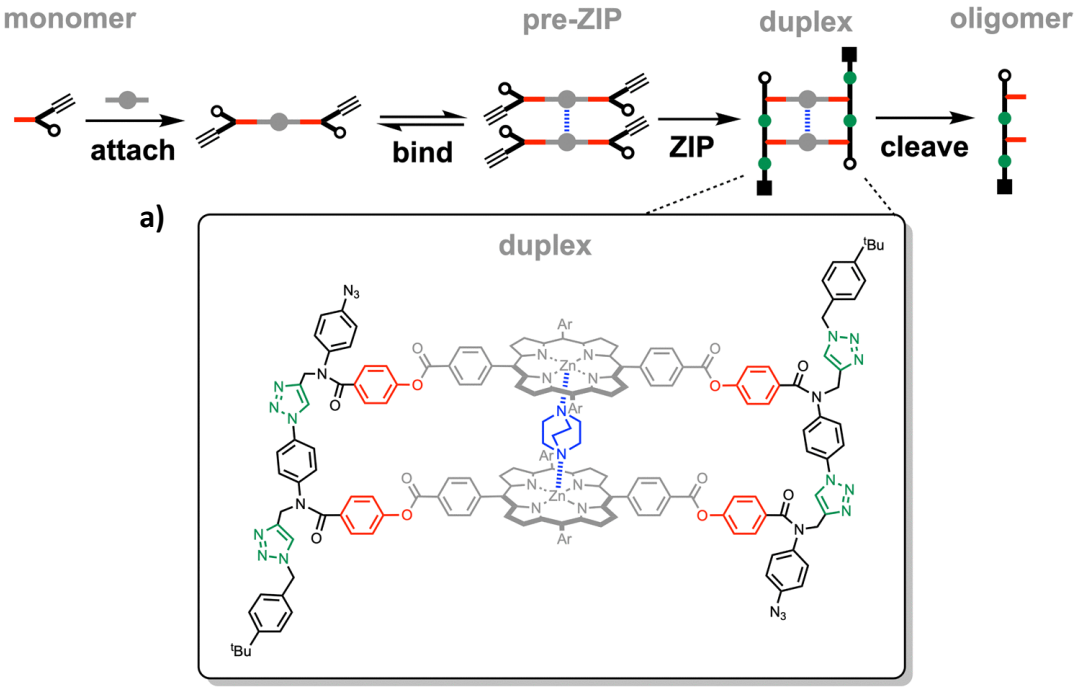

Scheme 2: Synthesis of desired oligomer from DABCO template by the aligning two porphyrin units and their azide and alkyne terminals.[23] Reprinted with permission from Ref. 23.

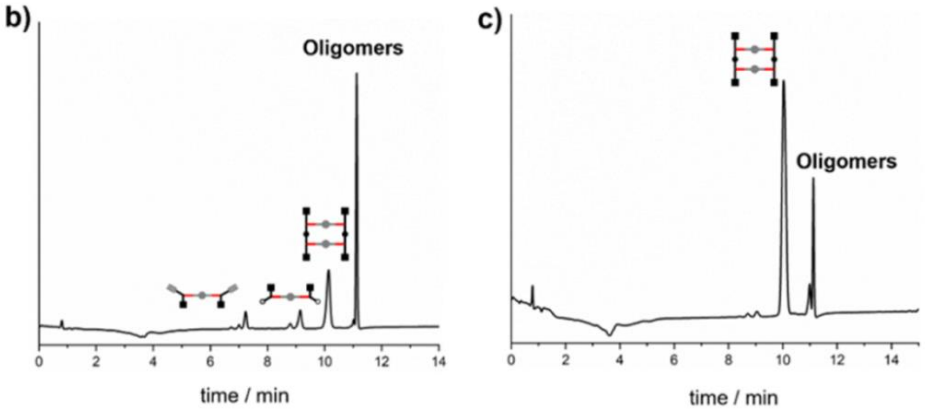

Figure 4: HPLC chromatograms of the product mixture obtained from the oligomerisation done without DABCO (b) and with DABCO (c).[23] Reprinted with permission from Ref. 23.

1.3 Butadiyne-Linked Porphyrin Oligomers and Nanorings

In 2007, Anderson *et al.* reported the first π-conjugated cyclic porphyrin macrocycle, the butadiyne-linked cyclic octamer ***c*-P8•T8 *5***.[25] The synthesis relies upon the cyclisation of ***l*-P8 *4***, whose central metal ions coordinate to the **T8** pyridine arms (**Scheme 3**). This approach laid the fundamentals for the synthesis of later butadiyene-linked rings. Furthermore, size matching of the nanoring's cavity and the template size requires a high degree of match. That without, the resulting distortion of the template would produce an additional unfavourable barrier to the preorganisation of the linear oligomers being converted to ***c*-PN** rings.

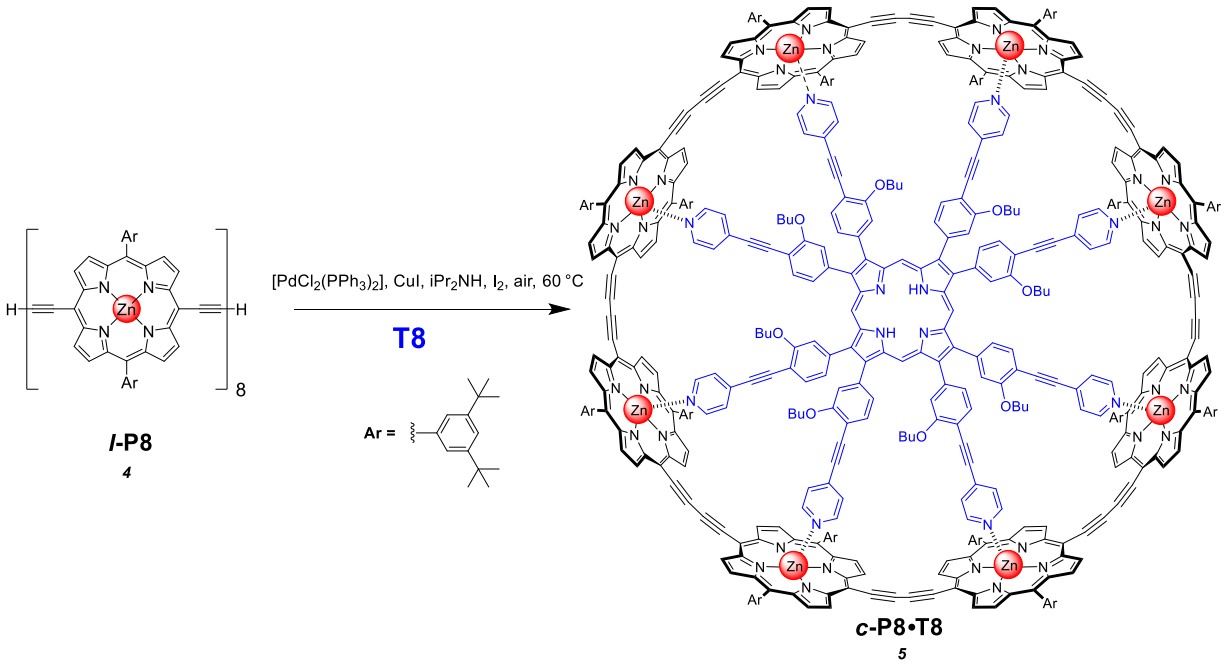

Scheme 3: ***c*-P8•T8 *5*** synthesis (55%) from ***l*-P8 *4***, zinc-pyridine from **T8** coordination helps preorganise the system massively favouring ***c*-P8 *5***.[25]

This successful synthesis would lead Anderson *et al.* to synthesise the smaller ***c*-P6•T6 *8*** nanoring in 2008 (**Scheme 4**).[26] The design of the new **T6** template combined with the innovation of using smaller linear oligomers, ***l*-P1 *7*** and ***l*-P2 *6***, would allow the synthesis of ***c*-P6•T6 *8*** to become comparatively facile compared to ***c*-P8•T8 *5*,** which required isolation of ***l*-P8 *4***. Despite these improvements, the use of smaller linear oligomer introduced a new entropic penalty in the formation of nanoring as the difficulty in arranging seven or four molecules is much higher than

the two in ***c*-P8•T8 *5*** synthesis. Combined with the greater need for purification to remove smaller linear oligomers, which have similar R_f values to ***c*-P6•T6 *8*** in the chromatographic conditions used for purification. This would result in the yield of ***c*-P8•T8 *5*** (55%) dropping to 21% for ***l*-P1** *7* and 44% for ***l*-P2 *6*** in the case of ***c*-P6•T6 *8***.

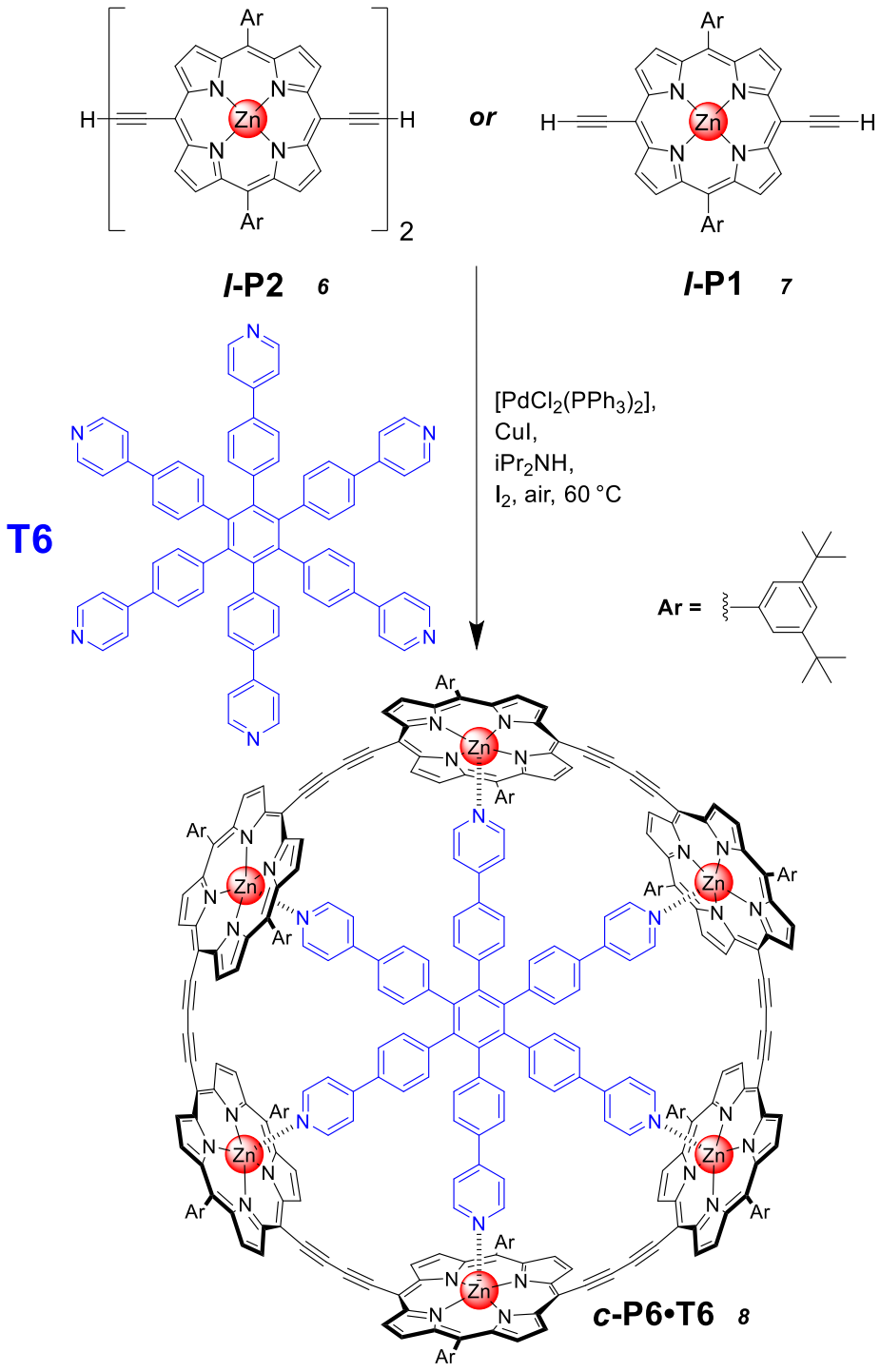

Scheme 4: ***c*-P6•T6 *8*** synthesis from ***l*-P2 *6*** and ***l*-P1** *7* yields of 44% and 21% respectively, once again highlighting the ability of the zinc-pyridine coordination to guide the reaction.

In recent years, attempts were made to move away from the 1:1 stoichiometry of the traditional template directed synthesis.[16] As such, the Vernier template method relies on the mismatch of the number of guest sites with the number of binding sites, forcing the smallest nanoring formation onto the lowest common denominator of both site numbers. This has allowed the synthesis of larger nanorings from smaller oligomers, for example ***c*-P10(T5)$_2$ *9*** from ***l*-P2 *6*** and **T5**. The Vernier template method proceeds *via* the "caterpillar track complex" which can be seen in **Figure 5**.[16]

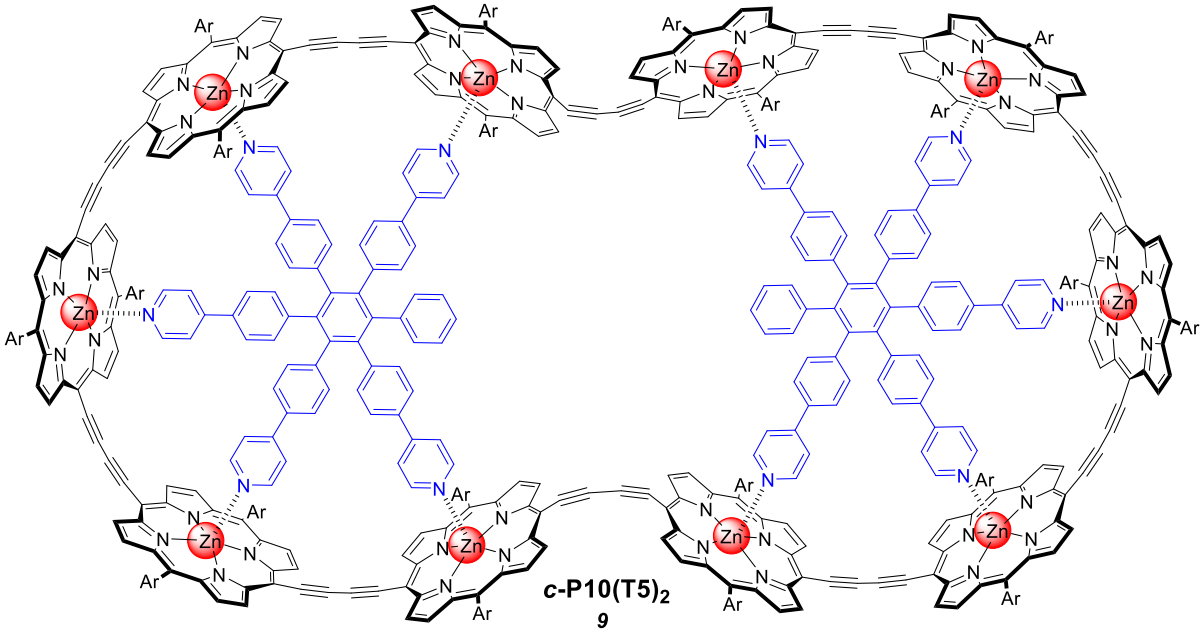

Figure 5: ***c*-P10(T5)$_2$ *9*** emergent from the ***l*-P2 *6*** and the **T5** complexes.[16]

1.4 Water-Soluble Porphyrins

Water-soluble porphyrin monomers are not new to the chemical scene. As far back as the 1950s, synthesis and study of these systems have been undertaken.[27] These research paths have included the elucidation of the bioinorganic mechanisms in the body or attempting to study their congregation into tumour tissue as a potential cancer treatment.[28] Water-soluble porphyrin centres are often found within fundamental structures of natural proteins, but these examples are solubilised by the protein groups providing limited information about how to best solubilise such systems.[10,11]

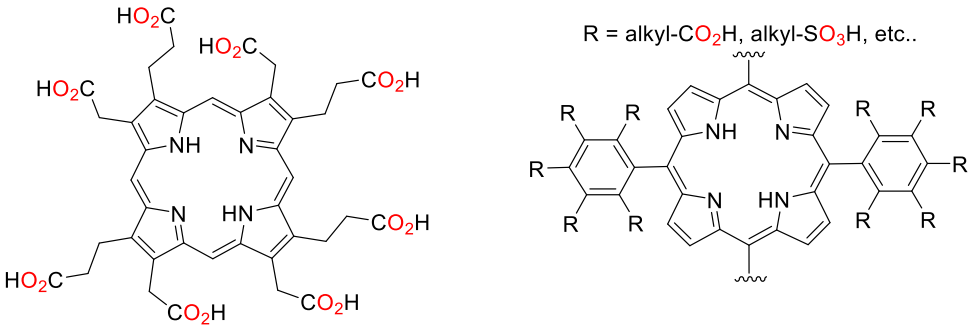

Figure 6: Left, **uroporphyrin I** ***10*** solubilised by carboxylic acid groups. Right, *meso*-tetraphenyl porphine modified with possible water-solubilising group examples.[27]

The naturally occurring uroporphyrins (**Figure 6**) present the main exception to these systems, solubilised instead by *β* functionalised alkyl carboxylate groups.[29] This comparatively simpler molecular family still presents a too complicated synthesis to be economically viable on an academic or industrial scale. As such, modification of the *meso*-tetraphenyl porphine family (**Figure 6**) has made its way to the forefront of water-soluble research due to its facile synthesis whilst still conferring the desired solubility.[30]

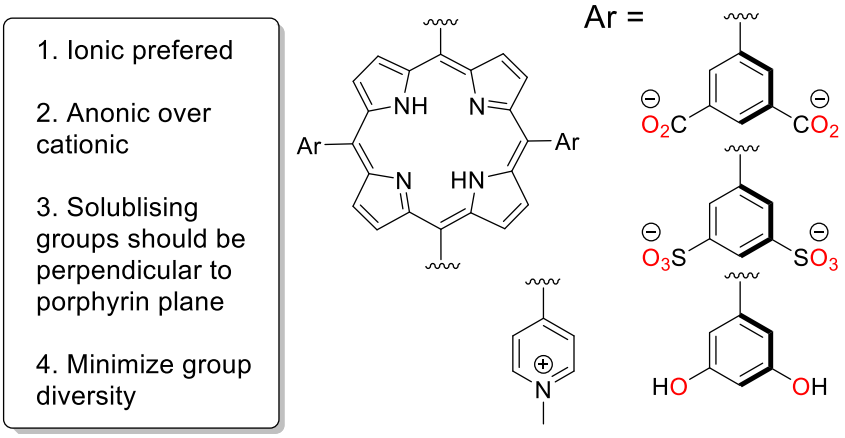

Figure 7: Simple criteria of water-soluble porphyrin monomers and examples of possible functional groups.[31]

Inspired from these earliest examples, a set of criteria (**Figure 7**)[31] can be established about the functional groups for best practices to confer solubility in water. First, ionic groups are more solubilizing than non-ionic groups for water. Second, anionic groups minimize non-specific binding to cellular structure and are preferred over cationic. Third, the projection of substituents

perpendicular to the porphyrin plane minimizes co-facial aggregation of porphyrins. Fourth, the diversity of solubilising groups should be minimized to allow for more facile synthesis and analysis.

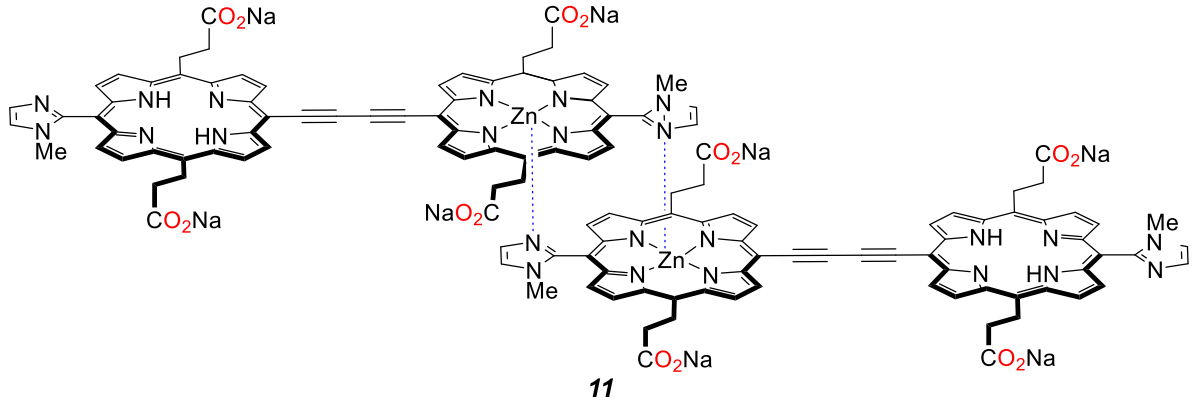

Figure 8: Water-soluble zinc porphyrin supramolecular array ***11*** synthesised by K. Ogawa.[32]

Successful limited *meso* functionalisation of porphyrins was demonstrated with water-soluble butadiyne-linked porphyrin dimers by the Ogawa group.[32] In their photodynamic therapy research, a water-soluble supramolecular porphyrin array (**Figure 8**) constructed from dimer was synthesised. The opposing *meso* positions decorated by single carboxylic acids can solubilise the entire array. This provides a clear example of how large porphyrin nanostructures can be solubilised despite the limited functionalisation of *meso* positions and how ***c*-P6**, which has half of its *meso* positions occupied, could theoretically be made water-soluble.

Work to water-solubilise ***c*-P6** nanoring was begun in the Anderson group in 2023. Initial attempts by Dr A. Rubio Rodríguez to use sulfonate groups to solubilise ***c*-P6** stalled due to problems deprotecting the sulfonate esters. Carboxylic acid became the next target, with J. Pickering completing the synthesis of carboxylic acid dendrimer **CAD NH *c*-P6 *12*** (**Figure 9**),[33] the first generation of water-soluble ***c*-P6** based upon the carboxylic acid dendrimer design. This original generation of water-soluble ***c*-P6** was limited in a restricted pH range with acidic conditions proving inaccessible. Furthermore, the acidic deprotection also resulted in the demetallation of the porphyrin cavities, which removed the ability to study the effect of zinc metal on ***c*-P6** binding.

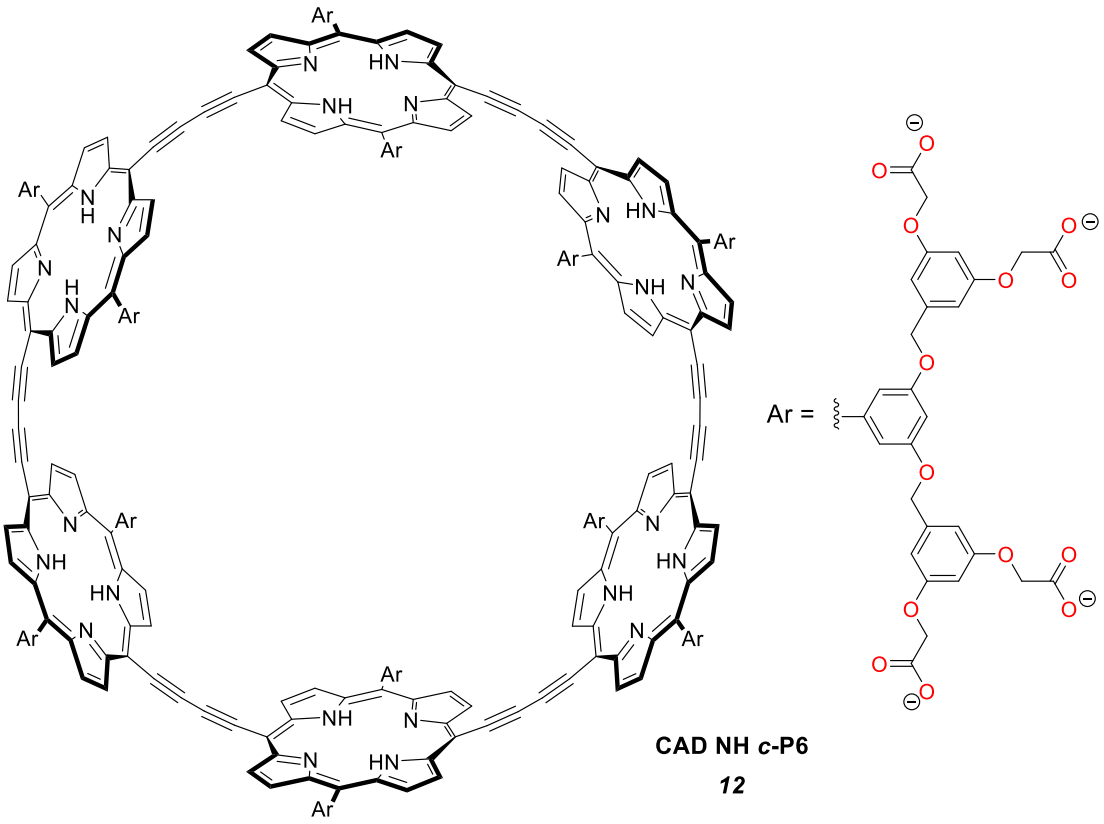

Figure 9: **CAD NH *c*-P6 *12*** the first water-soluble ***c*-P6** nanoring structure developed by J. Pickering.[33]

1.5 Carboxylic Acid Derivatives

This section will focus on the conversion of the carboxylic acids to three main derivatives, amides, activates esters, and ester sulfonates, to add a sulfonate group in place of the carboxylate (**Scheme 5)**. The conditions of these conversions however, are limited by the pre-existing design structure of the ring, namely the ether group linkers inside solubilising groups and the butadiyne bridges.[33]

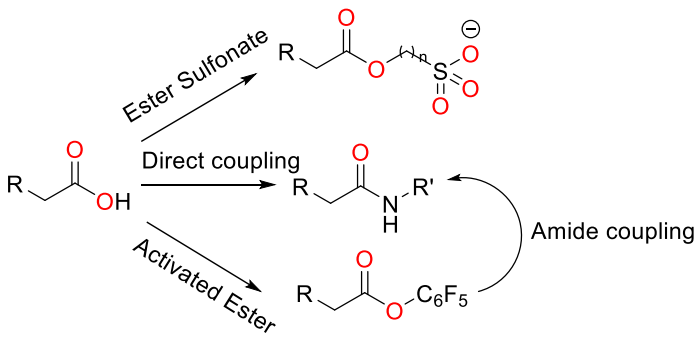

Scheme 5: The three main carboxylic acid derivatives focused upon in this thesis.

Whilst there are many harsh conditions to convert carboxylic acids to other functional groups,[34] the butadiyne links between porphyrin units provide a heavy limitation on how extreme these conditions can get. Alkyne systems are already reactive to many traditional conversion reagents for carboxylic acids, like acid-catalysed conversion, however in the case of ***c*-P6** rings their butadiyne linkers are strained by the curvature of the macrocycle (**Figure 10**). This results in an activated alkyne system capable of reaction even under mild conditions.[36,37]

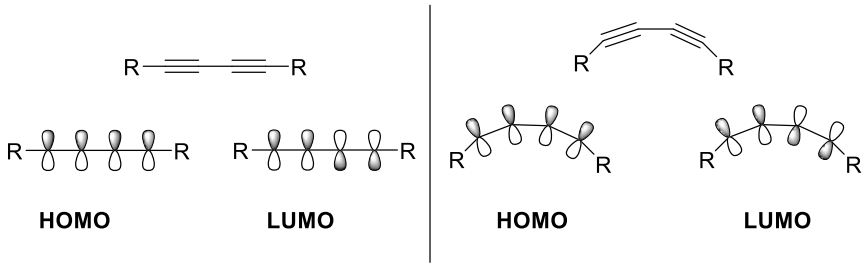

Figure 10a: Distortion of the π orbitals of a butadiyne bridge upon bending to become a part of a ***c*-P6** nanoring.

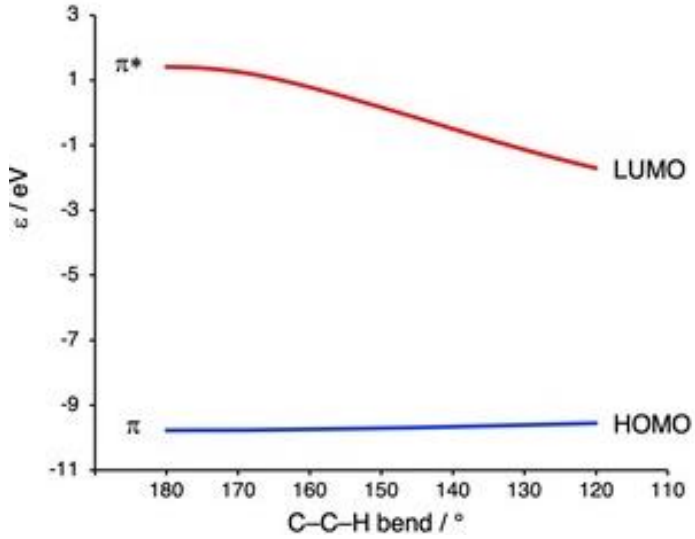

Figure 10b: Graph of change in HOMO-LUMO energy of a free terminal alkyne as the C-C-H bend change by T. A. Hamlin.[37] Reprinted with permission from Ref. 37.

These limitations result in the most reliable way of activating carboxylic acid in **CAD** based porphyrin and nanorings being through the established mild amide coupling agents like EDC, DCC, HBTU, and HATU.[34]

1.6 Aims of Thesis

This thesis aims to build upon the recent work of the Anderson group in creating a new water-soluble ***c*-P6** nanoring based on sulfonate solubilising groups instead of carboxylic acid. The synthesis of a sulfonate-based water-soluble ***c*-P6** nanoring was pursued to overcome the pH limitations conferred by the established **CAD NH *c*-P6 *12*** use of carboxylic acid as the solubilising groups. This new acidic pH water-solubility would allow for more detailed studies of the molecular recognition in water of porphyrin-based nanoring, to create models of binding for use in larger ***c*-PN** nanorings hoped to encapsulate proteins. This project targeted two directions. First the modification of **CAD NH porphyrin *16*** to convert carboxylic acid groups to sulfonate groups while preserving the core of **CAD NH *c*-P6 *12*** synthesis. Second, the use of a sulfonate ester protecting groups to allow for the synthesis of a sulfonate ***c*-P6** nanoring from first design principles whilst maintaining the ability to deprotect the sulfonate ester system. Therefore, the total aim of this thesis was to lay the foundation for a second-generation water-soluble sulfonate-based ***c*-P6** nanoring to remove the barriers to future molecular recognition work.

2 Results and Discussion

2.1 Design of Water-soluble *c*-P6 Nanorings

In order to make a porphyrin nanoring water-soluble a key question is what solubilising groups to use and when they should be introduced in the course of the synthesis. A crucial requirement for the water-solubilising group is not to include strongly coordinating heteroatoms which would disrupt template-directed synthesis, which clashes with the anionic preference discussed in section **1.4**. Fortunately, the protection strategy has shown itself as a robust way to include these water-solubilising groups in traditionally organic solvent-based syntheses.[38] In the case of water-soluble nanorings, protecting groups create two main benefits. First, they impart solubility in organic solvents, facilitating the use of the pre-existing methods for achieving synthesis of the porphyrin nanorings (**Scheme 6**).[26] Finally, they allow control over compound polarity, which allows effective flash column chromatography making purification more straightforward. However, the diverse conditions involved in the multiple reactions required to yield ***c*-P6** requires these groups to be resilient to pH conditions ranging from mildly acidic to strongly basic.[26, 33] Furthermore, these groups must be resilient to small nucleophiles, particularly fluorides due to the use of TBAF.

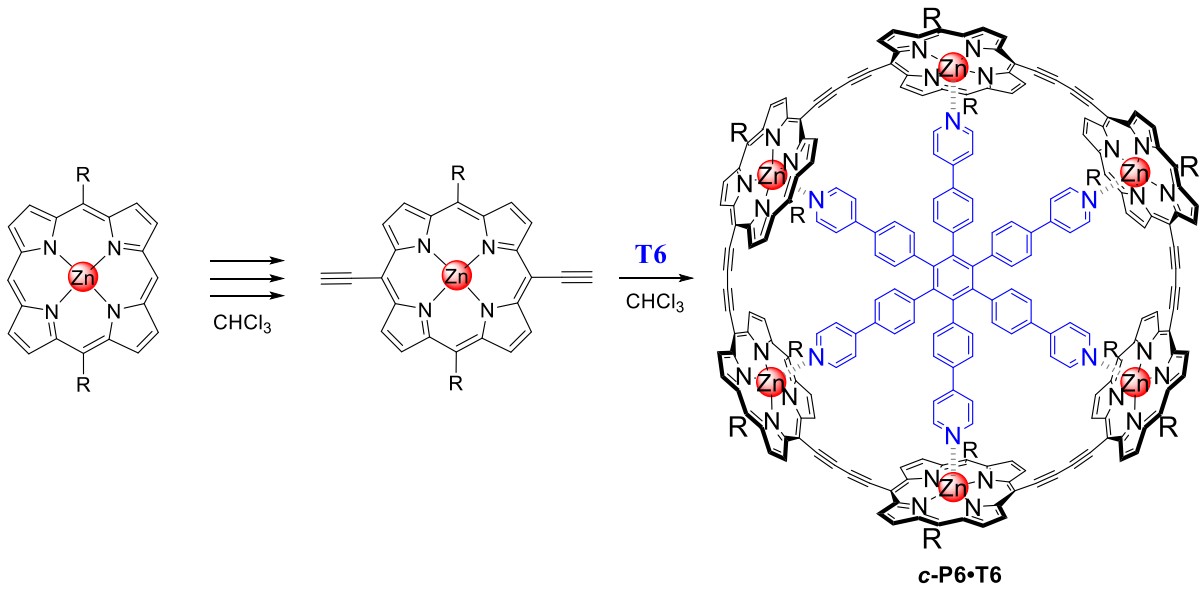

Scheme 6: Simplified synthesis of a general ***c*-P6•T6** nanorings in organic solvents.

Incorporation of sulfonate groups is a common way to impart water-solubility to organic compounds.[39] Therefore, sulfonate groups became the first target to incorporate into a ***c*-P6** nanoring. Protection for these groups generally relies upon the formation of a sulfonate ester, which can be cleaved under specific conditions. While there is a plethora of protecting esters, three sulfonate esters (**Figure 13**) stand out as the most resilient.[40]

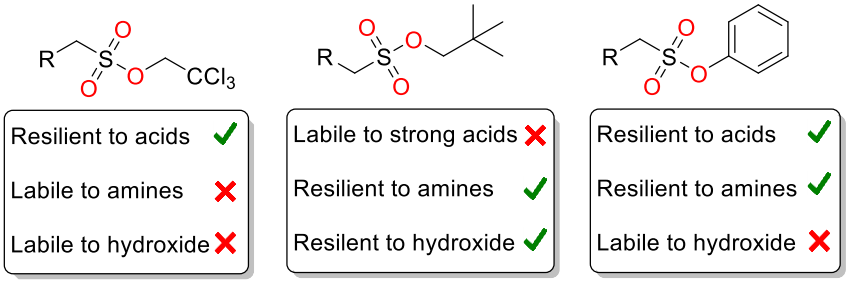

Figure 13: (Left to right) trichloroethyl (TCE), neo-pentyl (neo-P) and phenol protecting groups for sulfonates and their main traits.

Initial work in the Anderson group by Dr A. Rubio Rodríguez ruled out the use of trichloroethyl (TCE) and neo-pentyl (neo-P) groups as protecting groups for the sulfonate esters. These groups allowed for the formation of ***c*-P6•T6** nanoring, but upon deprotection of sulfonate protecting groups, the UV/Vis signature of ***c*-P6•T6** nanoring deteriorated. We concluded that the butadiyne linkers were destroyed, probably due to their activated nature making them sensitive to the deprotection conditions as discussed in section **1.5**. This resulted in the abandonment of sulfonate groups in favour of carboxylic acid.

Later work by J. Pickering would utilise the *tert*-butyl protecting group on carboxylic acids to construct the dendrimer framework (**Figure 14**) to solubilise ***c*-P6** nanoring in organic solvents and later water.[33] The dendrimer framework was used to ensure carboxylates would be able to impart water-solubility without a large number of the functional groups, as only the 5,15 *meso* positions were available for functionalisation. This work was successful in constructing carboxylic acid dendrimer (**CAD**) **NH *c*-P6 *12***, the first water-soluble nanoring. However, the use of carboxylic acid as the solubilising group meant that the ring (**CAD NH *c*-P6 *12***) was only soluble under basic

conditions. This, combined with the acidic conditions for deprotection of the *tert*-butyl groups, which also cause demetallation, does not allow the study of **CAD Zn *c*-P6.**

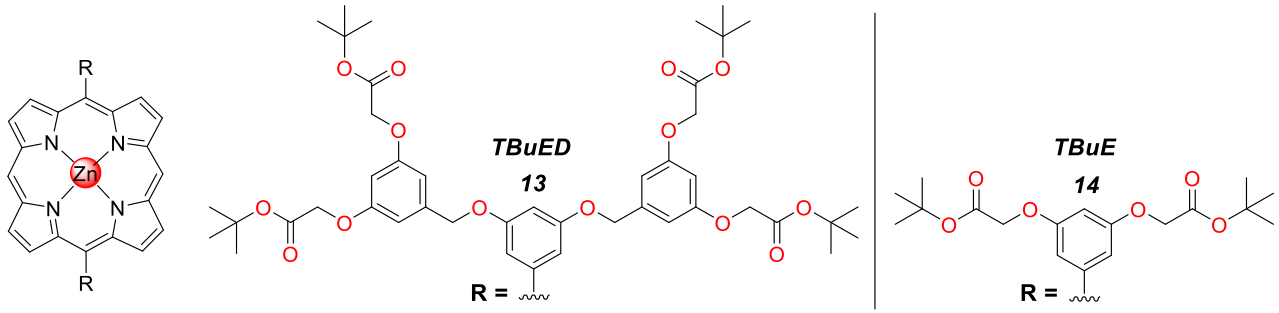

Figure 14: Left, the original 8-fold dendrimer system *tert*-butyl-ester dendrimer (**TBuED *13***) developed by J. Pickering. Right, the shortened 4-fold system *tert*-butyl-ester system (**TBuE *14***) developed by M. Foster.

M. Foster took over developments of the carboxylic acid dendrimer system, namely shortening the dendrimer chains from 8-fold to 4-fold (**Figure 14**) while maintaining water-solubility. He also refined the synthetic procedure for synthesis of **CAD NH *c*-P6 *12***.

Collectively, this work would return the synthesis of a sulfonate-based water-soluble nanoring to the forefront. I investigated two possible pathways. Firstly, adapting the **CAD NH *c*-P6 *12*** synthesis by creating a method of post-porphyrin side chain modification, allowing for the conversion of the **CAD** groups into sulfonate ones imparting acidic water-solubility *via* amide coupling (**Figure 15).** Secondly, synthesis of a new porphyrin functionalised with phenol-protected sulfonates, the last robust sulfonate ester group which has not been tested (**Figure 15**).[40] These phenol-protected sulfonates can be deprotected under basic conditions in contrast to the acidic conditions of neo-P or the reducing conditions of TCE. It was hoped that the basic conditions employed would neither cause demetallation nor cause degradation of the butadiyne linkers.

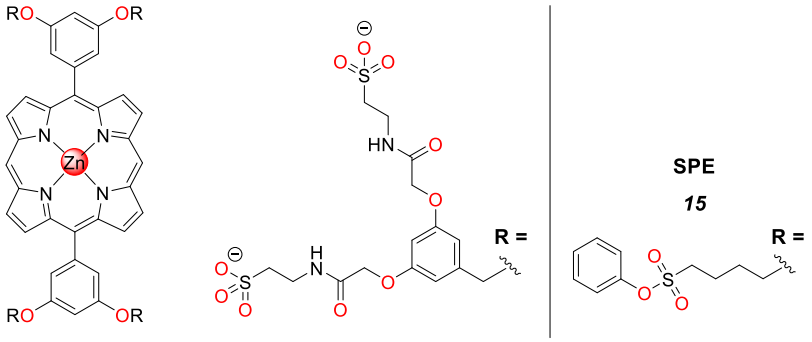

Figure 15: (Left) **CAD** system amide-coupled with taurine. (Right) the sulfonate phenyl ester (**SPE Zn porphyrin *15***) system derived from phenol protecting groups.

I attempted **CAD** side chain conversion utilising mild amide coupling reagents to attach an amino-alkane-sulfonate (**Scheme 7**). This was done in the hope that the sulfonate group would be inactive to the amide coupling agents, therefore bypassing the need for a sulfonate ester. This would avoid the addition of deprotection-amide coupling-deprotection final steps to the ***c*-P6** nanoring synthesis.

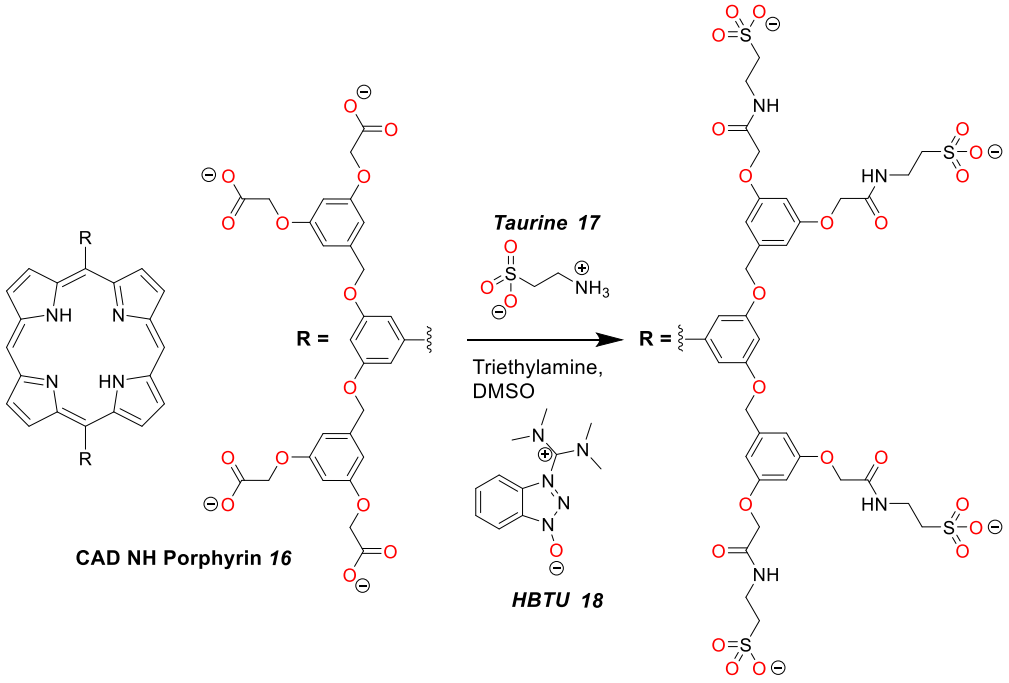

Scheme 7: **CAD NH porphyrin *16*** amide coupling by HBTU ***18*** with Taurine ***17***.

The sulfonate phenyl ester (**SPE**) ***c*-P6•T6 *27*** synthesis built on the work of the previous members of the group in incorporating the new side chain. Utilising the new 4-fold dendrimer and the demonstrated ability of 3,5-dihydroxybenzaldehdye ***23*** to act as a nucleophile towards primary halide groups, the sulfonate phenyl precursor was constructed by the catalytic ring opening of

butansultone ***19*** positioning chloride groups onto the termini of the compound. The formed sulfonyl chloride ***20*** reacts preferentially with phenol over the primary alkyl halide forming phenyl 4-chlorobutanesulfonate ***21*** ready for incorporation into the dendrimer, shown in **Scheme 8**. This aldehyde dendrimer ***22*** was then reacted with di-(2-pyrrolyl)-methane (**DPM**) to form a porphyrin, **SPE Zn porphyrin *15***, shown in **Figure 16**. The hydrophobic nature of the sulfonate phenyl ester combined with its UV activity make silica gel chromatographic purification facile.

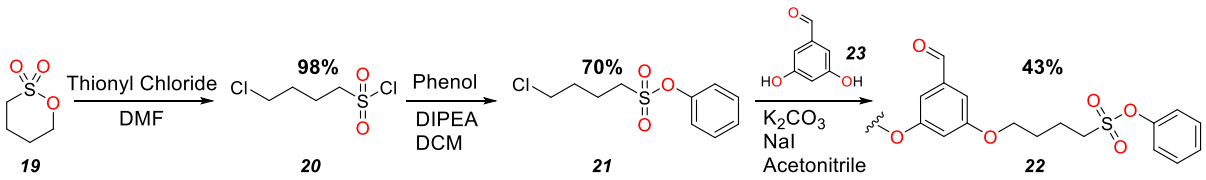

Scheme 8: Conversion of butanesultone ***19*** into aldehyde dendrimer system ***22***.

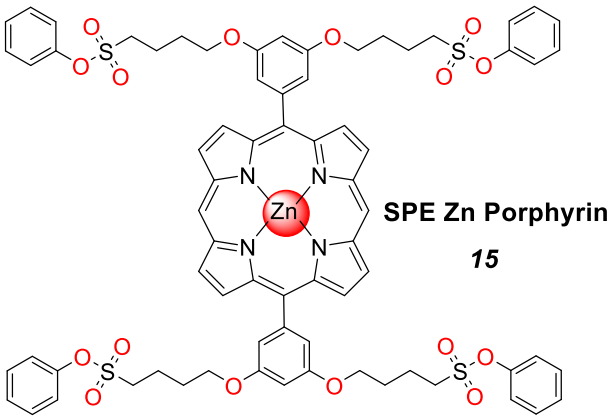

Figure 16: **SPE Zn porphyrin *15***, adapting the 4-fold dendrimer and sulfonate ester design together.

Upon successful synthesis of this monomer unit, the focus switched to functionalisation the porphyrin for incorporation as a monomer into a ***c*-P6** nanoring,[26] which had already been shown to work with *tert*-butyl-ester dendrimer (**TBuED**) side chain porphyrins (**Scheme 9**).

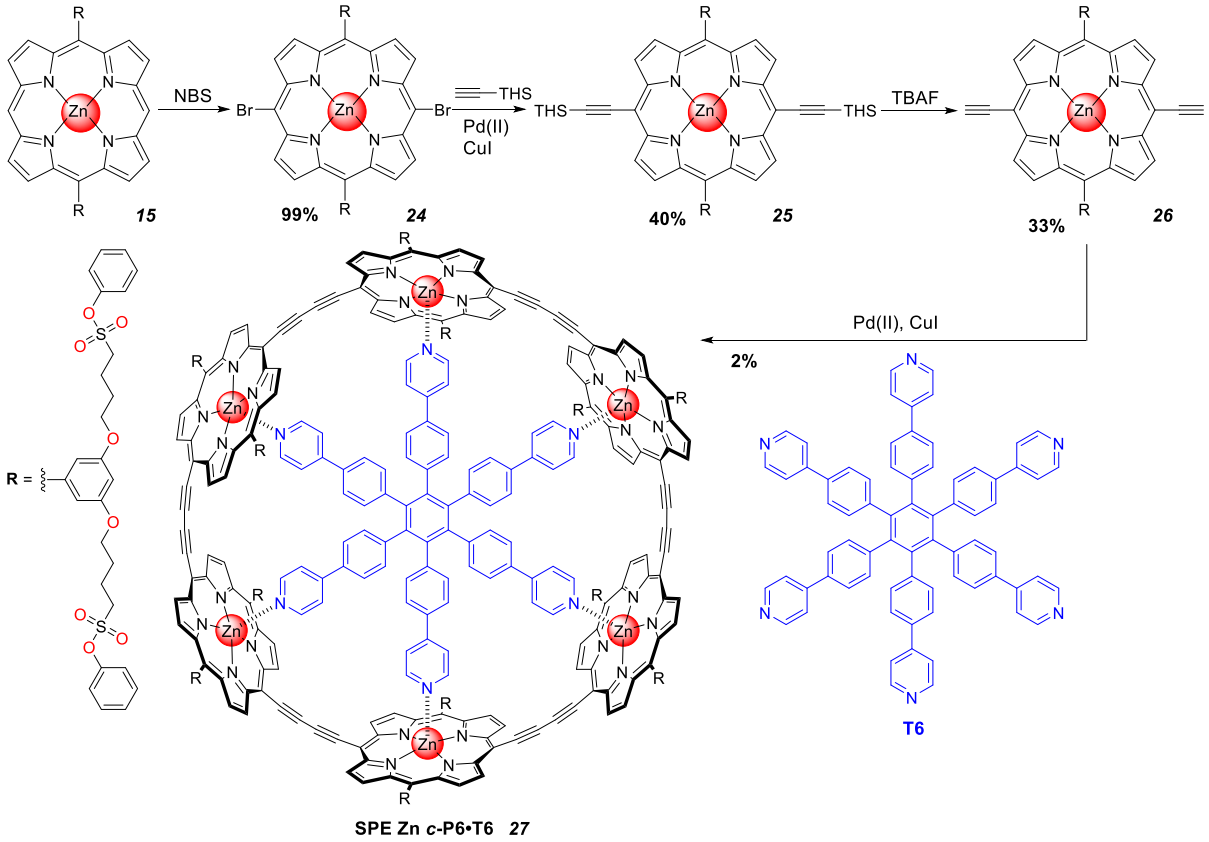

Scheme 9: Simplified post-porphyrin synthesis of **SPE Zn *c*-P6•T6 *27***.

Once **SPE Zn *c*-P6•T6 *27*** was synthesised, basic hydrolysis of the phenyl sulfonate esters to reveal the water-solubilising sulfonate was performed, revealing water-soluble sulfonic acid dendrimer (**SAD**) **Zn *c*-P6•T6 *28*** nanoring (**Scheme 10**).[40]

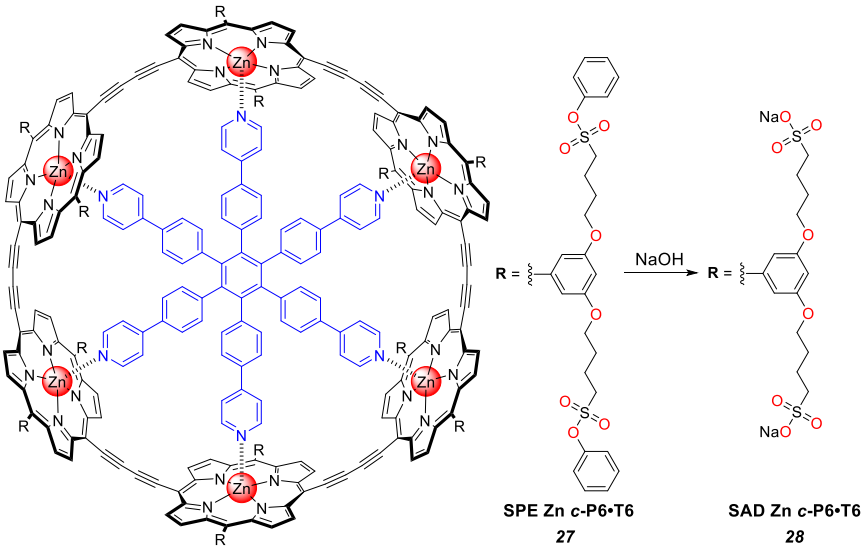

Scheme 10: Simplified deprotection of **SPE Zn *c*-P6•T6 *27*** to form **SAD Zn *c*-P6•T6 *28***.

2.2 Established CAD NH *c*-P6 synthesis

Work began with the synthesis of **TBuED Zn *c*-P6•T6 *37*** and its monomer **TBuED Zn porphyrin *13*** (**Scheme 11**), ready for attempts at post-porphyrin modifications. This work proceeded by the improved synthesis developed by J. Pickering, namely the synthesis of porphyrin dimer was focused upon, rather than monomer, in order to produce better yields of **TBuED Zn *c*-P6•T6 *37***.[33]

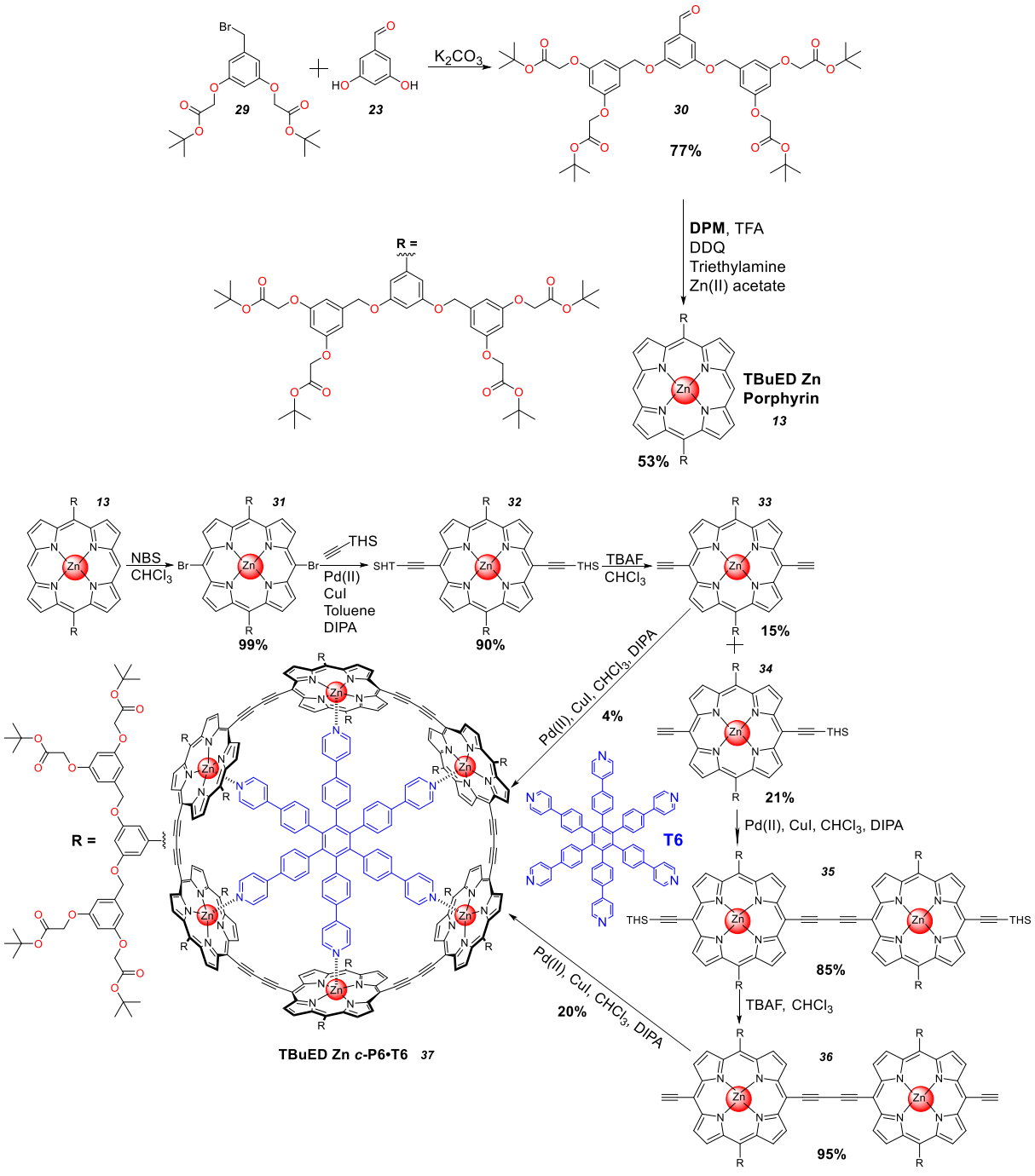

Scheme 11: **TBuED *c*-P6•T6 *37*** nanoring and **TBuED Zn porphyrin *13*** monomer synthesis.

Once the synthesis was completed, acidic deprotection of **TBuED Zn porphyrin *13*** (**Scheme 12**) was performed to produce **CAD NH porphyrin *16*** ready for amide coupling attempts.

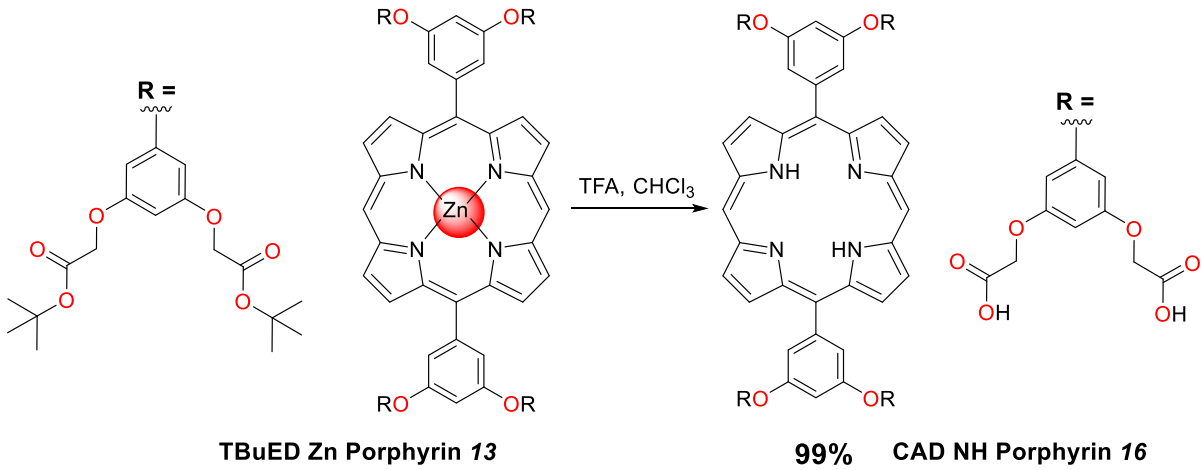

Scheme 12: **TBuED Zn porphyrin *13*** deprotection to form **CAD NH porphyrin *16***.

2.3 Post-Porphyrin CAD Modification

While a plethora of amide coupling conditions exist,[41] the methodology of any successful coupling is limited by the solubility of the two reactants, the amino-alkane-sulfonic acid and the **CAD NH porphyrin *16***. These reagents were found to be soluble only in water or in polar organic solvents, like DMSO or DMF. It was considered prudent to avoid water due to two reasons: amide coupling conditions affording higher yields were developed in organic solvents and to reduce drying time of product. Therefore, a test reaction adapting the method of N. P. Sargaeva *et al.*[42] for amide coupling was performed on **CAD NH porphyrin *16*** with taurine in DMSO (**Scheme 13**).

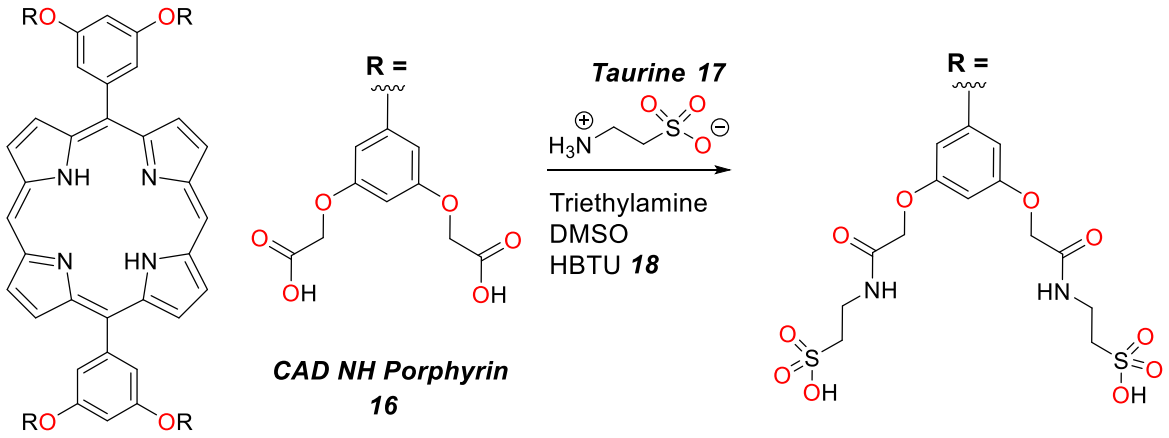

Scheme 13: General taurine *17* amide coupling derived from Sargaeva *et al.*[42]

After limited success, attempts to further the amide coupling were pursued. These ranged from higher temperatures, greater molar ratios of reagents to **CAD NH porphyrin *16***, attempts to shorten the alkyl backbone of the amino-alkane-sulfonic acids to improve its solubility in DMSO and different coupling reagents (**Appendix I**). While these changes improved the relative absorbance of substituted products in HPLC trace, full conversion proved impossible by HPLC (**Figure 17**). These results lead to increased doubt about the viability of an unprotected amino-alkane-sulfonates in amide coupling with **CAD NH porphyrin *16***. While the use of protecting groups were considered, this would defeat the purpose of avoiding additional deprotection steps. This was to minimise the exposure of the butadiyne bridges to further conditions in case of reaction in ***c*-P6**.

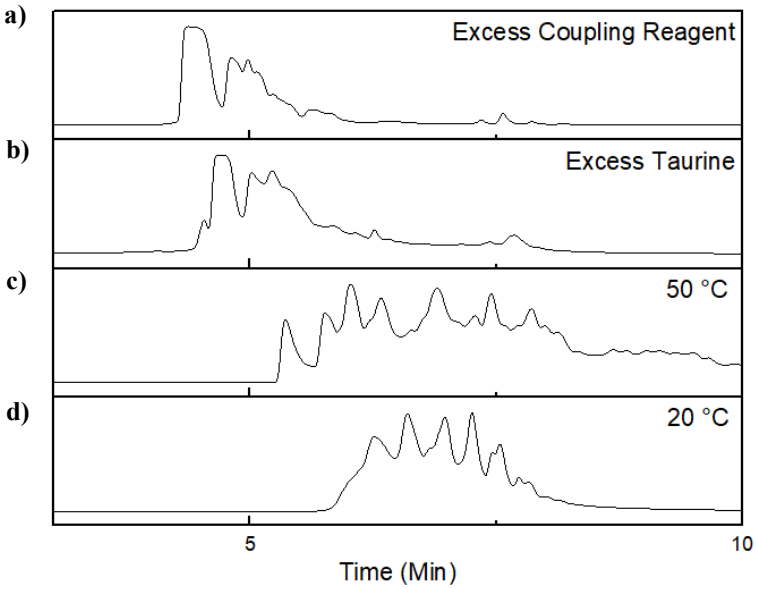

Figure 17: HPLC traces (420 nm, water: acetonitrile 95-20%, 30 mins) of **CAD NH porphyrin *16*** amide coupling with taurine ***17*** using HBTU ***18*** as the coupling reagent, demonstrating the improvement and stagnation of reaction after 12 hours. **d)** 1 eqv **CAD NH porphyrin**, 8.8 eqv taurine, 12 eqv HBTU, 20 ºC. **c)** all same as **d)** except for 50 ºC. **b)** all same as **d)** except for 16 eqv taurine, 50 ºC. **a)** all the same as **d)** except for 16 eqv taurine, 24 eqv HBTU, 50 ºC.

After extensive work, with limited success in purification and analysis of the material by HPLC, it was concluded that the reaction of amino-alkane-sulfonic acids was probably impossible due to the

polymerisation of sulfonic chains by the amide coupling reagents (**Scheme 14**).[43-46] This resulted in a too-diverse range of products, which reduced the yield of any of these products individually.

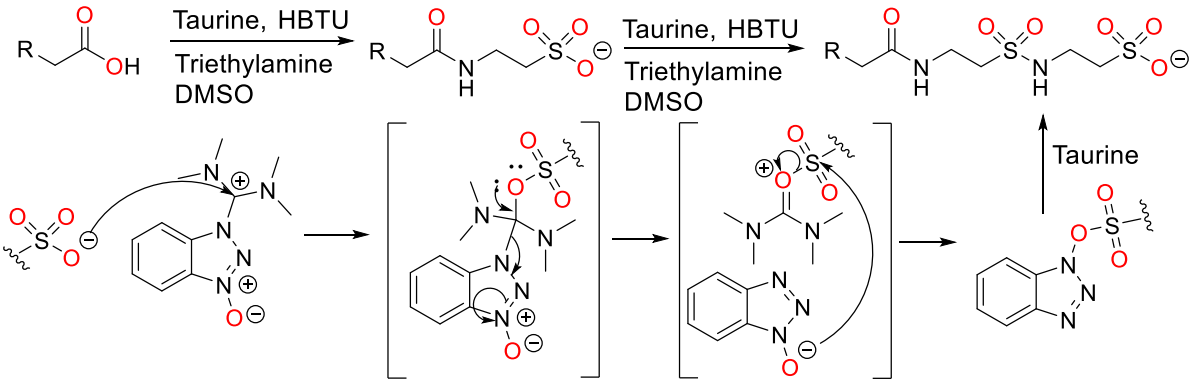

Scheme 14: Hypothesised mechanism of polymerisation of amino-alkane-sulfonic acids by HBTU ***18***.[43-46]

With amino-alkane-sulfonic acids proving impossible to convert in good yields, attention shifted to amino-sorbitol ***38*** (**Scheme 15**) due to its greater solubility in DMSO. The hypothesis was that by increasing the solubility and thus the concentration of the amine in the coupling but maintaining the molar ratio, these new conditions would favour the total conversion of the carboxylic acids. The less substituted material would react faster under the more concentrated conditions, narrowing the range of products.

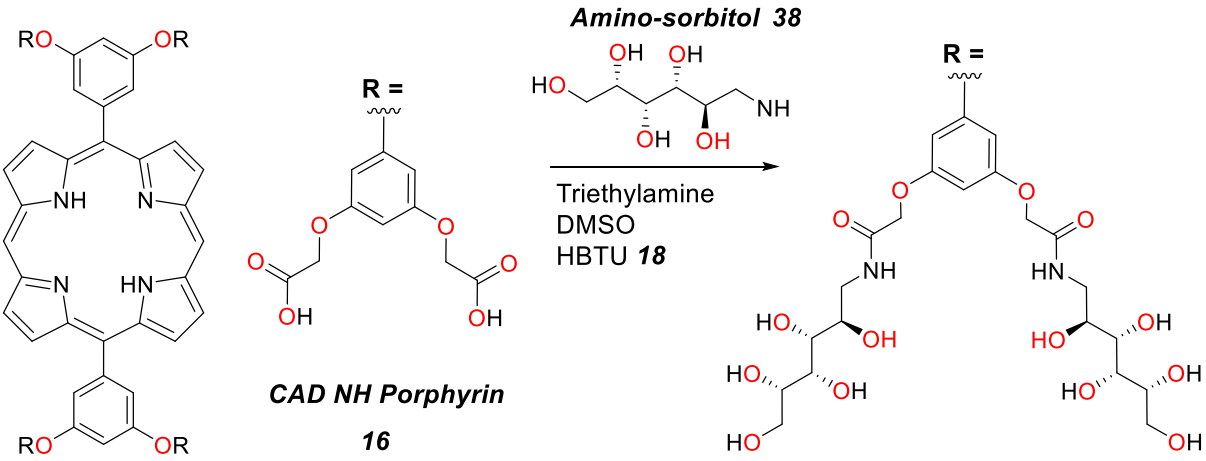

Scheme 15: General amide coupling conditions for amino-sorbitol ***38***.

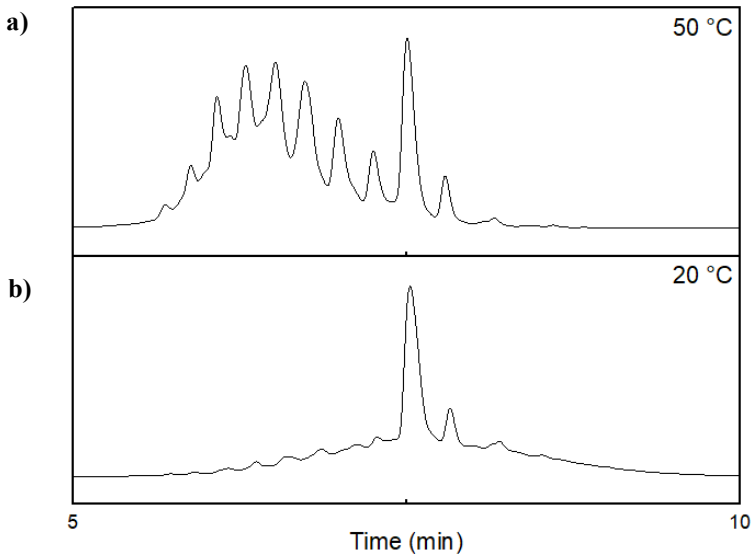

Figure 18: HPLC traces (420 nm, water: acetonitrile 95-20%, 30 mins) of **CAD NH porphyrin *16*** amide coupling with amino-sorbitol ***38*** using HBTU ***17*** as the coupling reagent after 12 hours, showing the coupling taking place but signs of polymerisation as the number of peaks do not correspond to the 8 possible substitutions. **b)** 1 eqv **CAD NH porphyrin**, 8.8 eqv amino-sorbitol, 12 eqv HBTU, 20 °C. **a)** all the same as **b)** except for 50 °C.

These attempts failed (**Figure 18**), resulting in the abandonment of in-situ activated ester formation by these amide coupling reagents in favour of the preformation of the activated ester. The chosen activated ester derives from pentaflourophenol alcohol ***39*** (**Scheme 16**).[47] This coupling was shown in DMF, allowing for solvent overlap needed to try **CAD** conversion.[48] Attempts of this conversion on the **CAD** system were unsuccessful, as the mono-substituted product precipitated out of reaction before full conversion. This was confirmed by MALDI-TOF (**Figure 19**).

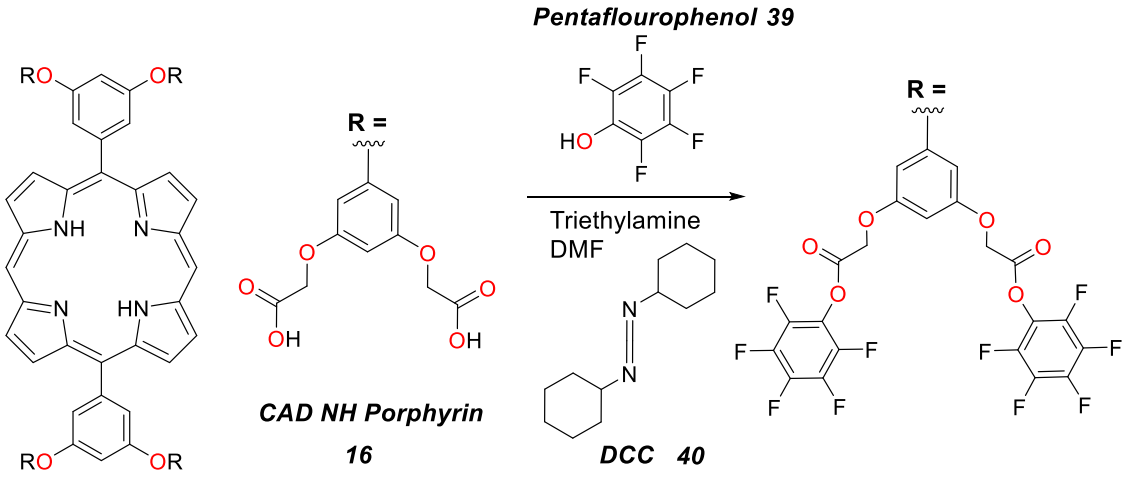

Scheme 16: **CAD NH porphyrin *16*** conversion into an activated ester *via* esterification with pentaflourophenol ***39***.

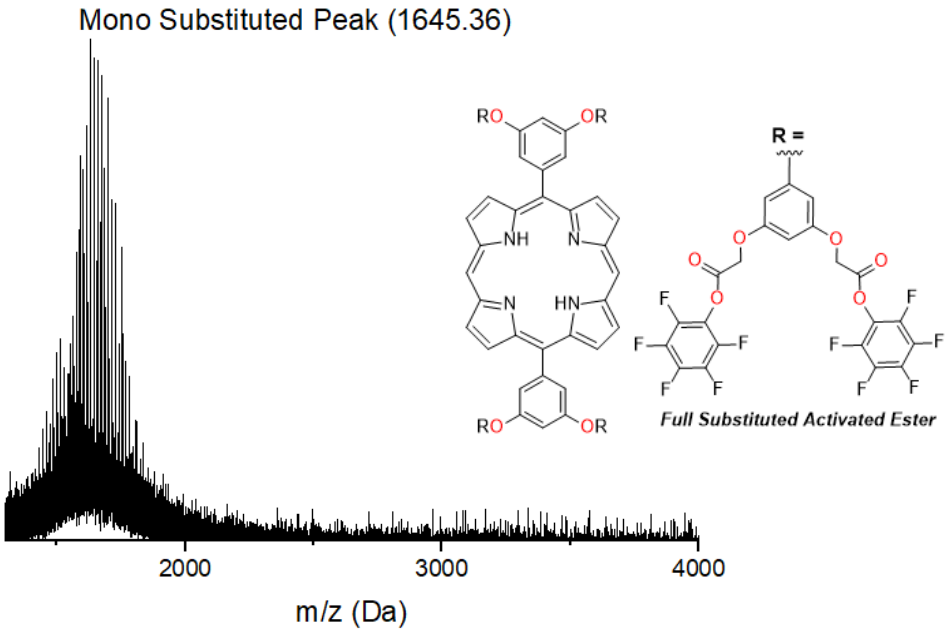

Figure 19: MALDI-TOF spectrum for crude reaction material from **Scheme 16**, only mono-substituted product is observed, the most abundant peak (1645.36 m/z). The expected mass for full substitution is 2815.89 m/z.

With **CAD**-amide conversion proving ineffective, the focus switched to the formation of an ester-linked sulfonic acid system. This utilised 4-iodobutanesulfonic acid derived from butansultone (**Scheme 17**),[49] which was then combined with **CAD NH porphyrin *16*** to attempt carboxylic acid conversion without the presence of a coupling reagent. Reaction side products from the amide coupling reagents had previously obscured ^{1}H NMR spectra, due to their overlapping of the relevant porphyrin ^{1}H NMR peaks.

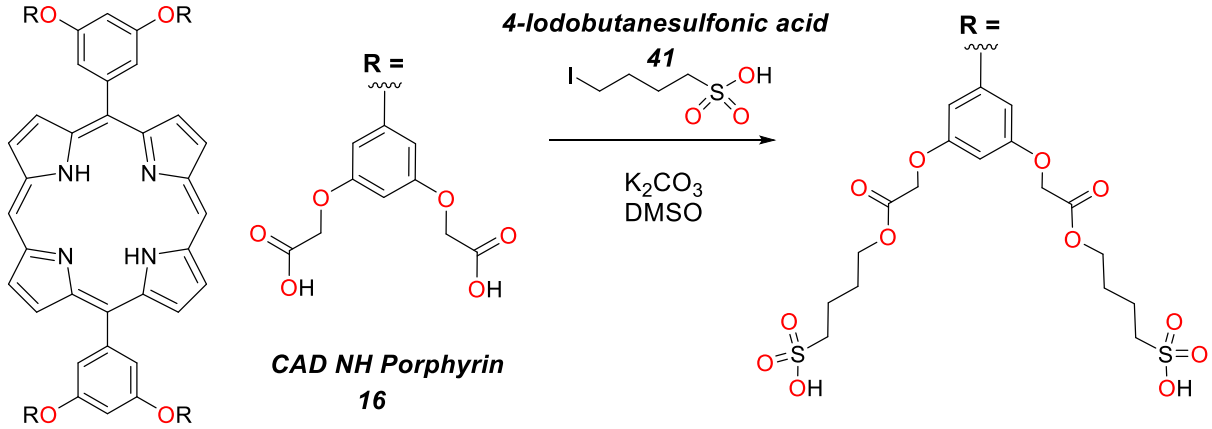

Scheme 17: **CAD NH porphyrin *16*** esterification with ***41***, performed to allow for NMR tracking of the system.

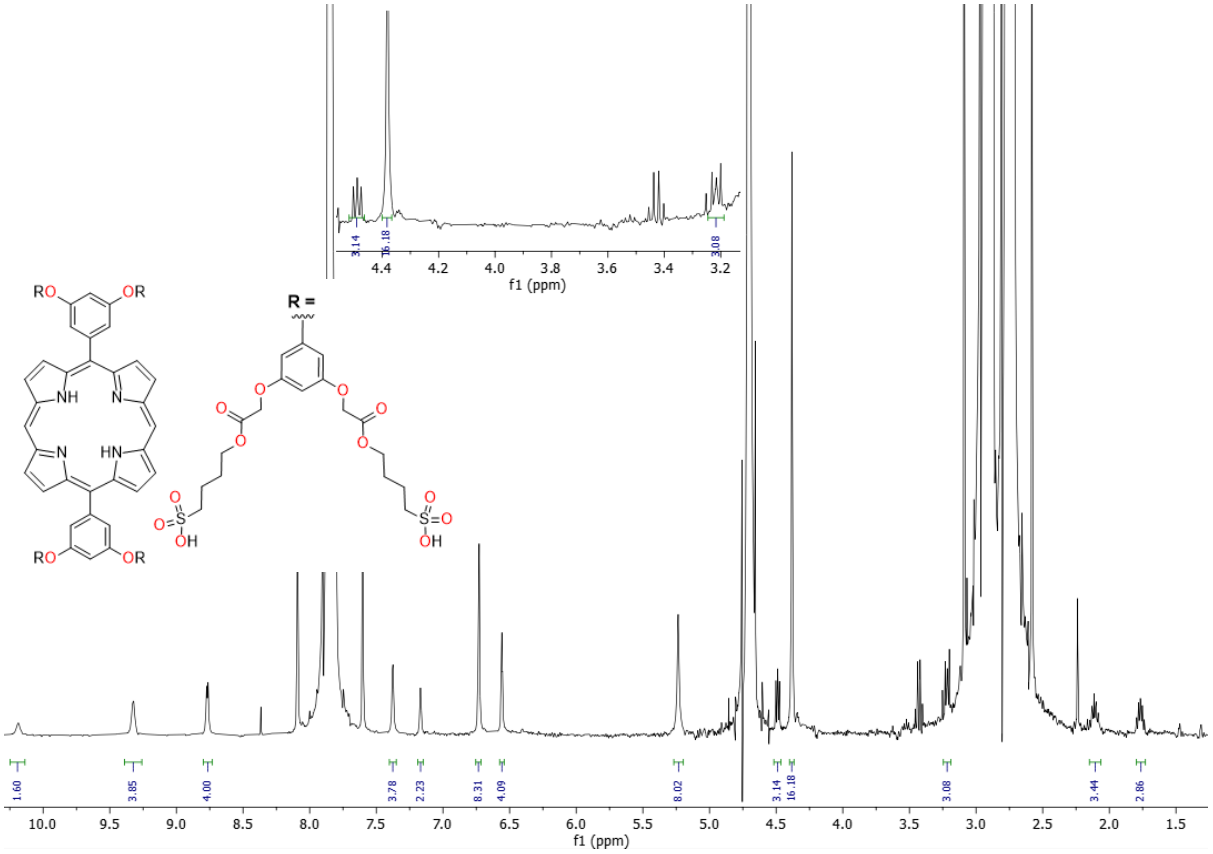

Figure 20: ^{1}H NMR (D_2O, 400 MHz) of the crude reaction product of **Scheme 17**. Peaks with integrals correspond to the desired product. The integral ratio between porphyrin peaks and the new triplets shows low conversion.

The ^{1}H NMR spectrum of the reaction mixture (**Figure 20**) once again showed only limited success in conversion. It was decided that further **CAD** modification attempts would be unfruitful. As such a return to designing new water-soluble side chains for ***c*-P6** synthesis was adopted, with two new water-solubilising groups derived from amino-sorbitol and the previous sulfonate systems.

2.4 Sorbitol Side Chain Synthesis

Amino-sorbitol, previously worked upon in section **2.3**, became the basis of a neutral charge side chain in the hope of imparting pH-independent water-solubility to ***c*-P6** rings. Drawing from work by Ik-Hyeon Paik *et al*.[50] selective protection of the alcohols in amino-sorbitol ***38*** in acid-catalysed acylation could be performed (**Scheme 18**). This penta-acetyl system ***42*** could then be bound to a bromo-acetyl bromide, forming a primary halide ***43*** already demonstrated by J. Pickering to incorporate into a dendrimer scaffold ***44*** (**Scheme 19**).[33]

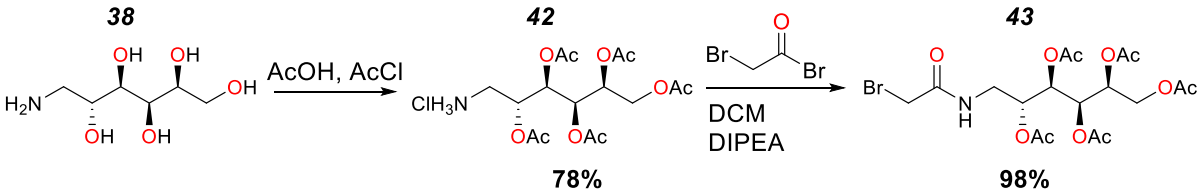

Scheme 18: Protection of amino-sorbitol's ***38*** alcohols,[50] followed by amide ***43*** formation.

While incorporation into a dendrimer system ***44*** was successful, the polar nature of the products made them impossible to purify on silica-gel chromatography. Despite this, attempts were made to use reverse-phase chromatography *via* preparative HPLC to isolate the desired product ***44***, shown in **Figure 21**.

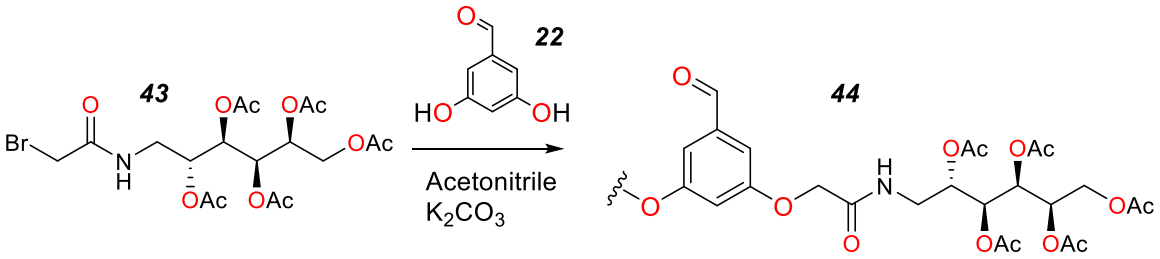

Scheme 19: The penta-acetyl system ***43*** incorporated into the aldehyde scaffold ***44*** ready for porphyrin synthesis.

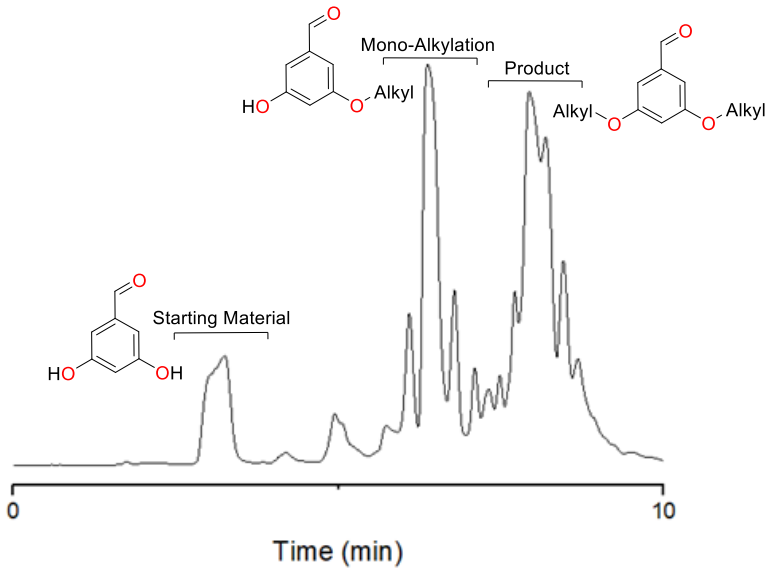

Figure 21: HPLC trace (220 nm, water: acetonitrile) of crude reaction mixture from dendrimer incorporation (**Scheme 18**). Reaction of ***43***, 3,5-dihydroxy-benzaldehyde ***23***, K_2CO_3 in acetonitrile at 82 °C under argon.

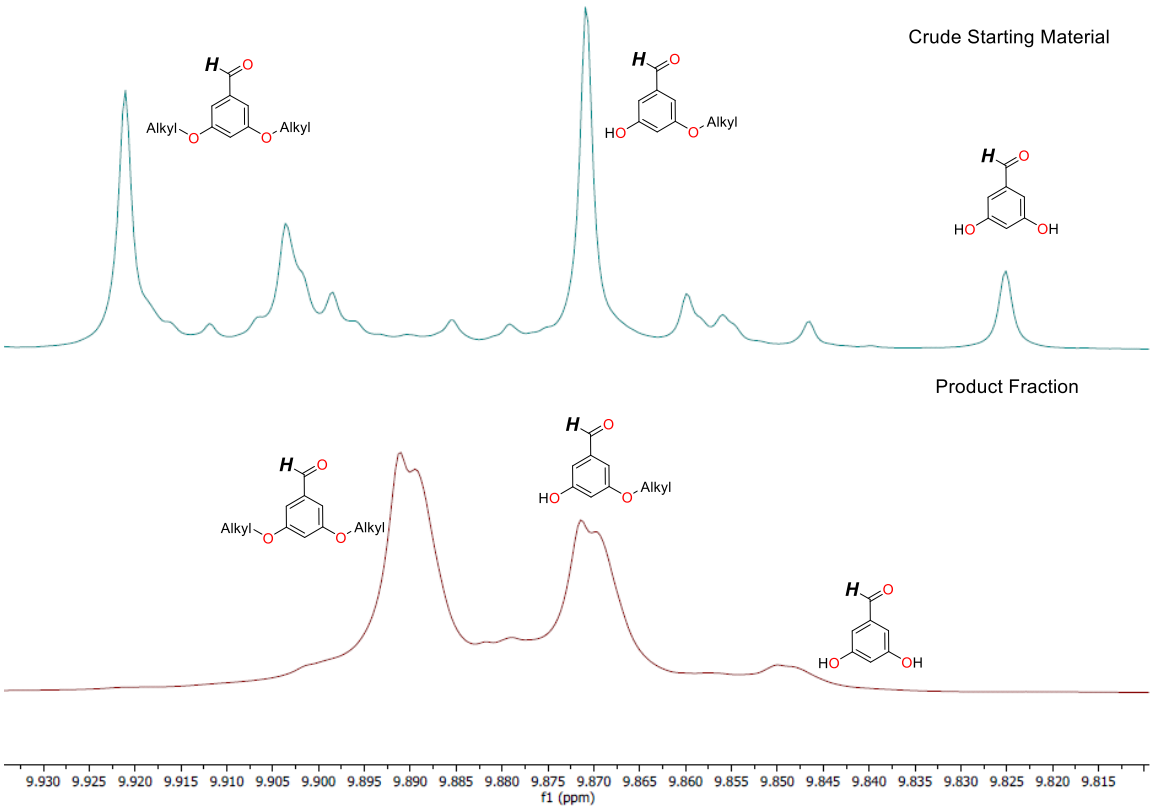

Figure 22: Comparison of aldehyde peaks of crude product material (**Scheme 19**) and the product material gained after HPLC (**Figure 21**) by ^{1}H NMR ($CDCl_3$, 400 MHz), demonstrating it is impossible to purify.

Isolation of the product ***44*** proved unsuccessful, with some mono and unsubstituted material remaining present in the 3rd fraction (**Figure 22**). A possible explanation is that the penta-acetyl protecting groups are too hydrophilic, resulting in favourable hydrogen bonding between alcohol groups present in the 3,5-dihydroxy-benzaldehyde ***23*** and its mono-substituted product and the product's acetyl groups. Thus, with purification of ***44*** not possible on a gram-scale, it was decided to proceed with the sulfonate design.

2.5 SPE Zn *c*-P6•T6 Synthesis

It was shown by G. Schwertz *et al.*[51] that butanesultone ***19*** could be ring-opened and simultaneously chlorinated at the new terminal positions by thionyl chloride and DMF. This allows for facile preparation of 4-chlorobutanesulfonyl chloride ***20*** from butanesultone ***19***, which could easily react with phenol to yield the desired sulfonate phenyl ester-protection group ***21***.[52] The primary chloro group then facilitated incorporation into the 4-fold dendrimer framework ***22***. This reaction proved

more difficult due to 3,5-dihydroxylbenzaldehyde ***23*** struggling to undergo S_n2 onto the primary chloro groups compared to bromo groups. This required the use of high-temperature reflux over a long period of time under argon. These conditions are notably harsher than the ones required under the synthesis reported by J. Pickering.[33] Altogether, this allowed for the synthesis of **SPE Zn porphyrin** ***15*** *via* condensation with **DPM** in gram-scale quantities (**Scheme 20**).

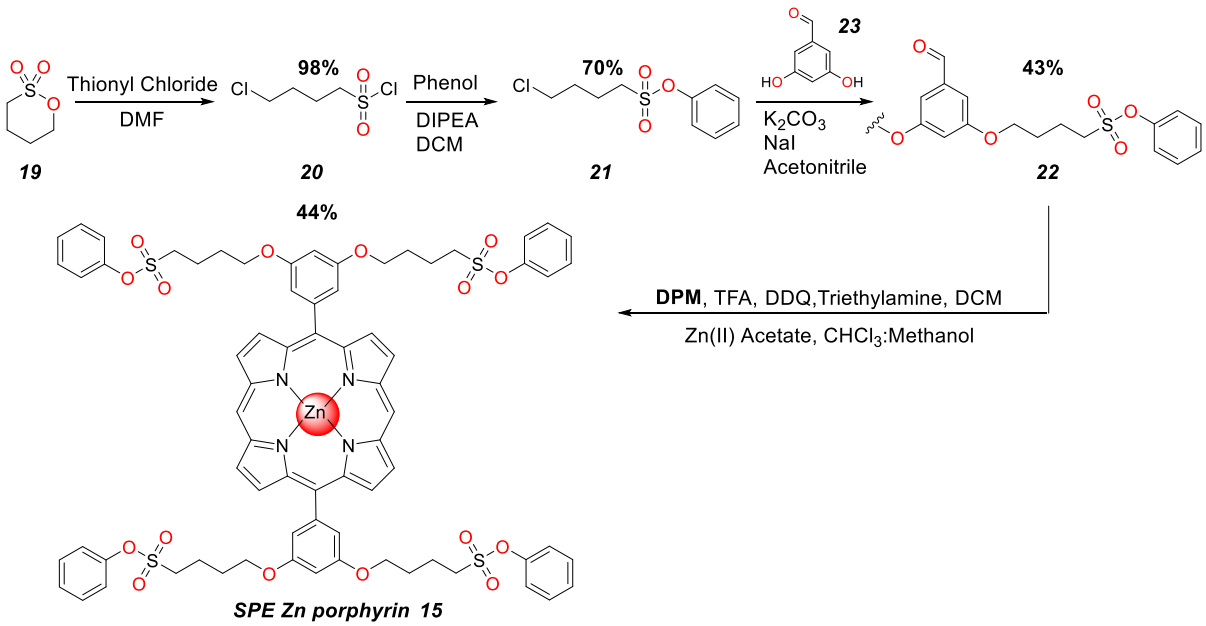

Scheme 20: **SPE Zn porphyrin** ***15*** synthesis from starting butanesultone ***19***.

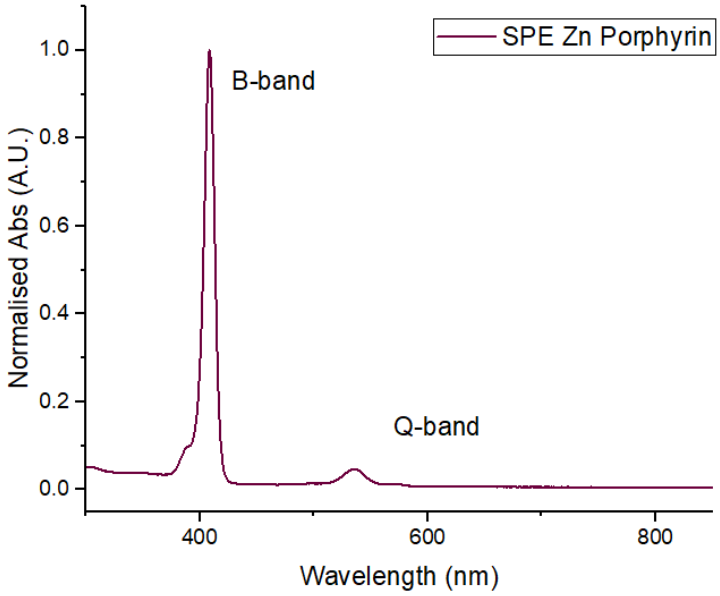

Figure 23: UV/Vis spectrum of **SPE Zn porphyrin** ***15*** in chloroform.

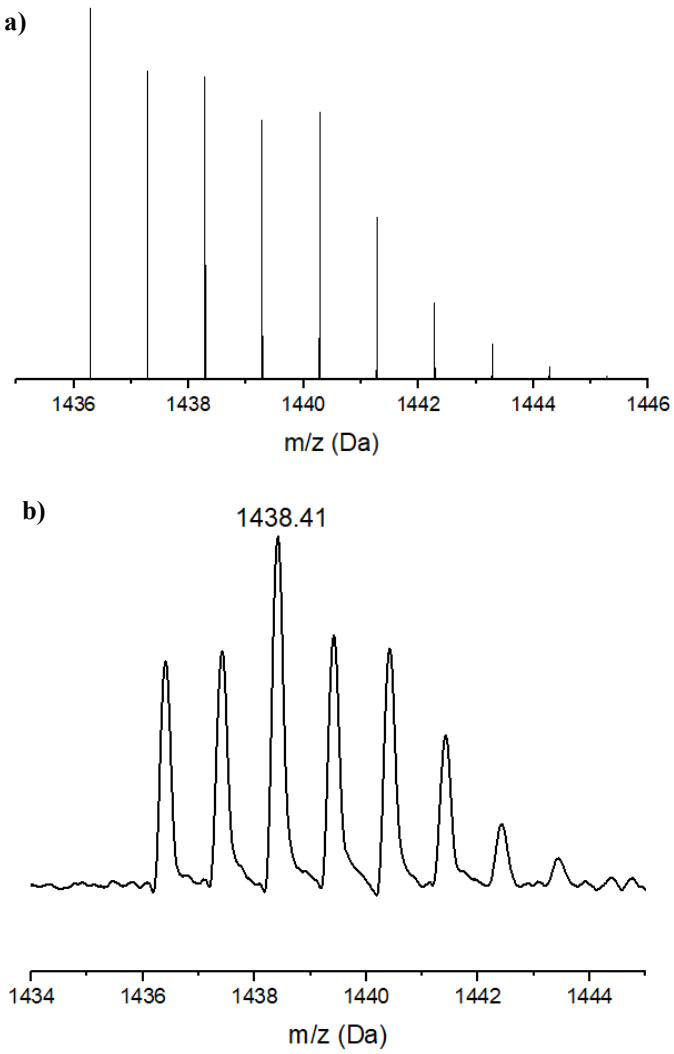

Figure 24: a) Calculated mass spectrum of **SPE Zn porphyrin *15***. b) MALDI-TOF spectrum of **SPE Zn porphyrin *15***, expected m/z of 1436.28.

With **SPE Zn porphyrin *15*** successfully synthesised (**Figure 23-24**), the established procedure of ***c*-P6** synthesis was conducted (**Scheme 21**).[26] First, *meso*-bromination by NBS to give ***24***, followed by Sonogashira coupling with trihexylsilyl (THS) acetylene ***56*** which produced the protected monomer ***25***. Standard TBAF deprotection of the THS groups could then reveal the **SPE *l*-P1 *26*** monomer ready for template-directed oxidative coupling. The **T6** template was synthesised according to the established procedure of 6-fold Suzuki coupling, combining 4-hexa-bromophenylbenzene and pyridine-4-boronic acid.[26] GPC trace of the crude reaction material is shown in **Figure 25**.

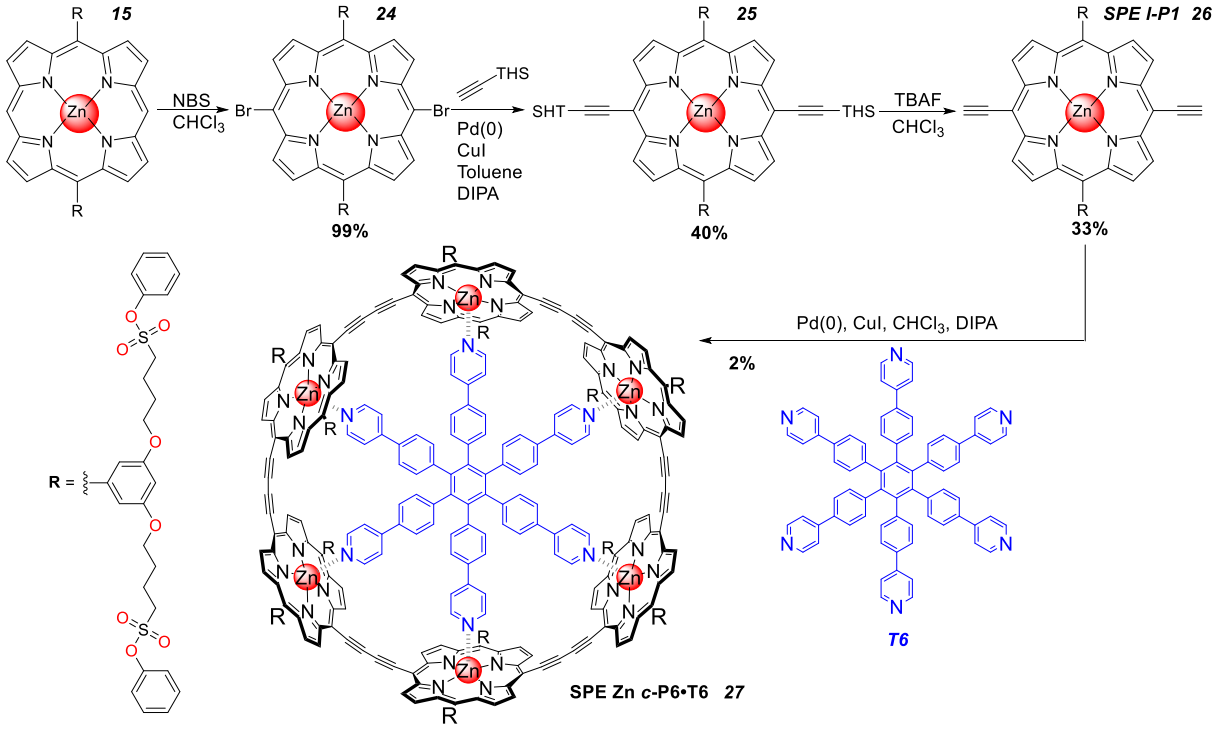

Scheme 21: **SPE Zn *c*-P6•T6 *27*** nanoring synthesis from **SPE Zn porphyrin *15*** monomer with yields.

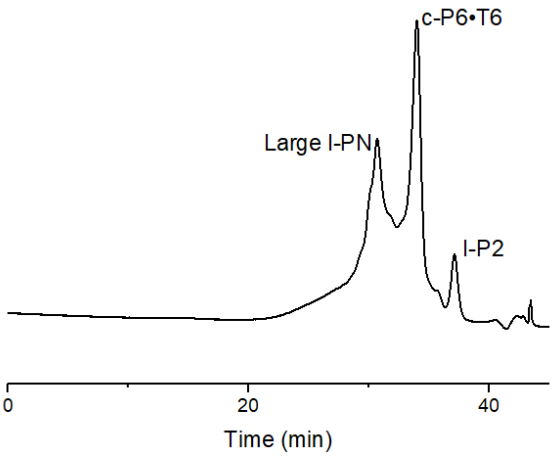

Figure 25: GPC (400 nm, THF: pyridine) of the reaction mixture from completed **SPE Zn *c*-P6•T6 *27*** synthesis.

Work by the Anderson group showed that ***c*-PN** oligomers obtain a unique UV/Vis signature due to the change in symmetry of the molecule (**Figure 26**).[26] This absorption change results in ***c*-P6•T6** nanorings showing a 3-peaked-crown forming in the Q band of the UV/Vis spectra of the material. As **SPE Zn *c*-P6•T6 *27*** is the only known material produced from the oxidative coupling with this unique signature, it was concluded the material produced was the desired ring.

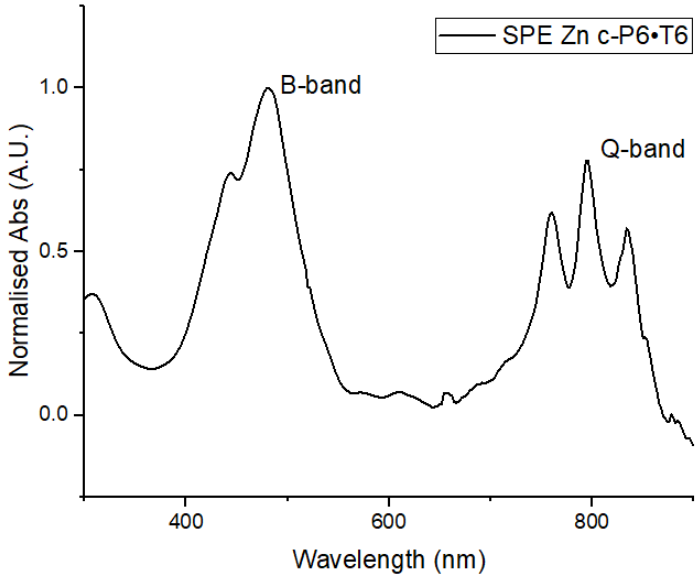

Figure 26: UV/Vis (chloroform) of **SPE Zn *c*-P6•T6 *27*** demonstrating the characteristic Q-band crown.

2.6 SPE to SAD Conversion

While the synthesis of **SPE Zn *c*-P6•T6 *27*** was ongoing, deprotection of the monomer **SPE Zn porphyrin *15*** was pursued to find conditions for revealing the sulfonic acid dendrimer (**SAD**) system. Adapting the work done by Stephen C. Miller, phenyl sulfonate esters were shown to be uniquely labile to NaOH cleavage.[40] This allowed for the use of NaOH dissolved in a DCM-methanol mixture (9:1 v/v) to completely cleave **SPE Zn porphyrin**'s (***15***) 4-fold phenyl sulfonate esters (**Scheme 22**) revealing the anionic sulfonate groups, as shown in **Figure 27**.

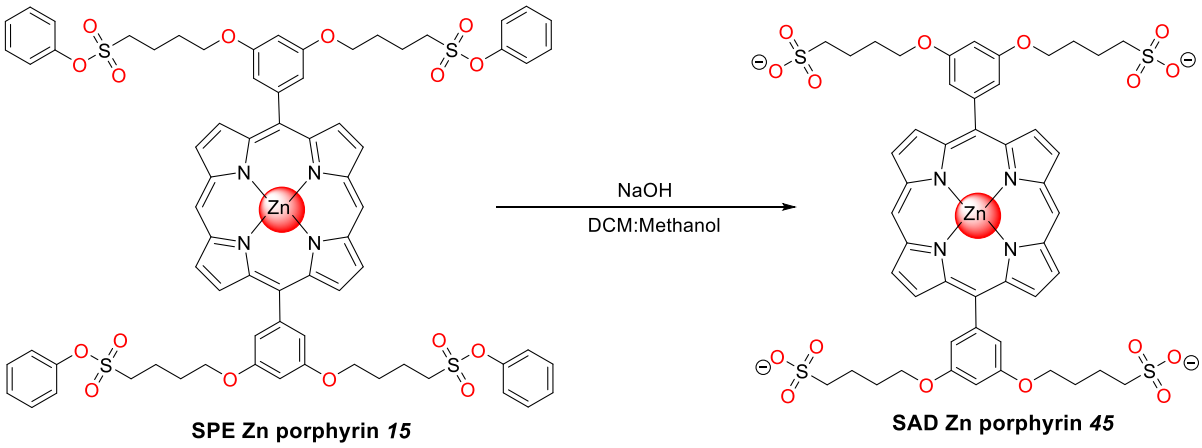

Scheme 22: Basic hydrolysis of **SPE Zn porphyrin *15*** producing **SAD Zn porphyrin *45***.

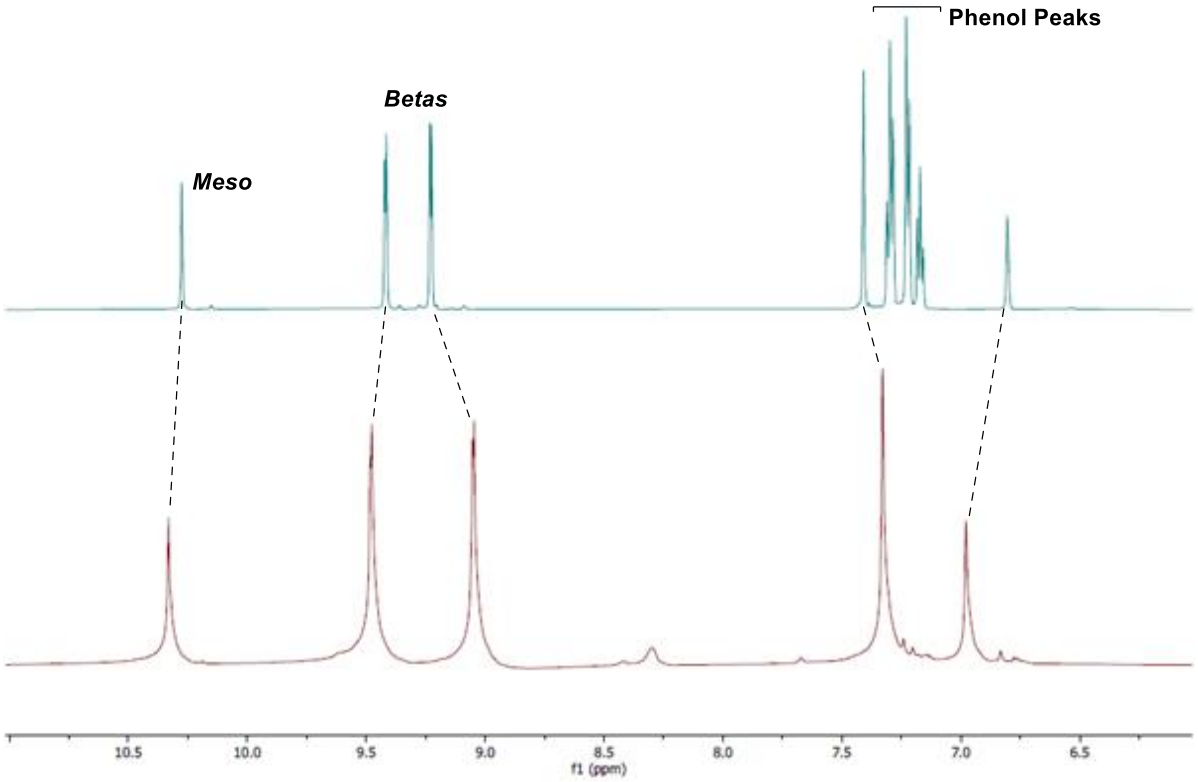

Figure 27: Top, ^{1}H NMR ($CDCl_3$, 600 MHz) of **SPE Zn porphyrin *15***. Bottom, ^{1}H NMR (DMSO, 600 MHz) of **SAD Zn porphyrin *45***. This demonstrates the collapse of the phenol related aromatic peaks upon cleavage.

The collapse of the phenol-linked aromatic peaks in the NMR combined with the solubility change demonstrates the success of this hydroxide cleavage. As such, attempts to cleave the **SPE Zn *c*-P6•T6 *27*** ring were pursued under the same conditions (**Scheme 23**).

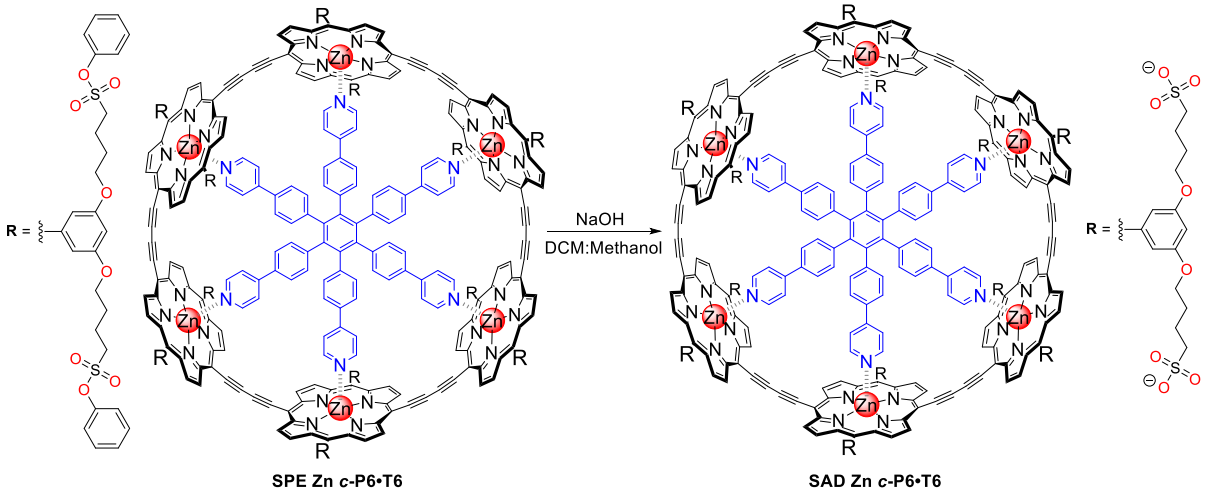

Scheme 23: Basic hydrolysis of **SPE Zn *c*-P6•T6 *27*** to form **SAD Zn *c*-P6•T6 *46***.

The main concern during this synthesis was the destruction of the butadiyne bridges, as demonstrated before by the loss of the unique UV/Vis signature of the sulfonate ***c*-P6** ring. However, despite the previously sulfonate deprotections proving incompatible with these bridges, the hydroxide cleavage would maintain the unique UV/Vis signature (**Figure 28**) of a ***c*-P6•T6** ring. A sulfonate-based water-soluble ***c*-P6•T6** nanoring was thus achieved *via* the conversion of **SPE** to **SAD** side chains.

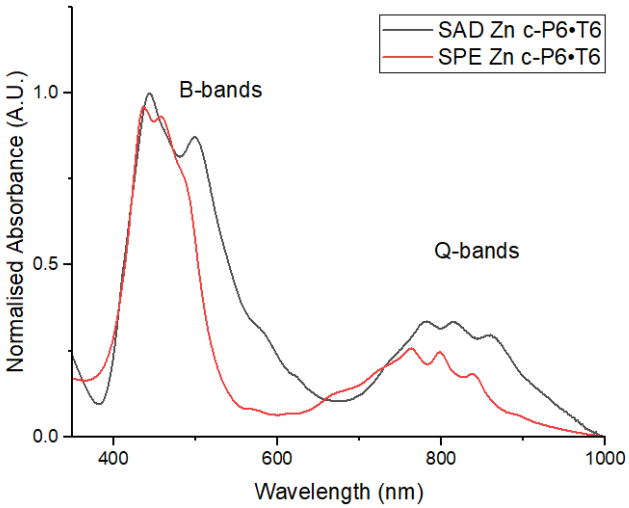

Figure 28: UV/Vis spectrum of **SAD** (H_2O) and **SPE** ($CHCl_3$) **Zn *c*-P6•T6** ***46*** and ***27*** nanorings, main emphasis is placed on the Q-bands which continue to show the "triple crown" after deprotection demonstrating the continued integrity of the butadiyne bridges. B-band distortion is attributed to self-complexation of **SAD** arms to Zn metal centres.

3 Conclusion

This thesis describes the successful synthesis of a sulfonate-based water-soluble ***c*-P6** nanoring - **SAD Zn *c*-P6•T6 *46***. This work demonstrates the importance of side chain design as the most important principle for constructing a water-soluble nanoring rather than post-porphyrin side chain modification of **CAD**. This confirms the limitation of late-stage functionalisation of **CAD NH *c*-P6 *47*** as a synthetic pathway to further water-soluble rings. Instead, the new **SAD** side chain design could allow for the study of the molecular recognition and biochemical properties of water-soluble ***c*-PN** nanorings in both acidic and basic conditions. Further, the orthogonality of deprotection and demetallation conditions allows for the future comparison of free-base vs metal-occupied porphyrin nanorings. This opens potential avenues for the study of the **SAD *c*-P6** family of compounds as possible ion channel transporters and their protein binding.

4 Experimental

4.1 General Methods

All commercial chemicals were used without further purification unless specified in synthesis. Solvent mixture ratios are reported by volume. Anhydrous solvents were retrieved from a MBraun MBSPS-5-BenchTop solvent purification system. All air-sensitive reactions were performed under argon using standard Schlenk procedures.

Thin layer chromatography (TLC) was performed on Merck TLC silica gel 60 F254. Size exclusion chromatography (SEC) utilised Bio-Rad Bio-Beads S-X1 (40-80 μm bead size). Analytical gel permeation chromatography (GPC) was carried out using JAIGEL-3H-A (8 × 500 mm) and JAIGEL-4H-A (8 × 500 mm) columns in THF + 1% pyridine as eluent with 1.5 mL/min flow rate or JAIGEL-3HR-A (8 × 500 mm) and JAIGEL-4HR-A (8 × 500 mm) columns in THF + 1% pyridine as eluent with 1.5 mL/min flow rate. Semi-preparative GPC was carried out using either Shimadzu recycling GPC system consisting of an SPD-20A UV detector, LC-20 AD pump, JAIGEL 3H (20 × 600 mm) and JAIGEL 4H (20 × 600 mm) columns in toluene + 1% pyridine as eluent with a flow rate of 3.5 mL/min or on a LaboACE LC-7080 Plus Series recycling GPC system consisting of a UV 4ch LA detector, P-LA80 pump, JAIGEL 3HR (20 × 600 mm) and JAIGEL 4HR (20 × 600 mm) columns in toluene + 1% pyridine as eluent with a flow rate of 10 mL/min.

Reverse phase High Performance liquid chromatography (HPLC) was performed at 298 K using an Agilent 1100 Series system comprising an autosampler (G1313A), a vacuum degassing unit (G1379A), a quaternary pump (G1311A), a column oven (G1316A), a diode array detector (G1315B), and a fraction collector (G1364C). For analytical HPLC an Agilent Eclipse XDB-C18 column (4.6 × 150 mm, 5 μm particle size) was used with a flow rate of 1.0 mL/min. For semi-preparative HPLC an Agilent Eclipse XDB-C18 column (9.4 × 250 mm, 5 μm) was used with a flow rate of 21.0 mL/min.

NMR spectra were recorded at 298 K using Bruker Avance III HD nanobay (400.1 MHz), Bruker Avance III HD (500.3 MHz) or a Bruker NEO 600 with broadband helium cryoprobe (600.4 MHz). Chemical shifts are quoted in parts per million (ppm) relative to the residual solvent peak. Coupling constants (*J*) are quoted in Hertz (Hz). Deuterated chloroform ($CDCl_3$) for NMR samples was stored over K_2CO_3 and passed through neutral activated alumina (Brockman I) before use.

MALDI-TOF mass spectrometry was carried out using an Autoflex MALDI-TOF instrument, using DCTB as the matrix and only molecular ions are reported.

UV-vis-NIR absorption spectra were measured on either a Perkin Elmer Lambda 20 spectrometer at 298 K, temperature controlled by a PTP-1 Peltier unit from Perkin Elmer, or Cary 60 UV-Vis spectrophotometer at 298 K, temperature controlled by Agilent Cary Single Cell Peltier Accessory Type SPVF-1x0. All sample solution were in quartz cuvettes (1 cm pathlength) or four-clear-sided polystyrene cuvettes (1 cm pathlength).

4.2 Synthesis of Relevant Compounds

All **TBuED** and **CAD** compounds were prepared according to the work of J. Pickering.[33]

TBuED Aldehyde *30*[33]

Benzyl bromide ***29*** was prepared using a published procedure.[53]

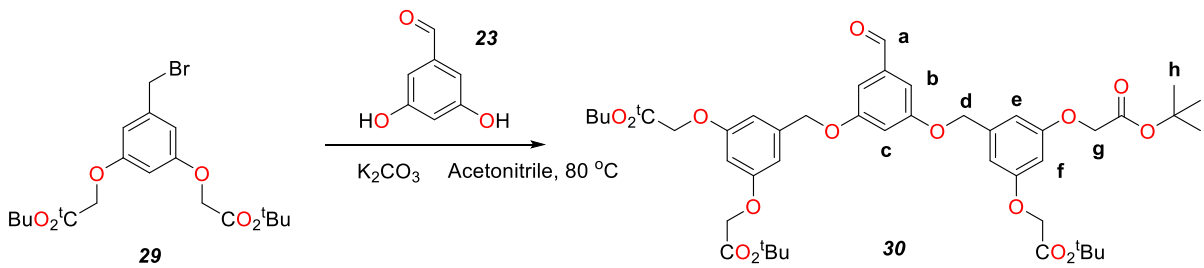

Benzyl bromide ***29*** (1.45 g, 3.36 mmol, 2.2 eqv) was added to 3,5-dihydroxybenzaldehyde ***23*** (0.211 g, 1.53 mmol, 1 eqv) and potassium carbonate (0.507 g, 3.67 mmol, 2.4 eqv) dissolved in acetonitrile under argon. The resulting mixture was heated to reflux at 82 °C for 14 hours. The mixture was then cooled to room temperature and acetonitrile was removed under reduced pressure. Water (50 mL) was added to the residue and extracted with ethyl acetate (30 mL) three times. The organic layer was then dried with sodium sulfate and concentrated under reduced pressure. This crude product was purified *via* silica gel column chromatography with 25:75 ethyl acetate: petroleum ether as eluent. The resultant yellow oil TBuED aldehyde ***30*** (0.985 g, 1.53 mmol, 77%) was collected.

^{1}H NMR (600 MHz, $CDCl_3$) **δ** 9.88 (s, 1H, H_a), 7.06 (d, J = 2.3 Hz, 2H, H_b), 6.80 (t, J = 2.3 Hz, 1H, H_c), 6.60 (d, J = 2.3 Hz, 4H, H_e), 6.44 (t, J = 2.3 Hz, 2H, H_f), 5.00 (s, 4H, H_d), 4.49 (s, 8H, H_g), 1.48 (s, 36H, H_h).

^{13}C NMR (151 MHz, $CDCl_3$**)** **δ** 191.1, 167.4, 160.0, 159.4, 139.9, 138.3, 108.6, 108.5, 106.8, 101.9, 82.8, 70.3, 65.8, 28.0.

TBuED Zn Porphyrin *13*[33]

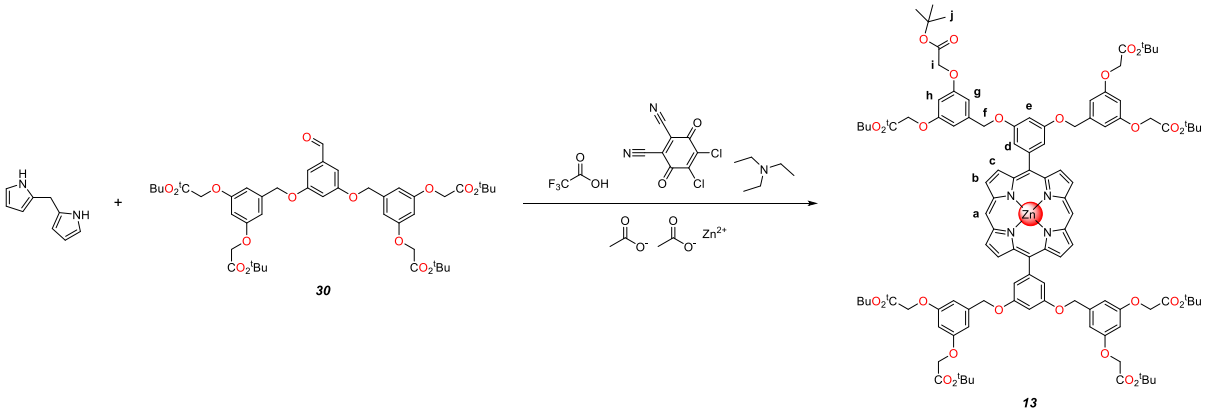

TBuED aldehyde ***30*** (4.15 g, 4.95 mmol, 2 eqv) and 2,2' dipyrromethane (0.723 g, 4.95 mmol, 2 eqv) dissolved in argon-saturated dichloromethane (1.37 L). TFA (10.1 mmol, 776 µL, 4.1 eqv) was added dropwise and the mixture stirred for 3 hours in the dark. DDQ (1.68 g, 7.42 mmol, 3

eqv) was added and the mixture stirred for 20 minutes. Triethylamine (19.8 mmol, 2.76 mL, 8 eqv) was then added and the solvent reduced under pressure. The crude mixture was then passed through a silica plug (25:75 ethyl acetate: petroleum ether eluent). The product, TBuED NH porphyrin ***48***, was dissolved in chloroform (20 mL) and then zinc(II) acetate (1.45 g, 7.91 mmol, 3.2 eqv) in methanol (10 mL) was added. The now purple solution was stirred for 1 hour at room temperature resulting in a pink solution. The solvent was removed under reduced pressure and the crude product purified by silica plug (25-40:75-60 ethyl acetate: petroleum ether) to give a red solid TBuED Zn porphyrin ***13*** (2.59 g, 1.30 mmol, 53%).

^{1}H NMR (600 MHz, $CDCl_3$) **δ** 10.32 (s, 2H, H_a), 9.43 (d, J = 4.4 Hz, 4H, H_b), 9.19 (d, J = 4.4 Hz, 4H, H_c), 7.52 (d, J = 2.2 Hz, 4H, H_d), 7.03 (t, J = 2.2 Hz, 2H, H_e), 6.69 (d, J = 2.2 Hz, 8H, H_g), 6.48 (t, J = 2.2 Hz, 4H, H_h), 5.16 (s, 8H, H_f), 4.47 (s, 16H, H_i), 1.44 (s, 72H, H_j).

^{13}C NMR (151 MHz, $CDCl_3$) **δ** 167.75, 159.32, 157.85, 149.82, 149.60, 144.56, 139.50, 132.55, 131.85, 119.57, 115.24, 106.69, 106.29, 101.73, 101.66, 82.41, 70.05, 65.80, 28.03.

λ_{max} ($CHCl_3$)/nm (ε /M^{-1} cm^{-1}) 413 (457809), 541 (17098)

TBuED NH Porphyrin *48*[33]

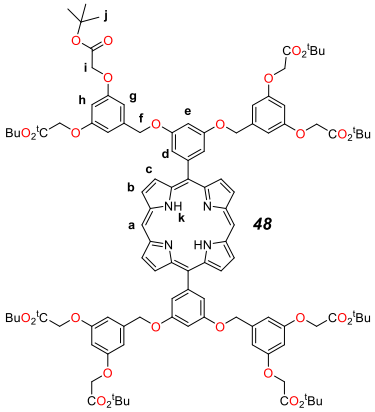

^{1}H NMR (600 MHz, $CDCl_3$) **δ**, 10.31 (s, 2H, H_a), 9.39 (d, J = 4.5 Hz, 4H, H_b), 9.11 (d, J = 4.5 Hz, 4H, H_c), 7.52 (d, J = 2.2 Hz, 4H, H_d), 7.05 (t, J = 2.2 Hz, 2H, H_e), 6.72 (d, J = 2.3 Hz, 8H, H_h), 6.52 (t, J = 2.3 Hz, 4H, H_e), 5.19 (s, 8H, H_f), 4.50 (s, 16H. H_i), 1.45 (s, 72H, H_j), -3.16 (s, 2H, H_k).

^{13}C NMR (151 MHz, $CDCl_3$) **δ** 167.76, 159.38, 158.12, 146.88, 145.30, 143.27, 139.49, 131.70, 131.07, 118.61, 115.39, 106.68, 105.32, 101.87, 101.71, 82.42, 70.08, 65.83, 28.04.

Meso Brominated TBuED Zn Porphyrin *31*[33]

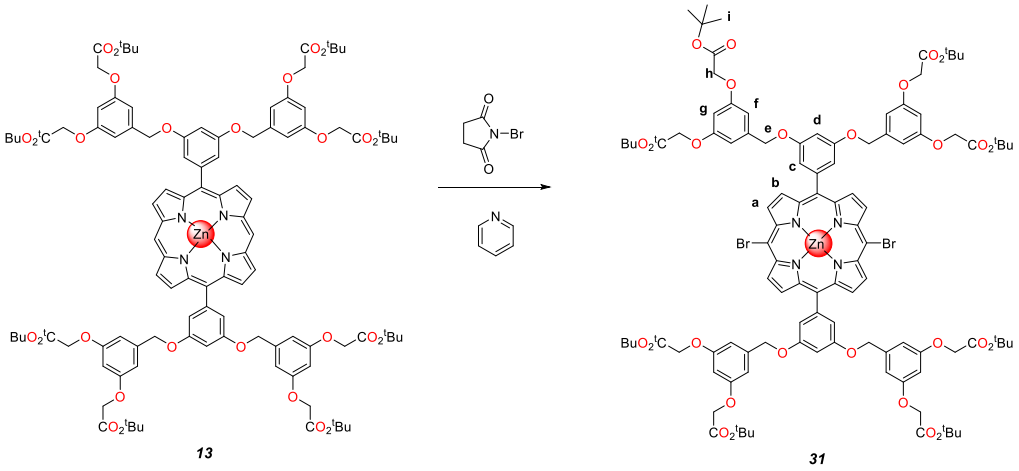

TBuED Zn porphyrin ***13*** (0.233 g, 117 µmol, 1 eqv) dissolved in chloroform (5.7 mL) with pyridine (0.140 g, 1.77 mmol, 142 µL). The solution was stirred absent of light at 0 °C. NBS (42.0 mg, 234 µmol, 2 eqv) dissolved in chloroform (5.7 mL) was added dropwise over 2 hours. The reaction mixture was then quenched with acetone and the solvent was then removed from the crude mixture under reduced pressure. Then purified by passing the mixture though a silica plug (20-30% ethyl acetate: pet ether) to give the green solid, *meso* brominated TBuED Zn porphyrin ***31*** (0.320 g, 117 µmol, 99%).

^{1}H NMR (600 MHz, $CDCl_3$) **δ** 9.64 (d, J = 4.6 Hz, 4H, H_a), 8.92 (d, J = 4.6 Hz, 4H, H_b), 7.39 (d, J = 2.2 Hz, 4H, H_c), 6.99 (t, J = 2.2 Hz, 2H, H_d), 6.69 (d, J = 2.3 Hz, 8H, H_f), 6.49 (t, J = 2.3 Hz, 4H, H_g), 5.15 (s, 8H, H_e), 4.49 (s, 16H, H_h), 1.45 (s, 72H, H_i).

^{13}C NMR (151 MHz, $CDCl_3$) **δ** 167.75, 159.33, 157.64, 150.44, 150.18, 144.52, 143.70, 139.44, 132.43, 131.17, 122.64, 115.34, 106.71, 101.57, 101.52, 82.43, 70.03, 65.81, 28.04.

Meso Alkynylated Protected TBuED Zn Porphyrin *32*[33]

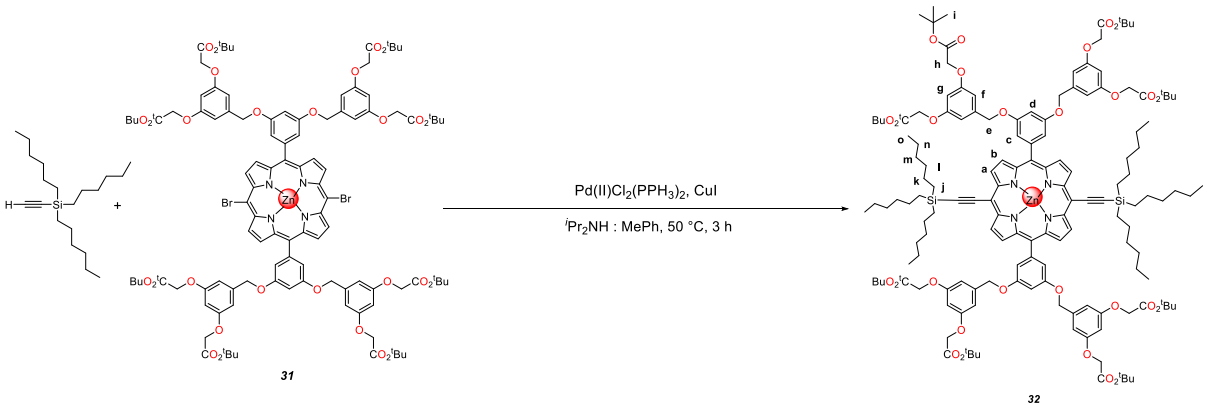

Meso brominated TBuED Zn porphyrin ***31*** (0.32 g, 0.15 mmol, 1 eqv), $Pd(PPh_3)_2Cl_2$ (21 mg, 30 µmol, 0.2 eqv) and CuI (2.8 mg, 15 µmol, 0.1 eqv) were dried under reduced pressure and then put under argon and dissolved in dry toluene (3.7 mL) and DIPA (3.7 mL) at room temperature. THS-acetylene (0.11 g, 0.37 mmol, 2.5 eqv) was added dropwise under argon and the reaction mixture was stirred for 3 hours at 50 °C. The mixture was then cooled to room temperature and purified through a silica plug (20:80 ethyl acetate:pet ether) and the solvent was removed under reduced pressure to give a green solid, *meso* alkynylated protected TBuED Zn porphyrin ***32*** (0.348 g, 134 µmol, 90%).

^{1}H NMR (600 MHz, $CDCl_3$) **δ** 9.65 (d, J = 4.5 Hz, 4H, H_a), 8.96 (d, J = 4.5 Hz, 4H, H_b), 7.43 (d, J = 2.3 Hz, 4H, H_c), 7.00 (t, J = 2.3 Hz, 2H, H_d), 6.71 (d, J = 2.3 Hz, 8H, H_f), 6.48 (t, J = 2.3 Hz, 4H, H_g), 5.14 (s, 8H. H_e), 4.49 (s, 16 H, H_h), 1.45 (s, 72H, H_i), 1.67 (m, 12H, H_n) 1.44 - 1.26 (m, 59 H, $H_{k, l, m, o}$), 1.04 (t, J = 6, 6 H, H_o), 0.91 (m, 29 H, $H_{k, l, m, o}$), 0.63 (t, 12H, H_j)

^{13}C NMR (151 MHz, $CDCl_3$) **δ** 167.76, 159.31, 157.83, 152.37, 149.78, 144.65, 143.14, 139.40, 132.43, 131.16, 121.80, 114.91, 109.08, 106.71, 101.65, 101.35, 99.76, 82.40, 70.08, 65.81, 33.44, 31.66, 28.03, 24.37, 22.70, 14.20, 13.89.

Meso Alkynylated Mono Protected TBuED Zn Porphyrin *34*[33]

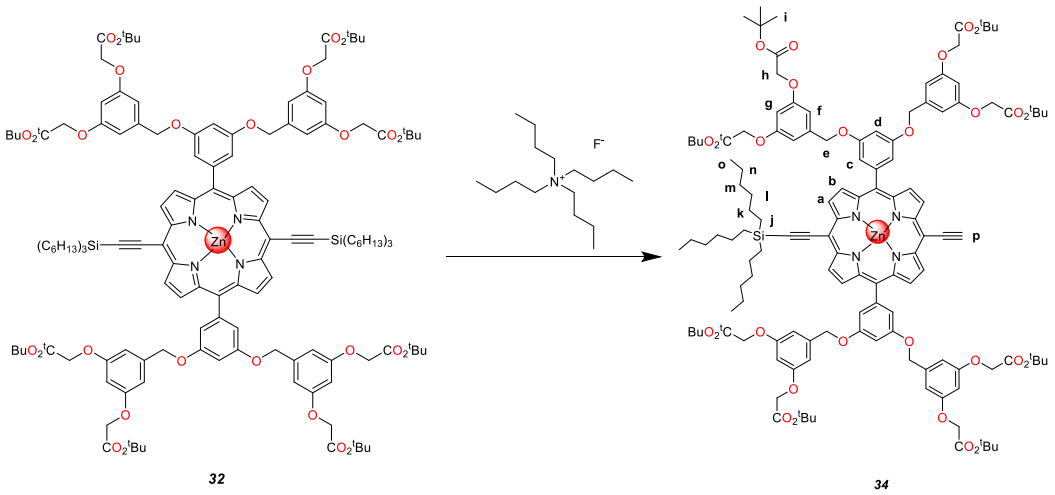

Meso alkynylated protected TBuED Zn porphyrin ***32*** (0.348 g, 134 µmol, 1 eqv) dissolved in chloroform (2.23 mL) and DCM (4.46 mL). TBAF in THF (1.0 M, 107 µL, 0.8 eqv) solution was added and the mixture stirred for 1 hour at room temperature. Another 0.1 eq of TBAF solution was added every 15 mins for 60 mins. Material separated by silica column chromatography (10-20-30-40% ethyl acetate: pet ether). Each green band collected and solvent removed under reduced pressure. The 2nd and 3rd most mobile band is *meso* alkynylated mono protected TBuED Zn porphyrin ***34*** (63.8 mg, 27.5 µmol, 21%) and *meso* alkynylated TBuED Zn porphyrin ***33*** (40.3 mg, 19.8 µmol, 15%) respectively.

^{1}H NMR (600 MHz, $CDCl_3$) **δ** 9.71 (dd, *J* = 16.2, 4.6 Hz, 4H, H_a), 8.97 (dd, *J* = 35.7, 4.5 Hz, 4H, H_b), 7.44 (d, *J* = 2.3 Hz, 4H, H_c), 7.01 (t, *J* = 2.3 Hz, 2H, H_d), 6.68 (d, *J* = 2.3 Hz, 8H, H_f), 6.46 (t, *J* = 2.3 Hz, 4H, H_g), 5.14 (s, 8H, H_e), 4.45 (s, 16H, H_h), 4.21 (s, 1H, H_p), 1.77 (m, 6H, H_a), 1.55 (m, 6H, H_n), 1.43 (s, 72H, H_i), 1.42-1.32 (m, 26 $H_{k, l, m, n, o}$), 1.06 – 1.00 (m, 8H, $H_{k, l, m, n, o}$), 0.90 (t, *J* = 7.1 Hz, 12H, H_j).

^{13}C NMR (151 MHz, $CDCl_3$) **δ** 167.76, 159.27, 158.1, 152.44, 152.40, 149.96, 149.93, 144.10, 139.38, 132.94, 132.75, 131.51, 131.26, 122.00, 114.93, 108.34, 106.70, 102.04, 101.94, 101.74, 101.66, 99.97, 85.91, 82.45, 70.09, 65.78, 33.33, 31.63, 28.07, 24.35, 22.68, 14.20, 13.82.

Meso Alkynylated TBuED Zn Porphyrin *33*[33]

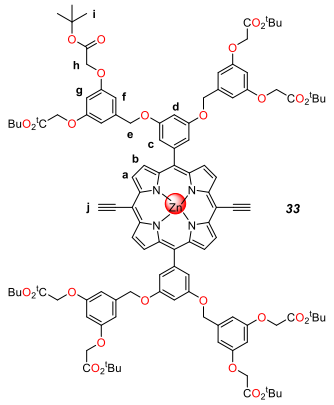

^{1}H NMR (600 MHz, $CDCl_3$) **δ** 9.70 (d, *J* = 4.5 Hz, 4H, H_a), 8.98 (d, *J* = 4.5 Hz, 4H, H_b), 7.43 (d, *J* = 2.2 Hz, 4H, H_c), 7.00 (t, *J* = 2.2, 2H, H_d), 6.67 (d, *J* = 2.3 Hz, 4H, H_f), 6.47 (t, *J* = 2.3 Hz, 8H, H_g), 5.15 (s, 8H, H_e), 4.46 (s, 16H, H_h), 4.18 (s, 2H, H_j), 1.43 (s, 72H, H_i).

^{13}C NMR (151 MHz, $CDCl_3$) **δ** 167.76, 159.28, 157.82, 152.40, 150.06, 144.03, 139.40, 132.98, 131.37, 122.07, 115.07, 107.71, 106.68, 101.64, 100.11, 85.85, 84.26, 82.40, 70.07, 65.79, 28.04.

Alkynylated Protected TBuED Zn Porphyrin Dimer *35*[33]

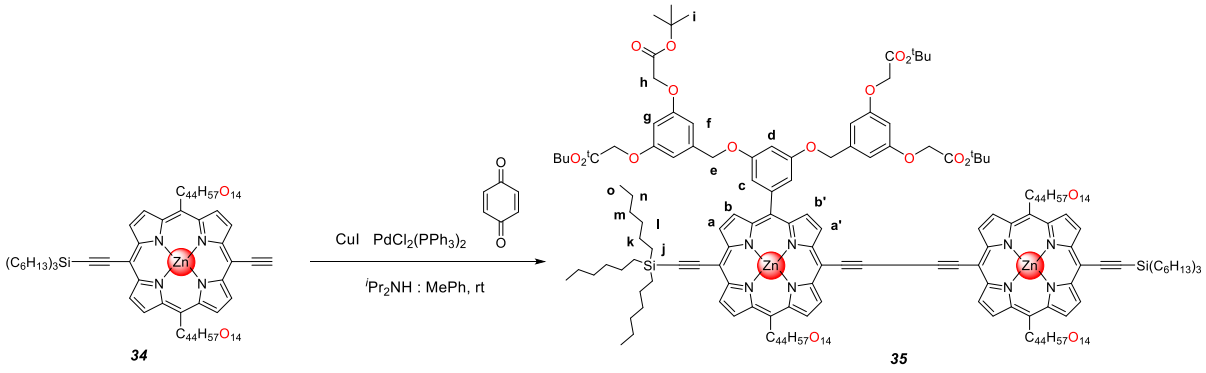

Meso alkynylated mono protected TBuED Zn porphyrin ***34*** (63.8 mg, 27.5 µmol, 1 eqv) was dissolved in toluene (2.75 mL) under an argon atmosphere. A solution of CuI (2.6 mg, 14 µmol, 0.5 eqv), $PdCl_2(PPh_3)_2$ (1.0 mg, 1.4 µmol, 0.05 eqv) and benzoquinone (5.9 mg, 55 µmol, 2 eqv) in dry toluene (2.75 mL) and DIPA (1.37 mL) was added to the reaction mixture. The mixture was stirred at room temperature for 1 hour and then purified by silica plug (petroleum ether: ethyl acetate 100-

70:0-30) collecting the green band. The solvent was then removed by reduced pressure producing green solid alkynylated protected TBuED Zn Porphyrin dimer ***35*** (54.2 mg, 11.7 µmol, 85% yield).

^{1}H NMR (600 MHz, $CDCl_3$) **δ** 9.96 (d, J = 4.6 Hz, 4H, $H_{a'}$), 9.72 (d, J = 4.6 Hz, 4H, H_a), 9.10 (d, J = 4.6 Hz, 4H, $H_{b'}$), 9.01 (d, J = 4.6 Hz, 4H, H_b), 7.49 (d, J = 2.2 Hz, 8H, H_c), 7.04 (t, J = 2.2 Hz, 4H, H_d), 6.70 (d, J = 2.3 Hz, 16H, H_g), 6.47 (t, J = 2.3 Hz, 8H, H_f), 5.17 (s, 16H, H_e), 4.48 (s, 32H, H_h), 1.83 – 1.74 (m, 13H, $H_{k, l, m, n, o}$), 1.56 (m, 14H, $H_{k, l, m, n, o}$), 1.42 (s, 159H, $H_{i, k, l, m, n, o}$), 1.08 – 1.02 (m, 13H, $H_{k, l, m, n, o}$), 0.91 (t, J = 7.0 Hz, 12H, H_j).

^{13}C NMR (151 MHz, $CDCl_3$) **δ** 167.76, 159.28, 157.95, 153.22, 152.48, 150.20, 149.74, 144.05, 139.33, 133.28, 132.85, 131.60, 131.17, 122.62, 114.91, 106.70, 102.64, 101.73, 101.67, 101.06, 100.00, 82.51, 82.41, 70.13, 65.80, 33.34, 31.64, 28.06, 28.03, 24.36, 22.70, 22.58, 14.21, 13.81.

Alkynylated TBuED Zn Porphyrin Dimer *36*[33]

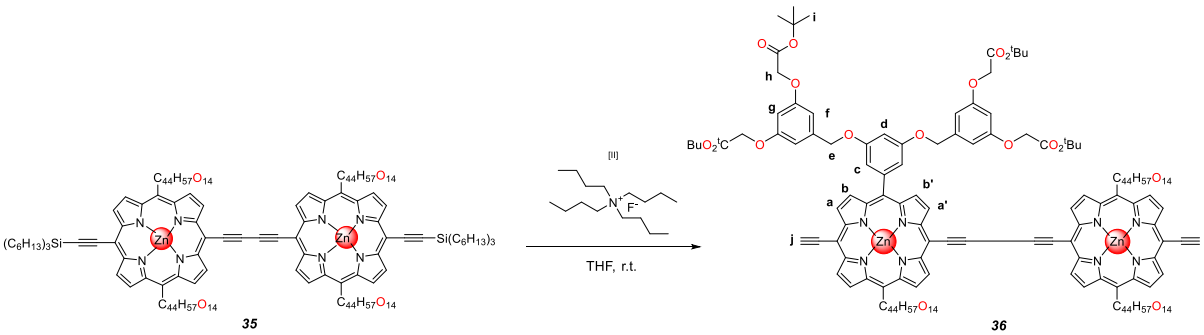

Alkynylated protected TBuED Zn Porphyrin dimer ***35*** (54.2 mg, 11.7 µmol, 1 eqv) dissolved in THF (1.72 mL). TBAF in THF (1.0 M, 29.2 µL, 2.5 eqv) solution was added and the mixture was stirred for 1 hour at room temperature. The solution was then passed through a silica plug (0-50 % ethyl acetate: petroleum ether) and the green band collected with solvent removed under reduced pressure. The resulting green solid alkynylated TBuED Zn porphyrin dimer ***36*** (45.3 mg, 11.1 µmol, 95%) was then collected.

^{1}H NMR (600 MHz, $CDCl_3$) **δ** 9.88 (d, J = 4.5 Hz, 4H, $H_{a'}$), 9.63 (d, J = 4.5 Hz, 4H, H_a), 9.03 (d, J = 4.5 Hz, 4H, $H_{b'}$), 8.89 (d, J = 4.5 Hz, 4H, H_b), 7.45 (d, J = 2.3 Hz, 8H, H_c), 7.00 (t, J = 2.3 Hz,

4H, H_d), 6.70 (d, J = 2.3 Hz, 16H, H_f), 6.47 (t, J = 2.3 Hz, 8H, H_g), 5.16 (s, 16H, H_e), 4.49 (s, 32H, H_h), 4.17 (s, 2H, H_j), 1.42 (s, 144H, H_i).

^{13}C NMR (151 MHz, $CDCl_3$) **δ** 166.73, 158.31, 156.72, 152.11, 151.36, 149.15, 148.67, 143.37, 138.40, 131.91, 131.68, 130.03, 129.90, 121.33, 114.22, 105.63, 100.64, 100.42, 98.94, 98.57, 87.13, 85.64, 82.39, 81.39, 81.23, 69.04, 27.02

TBuED Zn *c*-P6•T6 *37* (Monomer Variant)[33]

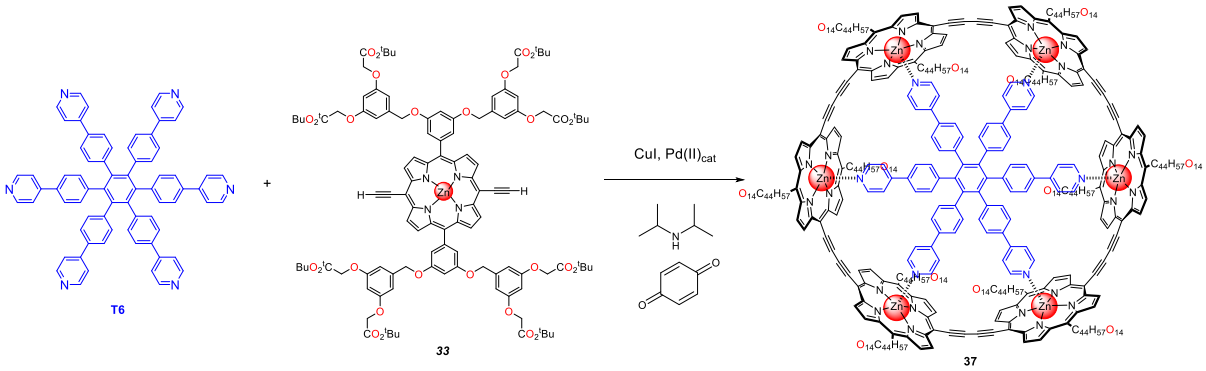

Meso alkynylated TBuED Zn porphyrin ***33*** (40.3 mg, 19.8 µmol, 5.7 eqv) and **T6** (3.5 mg, 3.5 µmol, 1 eqv) were dissolved in chloroform (165 mL) and the mixture sonicated for 30 mins. $PdCl_2(PPh_3)_2$ (1.7 mg, 2.4 µmol, 0.7 eqv), CuI (4.0 mg, 21 µmol, 6 eqv) and benzoquinone (3.8 mg, 35 µmol, 10 eqv) were dissolved in chloroform (10 mL) and DIPA (132 µL) and added slowly to the mixture. The mixture was then stirred at room temperature over 16 hours then the solvent was removed under reduced pressure. The crude was then pre-purified by silica plug (chloroform: methanol 90:10) and the dark band was collected. The solvent was then reduced under pressure and the resulting crude passed through a SEC (toluene: pyridine 1%). The solvent was then removed under pressure and the crude purified on preparative GPC (toluene: pyridine 1%) to give an amber solid TBuED Zn *c*-P6•T6 ***37*** (2.0 mg, 0.15 µmol, 4%).

TBuED Zn *c*-P6•T6 *37* (Dimer Variant)[33]

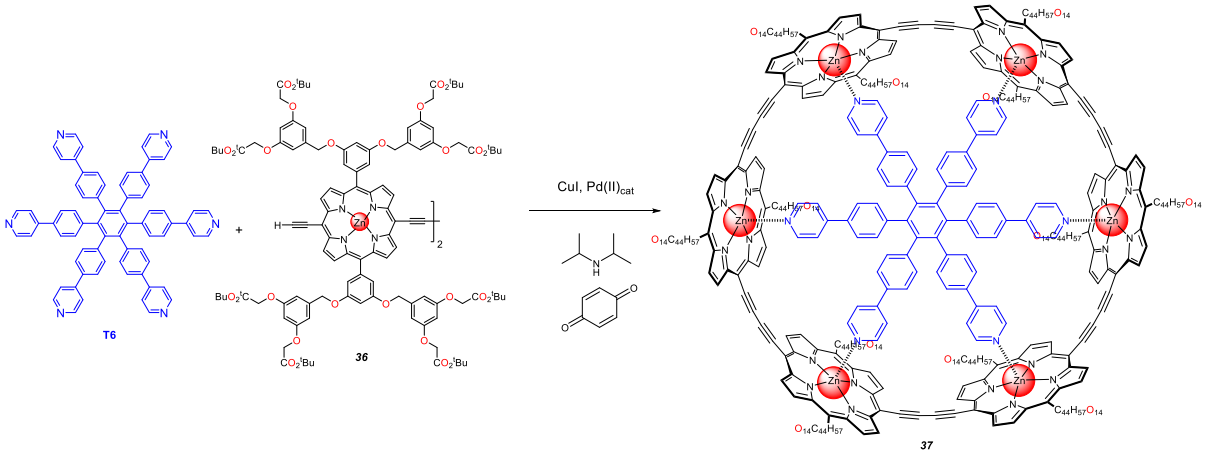

TBuED Zn porphyrin dimer ***36*** (45.3 mg, 11.1 µmol, 3 eqv) and **T6** (3.7 mg, 3.7 µmol, 1 eqv) were dissolved in chloroform (92.6 mL) and the mixture sonicated for 30 mins. A solution of $PdCl_2(PPh_3)_2$ (1.8 mg, 2.6 µmol, 0.7 eqv), CuI (4.2 mg, 22 µmol, 6 eqv) and benzoquinone (4.0 mg, 37 µmol, 10 eqv) was created in chloroform (10 mL) and diisopropylamine (141 µL) and added slowly to the mixture. The mixture was then stirred at room temperature over 16 hours then the solvent was removed by reduced pressure. The crude was then purified *via* silica plug (chloroform: methanol 90:10) and the dark band was collected. The solvent was then reduced under pressure and the resulting crude purified by passing through a SEC (toluene: pyridine 1%, SX1 bio-beads). The solvent was then removed under pressure and the crude run on preparative GPC (toluene: pyridine 1%) to give an amber solid TBuED Zn *c*-P6•T6 ***37*** (9.8 mg, 0.74 µmol, 20%).

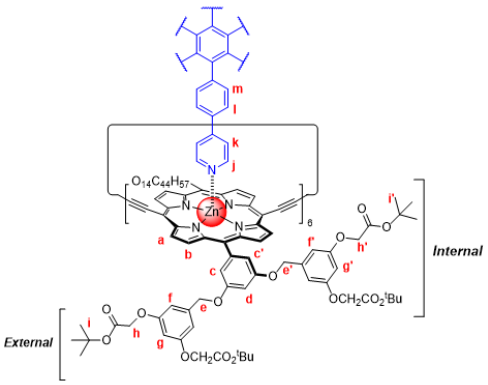

^{1}H NMR (600 MHz, $CDCl_3$) **δ** 9.53 (d, J = 4.3 Hz, 24H, H_a), 8.81 (d, J = 4.3 Hz, 24H, H_b), 7.52 (s, 12H, $H_{c'}$), 7.13 (s, 12H, H_c), 6.94 (s, 12H, H_k), 6.68 (d, J = 2.3 Hz, 24H, $H_{f'}$), 6.65 (d, J = 2.3 Hz, 24H, H_f), 6.46 (t, J = 2.3 Hz, 12H, $H_{g'}$), 6.40 (t, J = 2.3 Hz, 12H, H_g), 5.53 (d, J = 9.0, 12H, H_l), 5.49 (d, J = 9.0, 12H, H_m), 5.22 (s, 24H, $H_{e'}$), 5.04 (d, J = 7.2 Hz, 41H, $H_{e,k}$), 4.48 (s, 48H, H_h), 4.47 (s, 48H, $H_{h'}$), 2.28 (m, 12H, H_j), 1.44 (s, 266H, H_i), 1.34 (s, 210H, H_i).

^{13}C NMR (151 MHz, $CDCl_3$) **δ** 166.70, 158.30, 158.25, 156.87, 156.78, 151.7, 148.35, 146.52, 144.09, 141.78, 140.40, 139.73, 139.23, 138.58, 131.86, 131.25, 130.41, 130.02, 123.82, 123.36, 118.14, 115.84, 114.03, 105.66, 105.26, 100.66, 100.63, 100.48, 100.21, 95.21, 88.33, 81.37, 81.24, 64.77, 64.73, 27.02, 26.94.

λ_{max} ($CHCl_3$)/nm (ε /M^{-1} cm^{-1}) 483 (257799), 763 (165656), 799 (215494), 840 (184774),

CAD NH Porphyrin *16*[33]

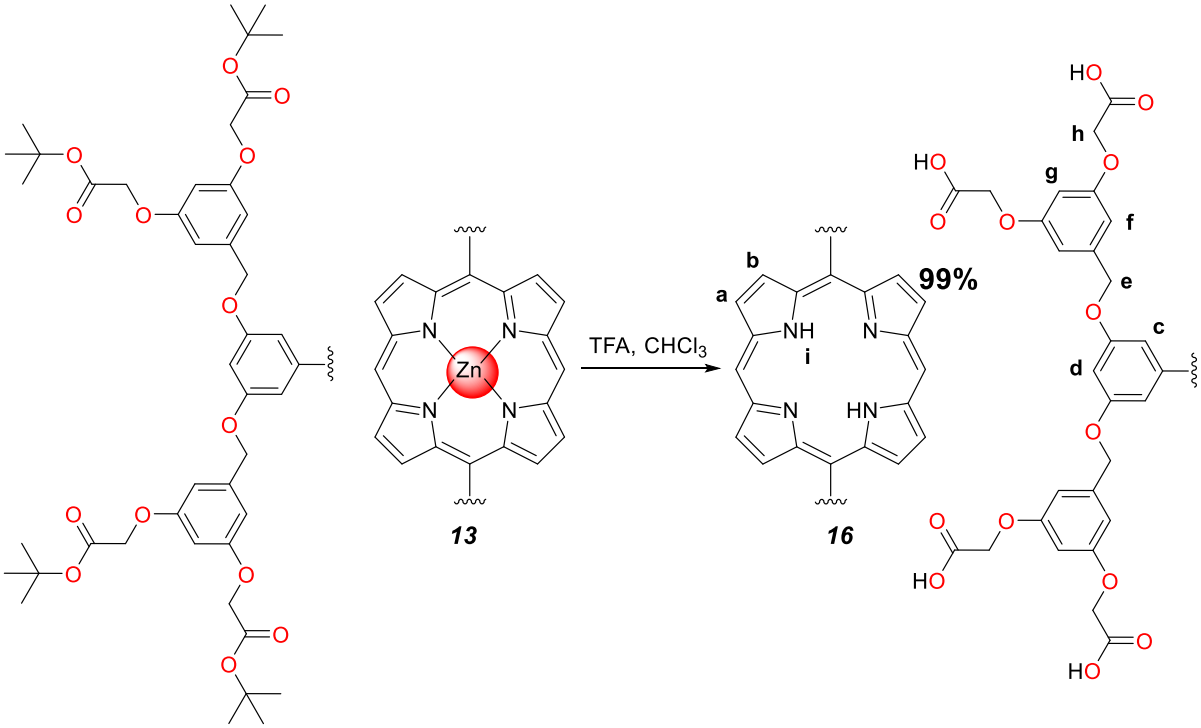

TBuED Zn Porphyrin ***13*** (12.4 mg, 3.11 µmol, 1 eqv) was dissolved in DCM (1 mL) and TFA (1 mL). The mixture was stirred for 2 hours at room temperature. Cold diethyl ether (0 °C) was then added to the reaction mixture to precipitate out and centrifuged (15 minutes at 40,000 RPM) to collect the product red solid CAD NH porphyrin ***16*** (9.1 mg, 3.1 µmol, 99%).

^{1}H NMR (600 MHz, DMSO) **δ** 10.61 (s, 2H, H_i), 9.62 (d, J = 4.5 Hz, 4H, H_a), 9.07 (d, J = 4.5 Hz, 4H, H_b), 7.55 (d, J = 2.2 Hz, 4H, H_c), 7.21 (t, J = 2.2 Hz, 2H, H_d), 6.75 (d, J = 2.3 Hz, 8H, H_g), 6.52 (t, J = 2.3 Hz, 4H, H_f), 5.28 (s, 8H, H_e), 4.69 (s, 16H, H_h), -3.29 (s, 2H, H_j).

^{13}C NMR (151 MHz, DMSO) **δ** 170.51, 159.50, 158.36, 146.66, 145.28, 142.81, 139.98, 133.24, 131.32, 118.84, 115.51, 107.12, 106.17, 102.53, 101.23, 69.81, 65.39.

CAD NH *c*-P6 *47*[33]

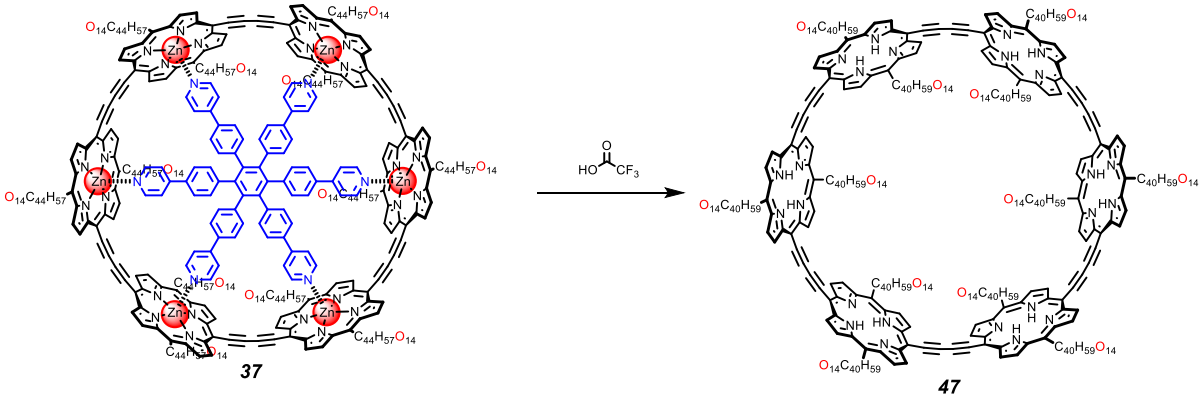

TBuED Zn *c*-P6 T6 ***37*** (10.2 mg, 0.771 µmol, 1 eqv) was dissolved in DCM (2 mL) and TFA (2.0 mL) and the resulting mixture was stirred at room temperature for an hour. The resulting mixture was then precipitated out by adding cold diethyl ether (0 °C) and the resulting precipitate was centrifuged for 15 minutes at 40,000 RPM. The precipitate was then washed with chloroform. The dark red precipitate CAD NH *c*-P6 ***47*** (6.7 mg, 0.63 µmol, 82%) was collected and dried.

^{1}H NMR (600 MHz, DMSO) **δ** 9.51 (s, 24H, H_a), 8.59 (s, 24H, H_b), 7.36 (s, 24H, H_c), 7.04 (s, 12H, H_d), 6.56 (s, 48H, H_f), 6.44 (s, 24H, H_g), 5.14 (s, 48H, H_e), 4.59 (s, 96H, H_h), -2.03 (s, 12H, H_i)

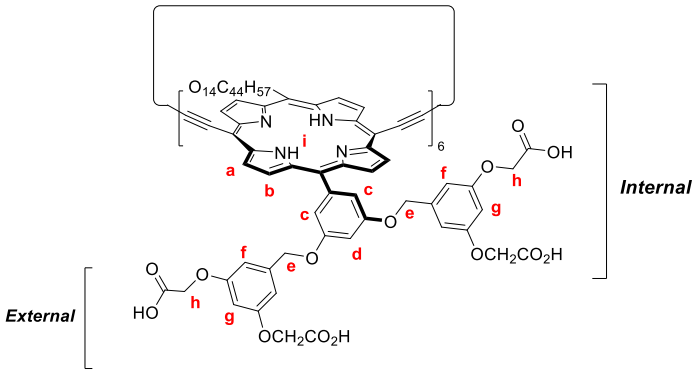

Bromo Acetyl Acylated Amino-Sorbitol *43*

Penta-acylated ammonium-sorbitol chloride ***42*** was prepared using a published procedure.[50]

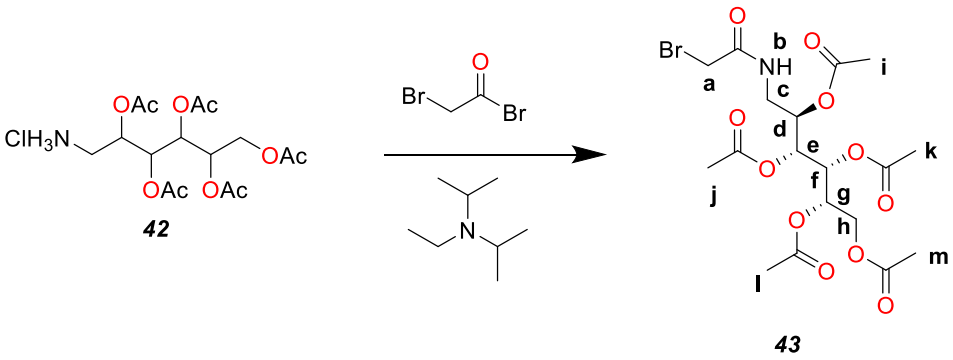

Penta-acetylated ammonium-sorbitol chloride ***42*** (800 mg, 1.87 mmol, 1 eqv) was dissolved in DCM (50 mL) under an argon atmosphere. The mixture was cooled to 0 °C and DIPEA (295 mg, 2.06 mmol, 1.1 eqv) was added dropwise. 2-bromo acetyl bromide (453 mg, 196 µL, 2.24 mmol, 1.2 eqv) was added in DCM (5 mL) dropwise. The mixture was stirred for 30 minutes at 0 °C and for a further 90 minutes at room temperature. The solvent was removed under reduced pressure, then redissolved in ethyl acetate (10 mL) and filtered. The filtrate was then purified *via* a silica plug (1:1 ethyl acetate: petroleum ether, followed by 1:1 acetone: DCM) collecting the orange fraction. The solvent was then removed under reduced pressure collecting the pale orange oil bromo acetyl acylated amino-sorbitol ***43*** (942 mg, 1.84 mmol, 98%).

^{1}H NMR (600 MHz, $CDCl_3$) **δ** 6.87 (t, J = 6.0 Hz, 1H, H_b), 5.48 (dd, J = 6.9, 4.3 Hz, 1H, H_f), 5.41 – 5.28 (m, 1H, H_e), 5.17 (td, J = 6.6, 4.5 Hz, 1H, H_d), 5.05 (td, J = 6.0, 3.2 Hz, 1H, H_g), 4.29 (dd, J = 12.4, 3.3 Hz, 1H, H_h), 4.14 (dd, J = 12.5, 5.4 Hz, 1H, H_h), 3.90 (s, 2H, H_a), 3.58 (dt, J = 13.7, 6.7 Hz, 1H, H_c), 3.49 (dt, J = 14.3, 5.0 Hz, 1H, H_c), 2.16 (s, 3H, H_i), 2.13 (s, 3H, H_j), 2.11 (s, 3H, H_k), 2.10 (s, 3H, H_l), 2.07 (s, 3H, H_m).

^{13}C NMR (151 MHz, $CDCl_3$) **δ** 170.77, 170.45, 170.26, 169.95, 169.92, 166.38, 69.94, 68.93, 68.83, 68.77, 68.74, 61.50, 40.31, 28.76, 20.77, 20.72, 20.69, 20.54

MS: m/z EI 512.007 ($C_{18}H_{27}BrNO_{11}$+ requires 512.06892)

SPE Aldehyde *22*

Phenyl 4-chlorobutane-1-sulfonate ***21*** was prepared using established procedure.[51, 52]

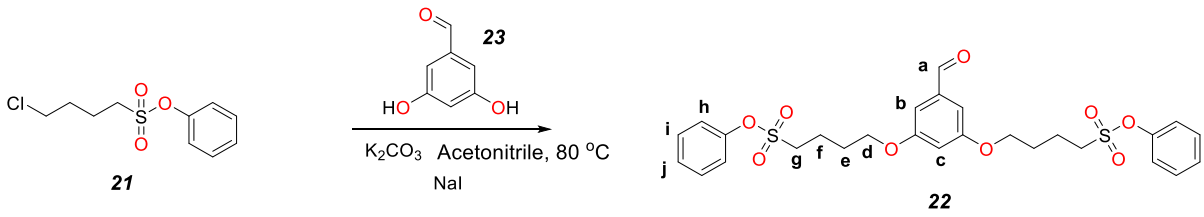

In a dry Schlenk tube under argon, 3,5-dihydroxybenzaldehyde ***23*** (495 mg, 3.59 mmol, 1 eqv), K_2CO_3 (4.95 g, 35.9 mmol, 10 eqv) and NaI (2.15 g, 14.3 mmol, 4 eqv) were dissolved in acetonitrile (86.0 mL). Phenyl 4-chlorobutane-1-sulfonate ***21*** (2.14 g, 8.60 mmol, 2.4 eqv) was added and the resulting mixture refluxed under argon at 82 °C for 48 hours. The solvent was then removed under reduced pressure and the residue was extracted by water (50 mL) and ethyl acetate (50 mL). The mixture was then washed with ethyl acetate (40 mL) three times. The combined organic layer was dried over Na_2SO_4 and concentrated under reduced pressure. The crude mixture was then purified *via* silica gel column chromatography (1:4 ethyl acetate: petroleum ether increasing to 2:3 ethyl acetate: petroleum ether) collecting the 2nd most mobile fraction. The solvent was then removed under reduced pressure to give a yellow oil SPE aldehyde ***22*** (871 mg, 1.55 mmol, 43%).

^{1}H NMR (600 MHz, $CDCl_3$) **δ** 9.90 (s, 1H, H_a), 7.43 – 7.37 (m, 4H, H_h), 7.34 – 7.26 (m, 6H, $H_{i,j}$), 7.01 (d, J = 2.3 Hz, 2H, H_d), 6.69 (t, J = 2.3 Hz, 1H, H_c), 4.06 (t, J = 5.9 Hz, 4H, H_d), 3.39 – 3.32 (m, 4H, H_g), 2.21 (tt, J = 7.7, 6.6 Hz, 4H, H_e), 2.01 (m, 4H, H_g).

^{13}C NMR (151 MHz, $CDCl_3$) **δ** 191.85, 160.33, 149.13, 138.46, 130.04, 127.32, 122.02, 107.98, 107.82, 67.29, 50.02, 27.52, 20.74.

MS: m/z EI 586.279 ($C_{27}H_{30}O_9S_2Na$+ requires 585.123)

SPE Zn Porphyrin *15*

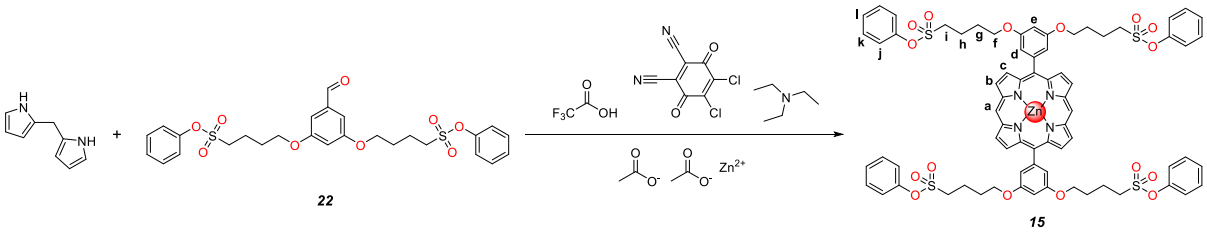

SPE aldehyde ***22*** (1.86 g, 3.31 mmol, 2 eqv) and 2,2' dipyrromethane (0.483 g, 3.31 mmol, 2 eqv) dissolved in degassed (with argon) dichloromethane (918 mL). TFA (773 mg, 6.78 mmol, 519 µL, 4.1 eqv) was added dropwise and the mixture stirred for 3 hours in the dark. DDQ (1.13 g, 4.96 mmol, 3 eqv) was added and the mixture stirred for 20 minutes. Triethylamine (1.34 g, 13.2 mmol, 1.84 mL, 8 eqv) was then added and the solvent reduced under pressure. The crude mixture was then passed through a silica plug (40:60 ethyl acetate: petroleum ether eluent) with all long wavelength UV active (red) bands collected and the solvent reduced under pressure. The product, SPE NH porphyrin ***49***, was dissolved in chloroform (20 mL) and then zinc(II) acetate (970 mg, 5.29 mmol, 3.2 eqv) in methanol (10 mL) was added. The purple solution was stirred for 1 hour at room temperature resulting in a pink solution. The solvent was removed by reduced pressure and the crude product run through a silica plug (40:60 ethyl acetate: petroleum ether) to give a red solid SPE Zn porphyrin ***15*** (1.03 g, 716 µmol, 43%).

^{1}H NMR (600 MHz, $CDCl_3$) **δ** 10.28 (s, 2H, H_a), 9.42 (d, J = 4.3 Hz, 4H, H_b), 9.23 (d, J = 4.3 Hz, 4H, H_c), 7.41 (m, 4H, H_d), 7.33 – 7.28 (m, 8H, H_j), 7.22 (m, 8H, H_k), 7.17 (t, J = 7.3 Hz, 4H, H_k), 6.80 (d, J = 2.5 Hz, 2H, H_e), 4.14 (t, J = 5.8 Hz, 8H, H_f), 3.33 (t, J = 7.8 Hz, 8H, H_i), 2.23 (m, 8H, H_h), 2.02 (m, 8H, H_g).

^{13}C NMR (151 MHz, $CDCl_3$) **δ** 157.82, 149.77, 149.55, 149.08, 144.69, 132.46, 131.87, 129.93, 127.18, 121.97, 119.51, 114.64, 106.29, 100.95, 67.21, 50.05, 27.70, 20.83.

λ_{max} ($CHCl_3$)/nm (ε /M^{-1} cm^{-1}) 409 (180902), 536 (66996)

MS: m/z MALDI-TOF 1436.397 ($C_{72}H_{68}N_4O_{16}S_4Zn$ requires 1436.280)

SPE NH Porphyrin *49*

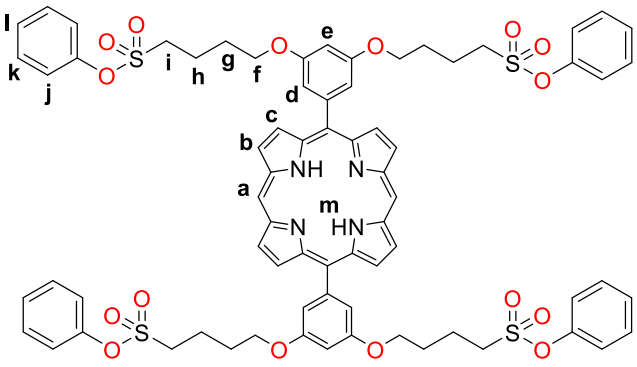

49

^{1}H NMR (600 MHz, $CDCl_3$) **δ** 10.31 (s, 2H, H_a), 9.44 (d, J = 4.4 Hz, 4H, H_b), 9.28 (d, J = 4.4 Hz, 4H, H_c), 7.43 (m, 4H, H_d), 7.35 – 7.29 (m, 8H, H_j), 7.23 (m, 8H, H_k), 7.22 (t, J = 7.2 Hz, 4H, H_k), 6.86 (d, J = 2.6 Hz, 2H, H_e), 4.27 (t, J = 5.7 Hz, 8H, H_f), 3.41 (t, J = 7.7 Hz, 8H, H_i), 2.29 (m, 8H, H_h), 2.11 (m, 8H, H_g), -3.76 (s, 2H, H_m).

^{13}C NMR (151 MHz, $CDCl_3$) **δ** 158.01, 149.83, 149.95, 149.25, 144.87, 132.64, 131.95, 130.22, 127.21, 122.04, 120.17, 114.90, 106.31, 101.02, 67.33, 50.21, 27.87, 20.89.

***Meso* Brominated SPE Zn Porphyrin 24**

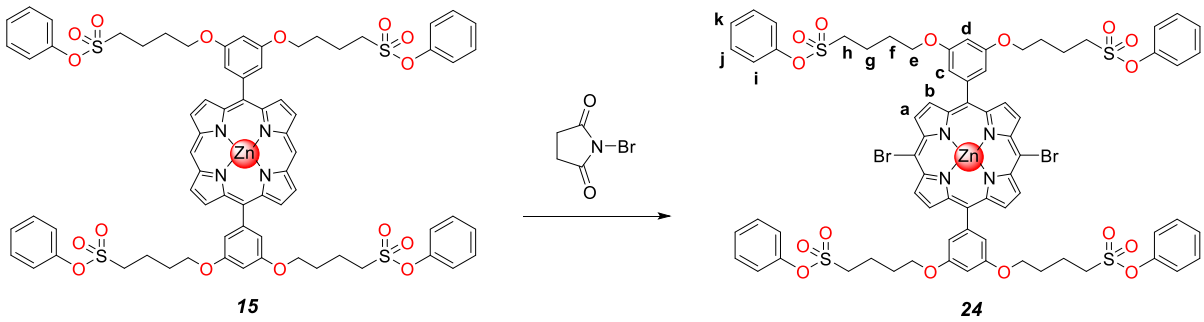

15 ***24***

SPE Zn porphyrin ***15*** (0.957 g, 666 µmol, 1 eqv) dissolved in chloroform (5.7 mL). The solution was stirred absent of light at 0 °C. NBS (0.237 g, 1.33 mmol, 2 eqv) dissolved in chloroform (33 mL) was added dropwise over 2 hours. The reaction mixture was then quenched with acetone and the solvent was then removed from the crude mixture under reduced pressure. Then purified by

passing the mixture though a silica plug (20-30% ethyl acetate: pet ether) to give the green solid, *meso* brominated SPE Zn porphyrin ***24*** (1.05 g, 658 µmol, 99%).

^{1}H NMR (600 MHz, $CDCl_3$) **δ** 9.73 (d, J = 4.7 Hz, 4H, H_a), 9.04 (d, J = 4.8 Hz, 4H, H_b), 7.37 – 7.31 (m, 12H, $H_{c,\,i}$), 7.26 (d, J = 7.9 Hz, 8H, H_j), 7.22 (t, J = 7.4 Hz, 4H, H_k), 6.85 (d, J = 2.3 Hz, 2H, H_d), 4.19 (t, J = 5.9 Hz, 8H, H_e), 3.39 (dd, J = 8.8, 6.8 Hz, 8H, H_h), 2.34 – 2.24 (m, 8H, H_f), 2.11 – 2.04 (m, 8H, H_g).

^{13}C NMR (151 MHz, $CDCl_3$) **δ** 157.84, 150.58, 150.32, 149.08, 144.08, 133.53, 133.38, 129.96, 127.22, 121.99, 121.74, 114.49, 105.33, 101.08, 67.24, 50.12, 27.74, 20.87.

Meso Alkynylated Protected SPE Zn Porphyrin *25*

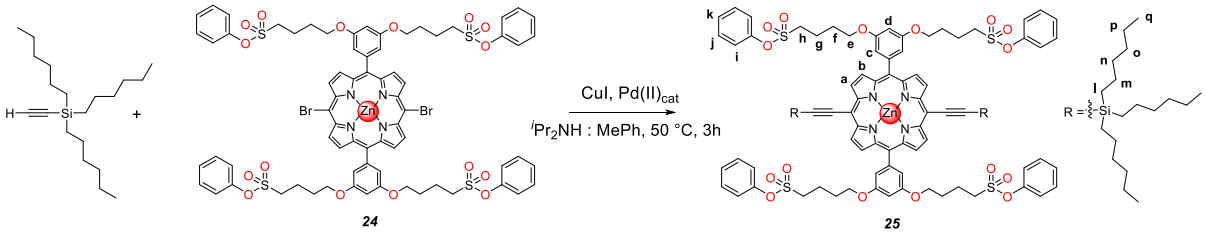

Meso brominated SPE Zn porphyrin ***24*** (0.975 g, 610 µmol, 1 eqv), $Pd(PPh_3)_2Cl_2$ (85.7 mg, 122 µmol, 0.2 eqv) and CuI (11.6 mg, 61.0 µmol, 0.1 eqv) were dried under reduced pressure and then put under argon and dissolved in dry toluene (15.3 mL) and DIPA (15.3 mL) at room temperature. THS-acetylene (0.471 g, 1.53 mmol, 2.5 eqv) was added dropwise under argon and the reaction was stirred for 3 hours at 50 °C. The mixture was then cooled to room temperature and purified through a silica plug (2:3 ethyl acetate: pet ether) and the solvent was removed under reduced pressure to give a green solid, *meso* alkynylated protected SPE Zn porphyrin ***25*** (0.502 g, 245 µmol, 40%).

^{1}H NMR (600 MHz, $CDCl_3$) **δ** 9.73 (d, J = 4.6 Hz, 4H, H_a), 9.01 (d, J = 4.5 Hz, 4H, H_b), 7.40 – 7.31 (m, 12H, $H_{c,\,i}$), 7.29 – 7.27 (m, 8H, H_j), 7.27 – 7.19 (m, 4H, H_k), 6.89 (t, J = 2.3 Hz, 2H, H_d), 4.23 (t, J = 5.8 Hz, 8H, H_e), 3.47 – 3.34 (m, 8H, H_h), 2.35 – 2.25 (m, 8H, H_g), 2.15 – 2.07 (m, 2H,

H_f), 1.82 (ddt, J = 11.7, 8.0, 6.2 Hz, 12H, H_m), 1.67 – 1.55 (m, 12H, H_n), 1.49 – 1.39 (m, 24H, $H_{o,p}$), 1.14 – 1.04 (m, 12H, H_l), 1.02 – 0.93 (m, 18H, H_q).

^{13}C NMR (151 MHz, $CDCl_3$) **δ** 157.88, 152.45, 149.84, 149.13, 144.49, 132.53, 129.97, 127.23, 122.01, 121.96, 114.37, 108.65, 101.67, 100.92, 67.25, 50.12, 33.38, 31.69, 27.80, 24.32, 23.78, 22.73, 22.68, 20.90, 14.24, 13.87.

Meso Alkynylated SPE Zn Porphyrin *26*

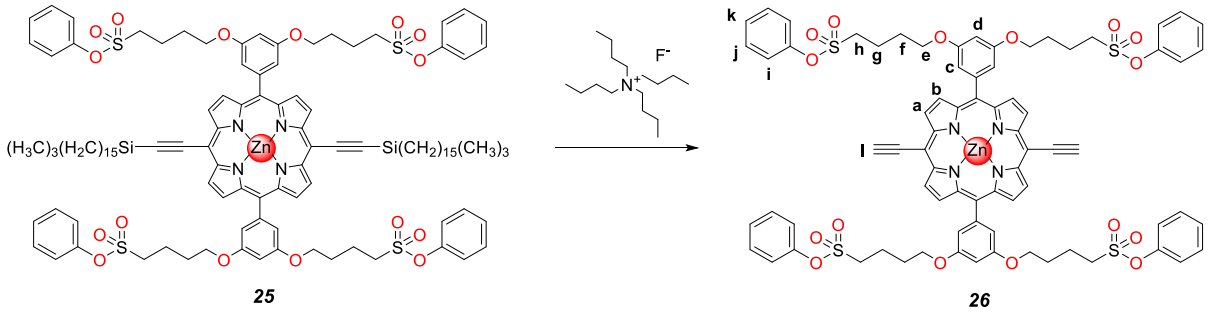

Meso alkynylated protected SPE Zn porphyrin ***25*** (0.502 g, 247 µmol, 1 eqv) dissolved in chloroform (4.12 mL) and DCM (8.24 mL). TBAF in THF (1.0 M, 198 µL, 0.8 eqv) solution was added and the mixture stirred for 1 hour at room temperature. Another 0.1 eqv (24.8 µL) of TBAF solution was added every 15 mins until TLC (petroleum ether: ethyl acetate, 1:1) resulted in 2nd most mobile spot being the most intense (90 minutes in total). Material separated by silica column chromatography (40-50-60% ethyl acetate: pet ether). Each green band collected and solvent removed under reduced pressure. The 3rd most mobile band is *meso* alkynylated SPE Zn porphyrin ***26*** (120 mg, 80.7 µmol, 33%), which was collected and solvent removed by reduced pressure.

^{1}H NMR (600 MHz, $CDCl_3$) **δ** 9.69 (d, J = 4.5 Hz, 4H, H_a), 9.00 (d, J = 4.6 Hz, 4H, H_a), 7.31 (ddt, J = 9.8, 4.8, 2.8 Hz, 12H, $H_{c,i}$), 7.24 (dd, J = 7.8, 1.6 Hz, 8H, H_j), 7.19 (m, 4H, H_k), 6.83 (t, J = 2.3 Hz, 2H, H_d), 4.17 (t, J = 5.9 Hz, 8H, H_e), 4.15 (s, 2H, H_l), 3.40 – 3.34 (m, 8H, H_h), 2.26 (dq, J = 12.7, 7.6 Hz, 8H, H_f), 2.06 (dq, J = 13.1, 6.3 Hz, 8H, H_g).

^{13}C NMR (151 MHz, $CDCl_3$) **δ** 157.86, 152.42, 150.05, 149.10, 144.23, 143.75, 132.86, 131.36, 129.96, 127.21, 122.00, 114.43, 101.00, 100.07, 85.88, 84.07, 67.23, 50.12, 27.75, 20.88.

SPE Zn *c*-P6•T6 *27*

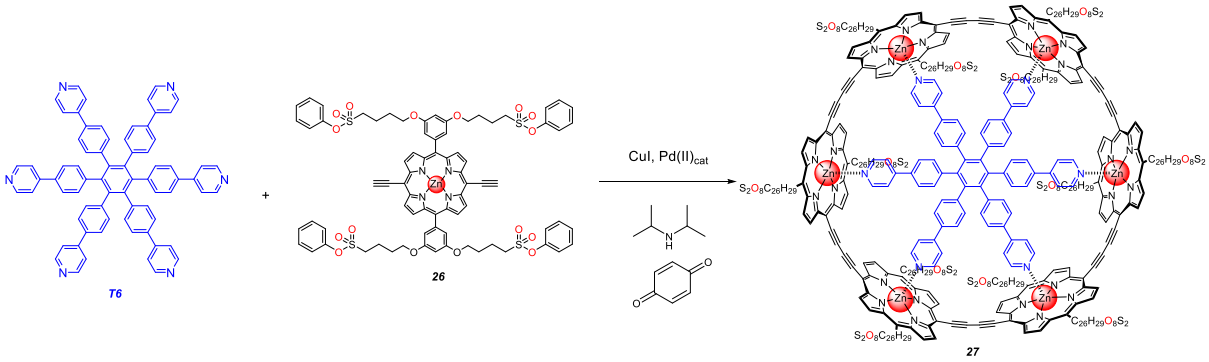

Meso alkynylated SPE Zn porphyrin ***26*** (120 mg, 80.7 µmol, 5.7 eqv) and **T6** (14.1 mg, 14.2 µmol, 1 eqv) were dissolved in chloroform (672 mL) and the mixture sonicated for 30 mins. A solution of $PdCl_2(PPh_3)_2$ (7.0 mg, 9.9 µmol, 0.7 eqv), CuI (16.2 mg, 84.9 µmol, 6 eqv) and benzoquinone (15.3 mg, 142 µmol, 10 eqv) was created in chloroform (10 mL) and diisopropylamine (539 µL) and added slowly to the mixture. The mixture was then stirred at room temperature over 16 hours then the solvent was removed by reduced pressure. The crude was then purified *via* silica plug (chloroform: methanol 90:10) and the dark band was collected. The solvent was then reduced under pressure and the resulting crude purified by passing through a SEC (toluene: pyridine 1%, SX1 bio-beads). The solvent was then removed under pressure and the crude run on preparative GPC (toluene: pyridine 1%) to give an amber solid SPE Zn *c*-P6 T6 ***27*** (3.1 mg, 0.19 µmol, 1%).

$\boldsymbol{\lambda_{max}}$ ($CHCl_3$)/nm (ε /M^{-1} cm^{-1}) 485 (342426), 762 (118248), 797 (118887), 837 (98876).

SAD Zn Porphyrin *45*

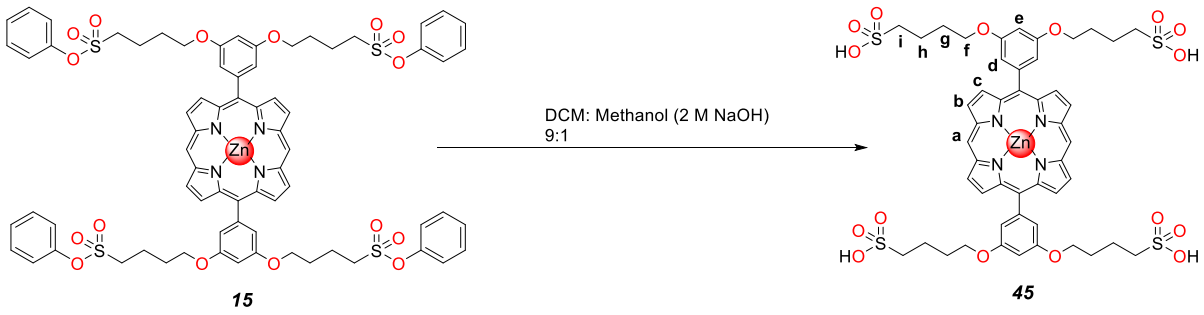

SPE Zn porphyrin ***15*** (10.8 mg, 7.51 µmol, 1 eqv) was dissolved in a solution of DCM (0.9 mL) and a NaOH solution in methanol (0.1 mL, 2 M). The reaction was stirred at room temperature for 24 hours. The reaction material was precipitated *via* addition of excess chloroform, the precipitate was collected *via* centrifuge (40,000 RPM for 15 minutes). The amber precipitate, SAD Zn porphyrin ***45*** (7.1 mg, 6.3 µmol, 84%), was dried under reduced pressure for 24 hours.[40]

^{1}H NMR (600 MHz, DMSO) **δ** 10.32 (s, 2H, H_a), 9.48 (d, J = 4.4 Hz, 4H, H_b), 9.05 (d, J = 4.4 Hz, 4H, H_c), 7.33 (m, 4H, H_d), 6.98 (m, 2H, H_c), 4.18 (m, 8H, H_f), 2.55 (m, 8H, H_i), 1.89 (m, 8H, H_g), 1.82 (m, 8H, H_h).

^{13}C NMR (151 MHz, DMSO) **δ** 167.31, 158.35, 149.40, 144.97, 132.46, 132.11, 119.19, 114.76, 106.39, 100.64, 68.19, 49.02, 28.65, 22.40.

SAD Zn *c*-P6•T6 *46*

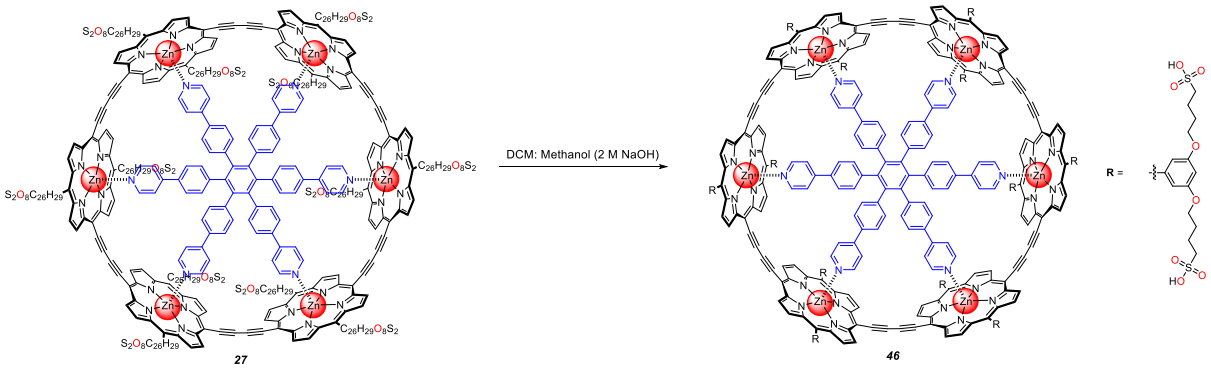

SPE Zn *c*-P6 ***27*** (3.1 mg, 0.30 µmol, 1 eqv) was dissolved in a solution of DCM (0.9 mL) and a NaOH solution in methanol (0.1 mL, 2.0 M). The reaction was stirred at room temperature for 24 hours. The reaction material was precipitated *via* addition of excess chloroform, the precipitate was collected *via* centrifuge (40,000 RPM for 15 minutes). The amber precipitate, SAD Zn *c*-P6 ***46*** (1.2 mg, 0.13 µmol, 43%), was dried by reduced pressure for 24 hours.[40]

λ_{max} (H_2O)/nm 444, 783, 818, 862.

4.3 CAD Porphyrins Modification

Amide Coupling Conditions

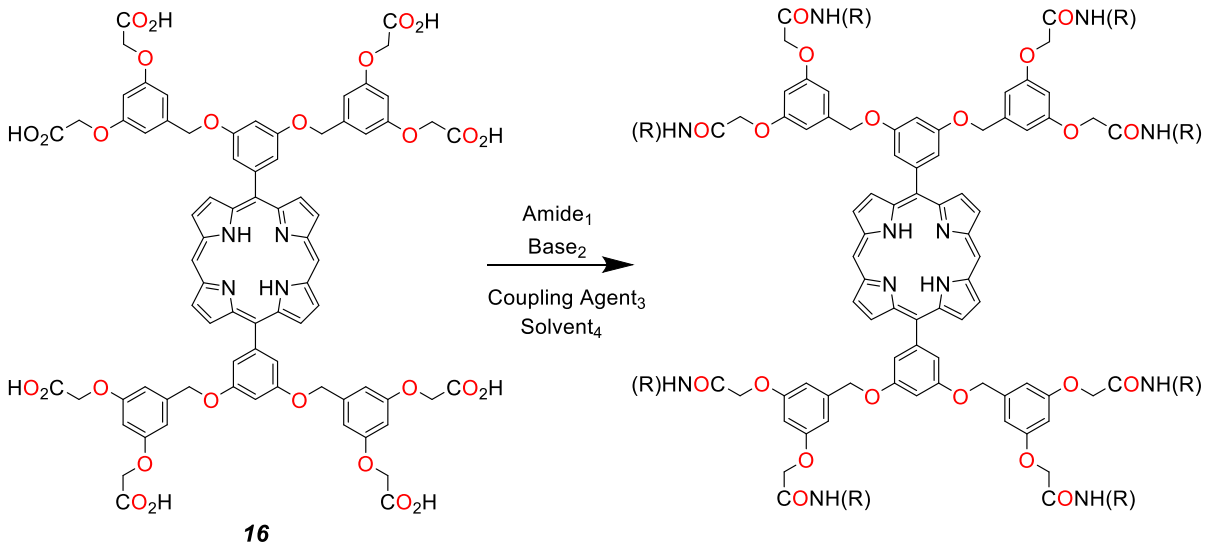

16

CAD NH porphyrin ***16*** (1 eqv), $amine_1$ (16, 32 or 64 eqv) and $base_2$ ($amine_1$ eqv x2) were dissolved in $solvent_4$ (5 mL) and stirred for 30 mins. $Coupling\ agent_3$ (12, 24 eqv) was then added and the resulting solution heated to $temperature_5$ for 14 hours. The resulting solution was then cooled and the product precipitated out using toluene (DMSO) or solvent was removed by reduced pressure (acetonitrile). HPLC (95:5 to 20:80 water: acetonitrile over 30 minutes) traces of the resulting precipitate were collected. These reactions did not go to completion and no analysable data of pure product was produced.[42]

Amine$_1$: aminomethanesulfonic acid, taurine, aminopropanesulfonic acid ***17***, 1-aminohexane-1,2,3,4,5,6-hexaol ***38***.

Base$_2$: triethylamine.

Coupling agent$_3$: HBTU ***18***, HATU, DCC ***40*** or none.

Solvent$_4$: DMSO, DMSO (5% water), acetonitrile.

Temperature$_5$: 20, 50, 70, 100 (°C).

Activated Ester Conditions

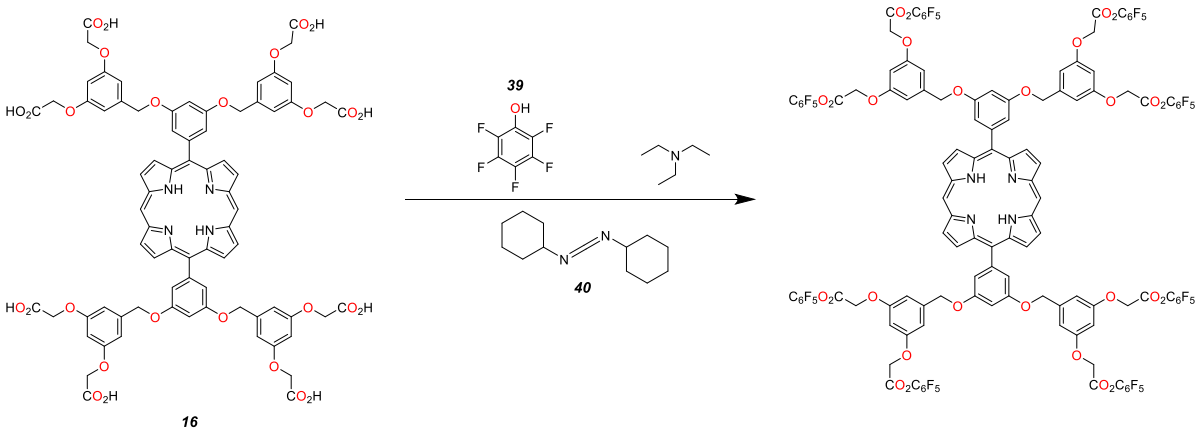

CAD NH porphyrin ***16*** (5.0 mg, 3.2 µmol, 1 eqv), DCC ***40*** (8.0 mg, 39 µmol, 12 eqv) and triethylamine (6.6 mg, 9.0 µL, 65 µmol, 20 eqv) were dissolved in DMF (3 mL) and stirred for 30 minutes. Pentaflourophenol ***39*** (7.2 mg, 39 µmol, 12 eqv) was then added dropwise at 0 °C. The mixture was then stirred under argon for 2 hours. The solvent was removed by reduced pressure and the residue collected. No evidence for complete reaction was found.[47]

Ester Sulfonate Conditions

4-Iodobutane-1-sulfonic acid ***41*** was prepared using established procedure.[49]

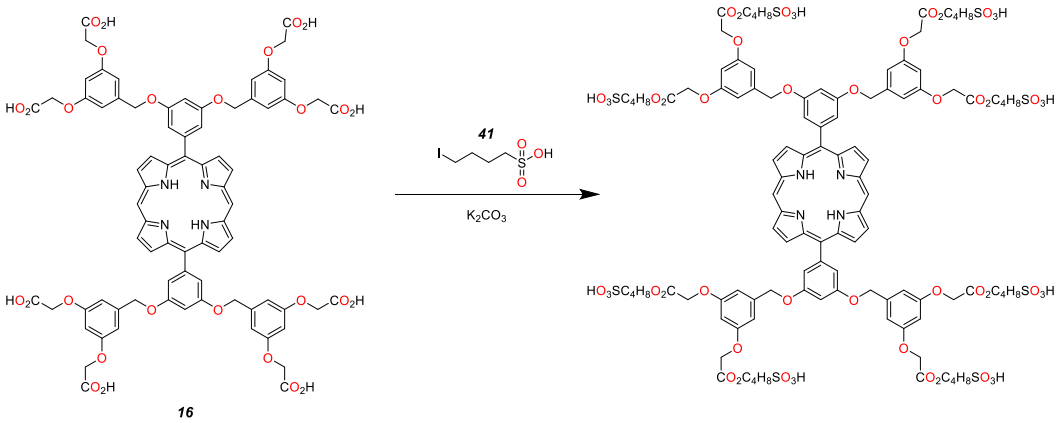

CAD NH porphyrin ***16*** (8.2 mg, 5.3 µmol, 1 eqv) and Na_2CO_3 (5.6 mg, 53 µmol, 10 eqv) was dissolved in DMF under argon and stirred for 30 mins. 4-Iodobutane-1-sulfonic acid ***41*** (12.4 mg, 53.2 µmol, 8.8 eqv) was then added and the reaction was stirred for 24 hours at room temperature. Cold diethyl ether (0 °C) was then added to precipitate out the red solid, which was collected by centrifuge (40,000 RPM for 15 minutes). The material proved unpurifiable by HPLC (attempts included, 95% to 20% water in acetonitrile over the course of 30 and 45 minutes) and could not be analysed by ^{1}H NMR in DMSO (d_6).[47]

Bibliography

1. M. Tahoun, *RSC Adv.*, **2021, 11,** 7552-7563.
2. Y. Shi, F. Zhang, R. J. Linhardt, *Dyes and Pigments*, **2021**, 188, 109136
3. E. B. Fleischer, *Acc. Chem. Res.*, **1970,** *3*, 105-112
4. International Union of Pure and Applied Chemistry, *IUPAC Compendium of Chemical Terminology*, 3rd ed, **2006**.
5. Moss, G.P., *Eur. J. Biochem*., **1988**, 178, 277-328.
6. A. Samrah, *Mater. Adv*., **2020**, 1, 1895-1908.
7. M. Gouterman, *J. Mol. Spec*., **1961**, 6, 138-163.
8. H. L. Anderson, *Chem. Commun*., **1999**, 23, 2323-2330.
9. R. S. Becker, J. B. Allison, *J. Phys. Chem.*, **1963**, *67*, 2662-2669.
10. R. J. Hill, W. Konigsberg, G. Guidotti, L.C. Craig, *J. Biochem*, **1961**, 237, 1549-1554.
11. Fischer, H., and Wenderoth, H., *Annalen*, **1940**, 545, 140.
12. I. G. Denisov, T. M. Makris, S. G. Sligar, I. Schlichting, *Chem. Rev.*, **2005**, *105*, 2253-2278.
13. Strain, H. H., M. R. Thomas and J. J. Katz, *Biochem. Biophys*., **1963**, 75, 306-311.
14. K. E. Redding, S. Santabarbara, *The Chlamyonmonas Sourcebook*, 3rd ed, **2023**.
15. Jui H. Wang, *Science*, **1961**, 133, 1770-1771.
16. P. S. Bols, H. L. Anderson, *Acc. Chem. Res*., **2018**, 51, 2083-2092.
17. Dixon, J. M., M. Taniguchi and J. S. Lindsey, *Photochem. Photobio*., **2005**, 81, 212-213.
18. J. T. Goodwin and D. G. Lynn, *J. Am. Chem. Soc.* **1992,** *114*, 9197-9198.
19. N Kamonsutthipaijit, H.L. Anderson, *Chem. Sci*., **2017**, 8, 2729-2740.
20. W. Shu-ping, S. Yan-Feng, Z. Ben-Yue, W. Jing, *Chem. Commun.*, **2016**, 52, 10205-10216.
21. S. Anderson, H. L. Anderson, J. K. M. Sanders, *J. Chem. Soc*., **1995**, 1, 2255-2267.
22. C.J. Pedersen, *Science*, **1988**, 241, 536-540.
23. F. Fasano, P. Bolgar, G. Iadevaia, C. Hunter, *Chem. Sci.*, **2022**, 13, 44, 13085-13093.
24. H.M. Pineda-Castaneda, Z. J. Rivera-Monroy, M. Maldonado, *ACS Omega*, **2023**, 8, 4, 3650–3666.
25. M. Hoffman, C.J. Wilson, B. Odell, H. L. Anderson, *Angew. Chem. Int. Ed*., **2007**, 46, 3122-3125.
26. M. Hoffman, J. Karnbratt, C. Ming-Hua, L. M. Herz, B. Albinsson, H. L. Anderson, *Angew. Chem. Int. Ed*., **2008**, 47, 4993-4996.
27. S.F MacDonald, R. J. Stedman, *Can. J. Chem*., **1954**, 32, 896-900.

28. S. R. Adapa, A. Sami, P. Meshram, G. Ferreira, R. H. Y. Jiang, *Genes (Basel)*, **2024**, 15, 961.

29. Yip KW Zhang et al, *PLOS ONE*, **2014**, 9, 1-9.

30. A.D. Alder, F, R, Longo, W. Shergalie, *J. Am. Chem. Soc*, **1964** ,86, 3145.

31. Muresan AZ, Lindsey JS. *Tetrahedron Let*., **2008**, 64, 11440-11448.

32. Ogawa K, Kobuke Y. *Biomed. Res. Int*., **2012**, 2013, 125658.

33. J. Pickering, Synthesis and Applications of a Water-Soluble Porphyrin Nanoring, MChem diss, Oxford University, **2024**.

34. A. Leggio et al, *RSC Adv*., **2016**, 6, 34468-34475.

35. K. M Freiberg et al, *Chem. Sci*., **2023**, 14, 3462-3469.

36. K. Miki, K. Ohe, *Chem. Eur. J*., **2020**, *26*, 2529.

37. Hamlin TA, Levandowski BJ, Narsaria AK, Houk KN, Bickelhaupt FM. *Chem. Eur*. **2019**, 25, 6342-6348.

38. P. Kocienski, *Protecting Groups*, 3rd ed, **2003**.

39. A. M. Mansour, *Dalton Trans*., **2021**, 50, 10701-10706.

40. S. C. Miller. *J. Org. Chem.*, **2010**, 75, 4632-4635.

41. E. Valeur, *Chem. Soc. Rev*., **2009**, 38, 606-631.

42. N. P. Sargaeva, *J. Am. Soc. Mass. Spec*., **2011**, 22, 480-491.

43. W. Yizhe, *Eur. J. Med. Chem*., **2021**, 223, 113637.

44. C. Shuqiang, *Eur. J. Med. Chem*., **2021**, 113544.

45. C. Li, *Bioorg. Med. Chem*., **2020**, 28, 115596.

46. N. B. Palakurthy, *Tetrahedron Let*., **2011**, 52, 7132-7134.

47. M. Adamczyk, *Biocon. Chem*., **1997**, 8, 253-255.

48. L.M. Gayo, *Tetrahedron Let*., **1996**, 37, 4915-4918.

49. Jermyn, M. A., *Aust. J. Chem.*, **1966**, 19, 1293 – 1295.

50. I. H. Paik, *Angew. Chem. Int. Ed*., **2007**, 46, 3284-3287.

51. G. Schwertz, *J. Med. Chem.*, **2017**, 60, 4840-4860.

52. Pavov, *J. Org. Chem. USSR*., **1976**, 12, 827-832.

53. Bhandari, P. J., *J. Org. Chem.*, **2021**, *86*, 8576–8589.

54. Paik, I.-H., *Angew. Chem. Int. Ed.*, **2007**, 46, 3284-3287.

55. Ngassa, F. N., *Trends Org. Chem.*, **2017**, 18, 1-14.

56. Chu, Y.-H., *Molecules*, **2022**, *27*, 25

57. Plater, M. J, *Tetrahedron*, **2002**, 58, 2405-2413.

Appendix I: Table of Amide Coupling Conditions

Amide	**Coupling Agent**	**Solvent**	**Temperature (°C)**	**Stoichiometry** (Amine per carboxylic acid sites)	**Stichometry** (Coupling agent per carboxylic acid sites)	**Result**
Taurine ***17***	HBTU ***18***	DMSO	20	2	1.5	No reaction
-	-	-	50	2, 4, 8	1.5, 3	Incomplete
-	-	-	100	2, 4, 8	1.5	Incomplete
-	-	DMSO (5% water)	50	4	1.5	Incomplete
-	-	-	70	4	1.5	Incomplete
-	-	Acetonitrile	50	4	1.5	Incomplete
-	DCC ***40***	Acetonitrile	50	4	1.5	Incomplete
-	HATU	DMSO	50	8	3	Incomplete
-	n/a	DMSO	50	4	1.5	No reaction
Aminomethanesulfonic acid	HBTU ***18***	DMSO	50	4	1.5	Incomplete
-	-	-	100	4, 8	1.5, 3	Incomplete
Aminopropanesulfonic acid	HBTU ***18***	DMSO	50	4, 8	1.5, 3	Incomplete
-	-	-	100	8	1.5, 3	Incomplete
1-aminohexane-2,3,4,5,6-pentol ***38***	HBTU ***18***	DMSO	50	4, 8	1.5, 3	Incomplete

Table 1: Reaction conditions attempted during **CAD NH porphyrin** amide conversion synthesis.

Appendix II: Synthesis of Supplementary Compounds

4-Chlorobutanesulfonyl Chloride *20*[51]

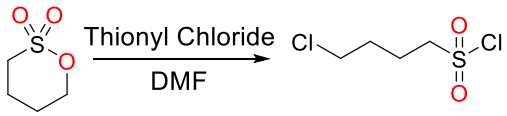

19 ***20***

Butanesultone ***19*** (1.50 mL, 14.7 mmol, 1 eqv) was added to thionyl chloride (2.13 mL, 29.4 mmol, 2 eqv) and DMF (0.1 mL). This mixture was heated to reflux under argon for 12 hours. The thionyl chloride and DMF were then removed by reduced pressure yielding a yellow oil 4-chlorobutanesulfonyl chloride ***20*** (2.75 g, 98%).[51]

^{1}H NMR (400 MHz, $CDCl_3$) **δ** 3.59 (m, 2H), 3.48 (m, 2H), 2.10 (m, 2H), 1.86 (m, 2H).

Phenyl 4-Chlorobutanesulfonate *21*[52]

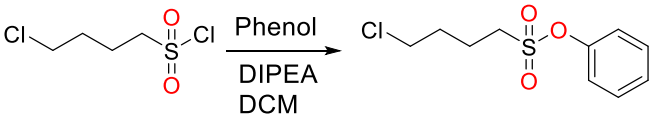

20 ***21***

Under argon, phenol (1.66 g, 17.6 mmol, 1 eqv) was dissolved in DCM (100 mL) then DIPEA (2.28 g, 17.6 mmol, 1 eqv) was added. The 4-chlorobutanesulfonyl chloride ***20*** (3.37 g, 17.6 mmol, 1 eqv) in DCM (10 mL) was added dropwise at 0 °C. The reaction mixture was stirred at 0 °C for 30 mins and then further stirred for 12 hours at room temperature. The solvent was then removed under reduced pressure, and the orange oil purified by silica column (petroleum ether: ethyl acetate, 9:1), yielding a yellow oil phenyl 4-chlorobutanesulfonate ***21*** (1.86 g, 43%).[52]

^{1}H NMR (400 MHz, $CDCl_3$) **δ** 7.15 (m, 2H), 6.83 (m, 1H), 6.86 (m, 2H), 3.55 (m, 2H), 3.43 (m, 2H), 2.04 (m, 2H), 1.84 (m, 2H).

Di-*Tert*-Butyl-Ester-Hydroxymethylbenzene *51*[33]

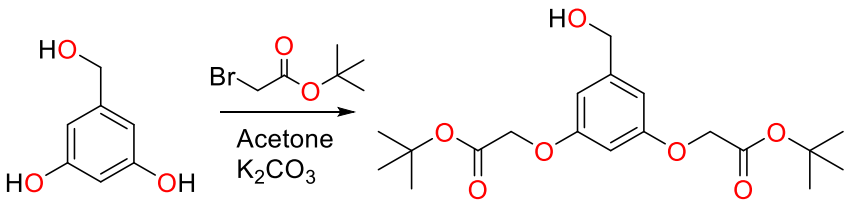

50 ***51***

Trihydroxymethylbenzene ***50*** (2.00 g, 14.3 mmol, 1 eqv.), K_2CO_3 (4.75 g, 34.4 mmol, 2.4 eqv.) and 18-crown- 6 (0.34 g, 1.28 mmol, 0.1 eqv.) were dissolved in acetone (143 mL). *Tert*-butyl 2-bromo-acetate (4.64 mL, 31.4 mmol, 2.2 eqv.) was then added and the mixture was heated to reflux for 36 hours. The reaction mixture was then cooled to room temperature and the acetone removed under reduced pressure. Water (30 mL) was added to the resulting residue and extracted with EtOAc (30 mL x3), with the combined organic layers being dried with Na_2SO_4. The crude product was then purified by silica column (petroleum ether: ethyl acetate 4:1) to give a yellow oil di-*tert*-butyl-ester-hydroxymethylbenzene ***51*** (2.39 g, 46%).[33]

^{1}H NMR (600 MHz, $CDCl_3$) **δ** 6.53 (d, J = 2.4 Hz, 2H), 6.40 (t, J = 2.3 Hz, 1H), 4.61, (s, 2H), 4.48 (d, J = 1.1 Hz, 4H), 1.48 (s, 18 H).

Di-*Tert*-Butyl-Ester-Bromomethylbenzene *29*[33]

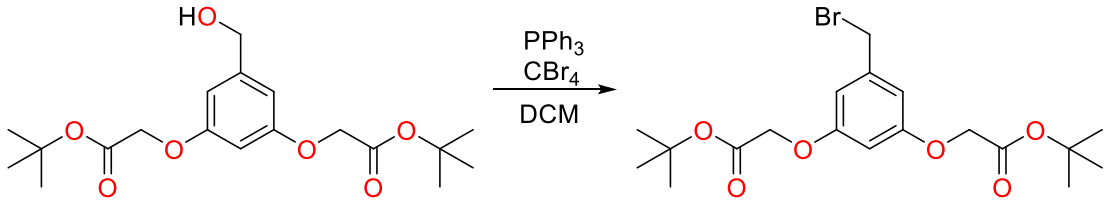

51 ***29***

Di-*tert*-butyl-ester-hydroxymethylbenzene ***51*** (2.58 g, 7.0 mmol, 1 eqv.) was dissolved in DCM (70 mL) and then CBr_4 (3.02 g, 9.10 mmol, 1.3 eqv.) was added. Next, a solution of PPh_3 (2.39 g, 9.1 mmol, 1.3 eqv.) in DCM (20 mL) was added dropwise to the solution at 0 °C and the solution was allowed to stir for 10 minutes at room temperature. Then water (30 mL) was added to the reaction mixture and extracted with DCM (30 mL x3). The combined organic layers were dried

with Na_2SO_4, and the resulting crude product was purified using silica column (petroleum ether: ethyl acetate 9:1), to give the white solid di-*tert*-butyl-ester-bromomethylbenzene ***29*** (1.46 g, 48%).[33]

^{1}H NMR (600 MHz, $CDCl_3$) **δ** 6.54 (d, *J* = 2.3 Hz, 2H), 6.41 (t, *J* = 2.3 Hz, 1H), 4.48 (s, 2H), 4.38 (s, 4H), 1.49 (s, 18H).

Penta-Acylated Ammonium-Sorbitol Chloride *42*[50]

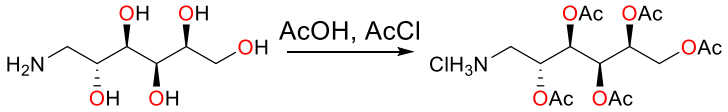

38 ***42***

Amino-sorbitol ***38*** (1.0 g, 5.52 mmol, 1 eqv) was dissolved in glacial acetic acid (10 mL, 87.4 mmol, 16 eqv). Acetyl chloride (22.6 mL, 140 mmol, 25 eqv) was then added dropwise at 0 °C. The reaction mixture was stirred for 18 hours. The solvent was removed under reduced pressure. The mixture was re-dissolved in methanol (8 mL) and ethanol (5 mL) then recrystalised at -20 °C to afford a white crystalline solid penta-acylated ammonium-sorbitol chloride ***42*** (1.84 g, 78%).[50]

^{1}H NMR (400 MHz, $CDCl_3$) **δ** 8.21 (s, 3H), 5.46 (dd, *J* = 6.9, 4.3 Hz, 1H), 5.38 – 5.27 (m, 1H), 5.16 (td, *J* = 6.6, 4.5 Hz, 1H), 5.03 (td, *J* = 6.0, 3.2 Hz, 1H), 4.28 (dd, *J* = 12.4, 3.3 Hz, 1H), 4.12 (dd, *J* = 12.5, 5.4 Hz, 1H), 3.54 (m, 2H), 2.15 (s, 3H), 2.12 (s, 3H), 2.10 (s, 3H), 2.09 (s, 3H), 2.06 (s, 3H).

2,2' Dipyrromethane (DPM)[57]

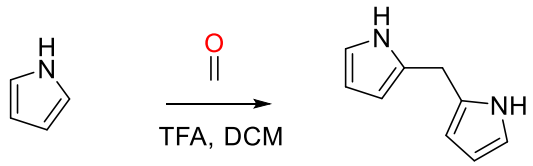

52 ***DPM***

Distilled, degassed pyrrole (250 mL, 10.9 mol, 22.3 eqv) and formaldehyde (14.7 g, 162 mmol, 22.3 eqv) were combined under argon. TFA (6.03 g, 52.9 mol, 0.1 eqv) was added and the mixture stirred for 5 mins. DCM (250 mL) was then added followed by a saturated solution of $Na_2CO_{3(aq)}$

(250 mL). The organic layer was then extracted and washed with saturated $Na_2CO_{3(aq)}$ (75 mL x3). The organic layer was dried over Na_2SO_4 and then concentrated under reduced pressure. The concentrate was then purified by silica column (85: 15 petroleum ether: ethyl acetate) to give **DPM** (0.50 g, 1%) as a white crystalline solid.[57]

^{1}H NMR (400 MHz, $CDCl_3$) **δ** 7.81 (s, 2H) 6.65 (tt, *J* = 2.6, 1.5 Hz, 2H), 6.16 (p, *J* = 3.1 Hz, 2H), 6.04 (q, *J* = 2.4 Hz, 2H), 3.97 (s, 2H).

T6[26]

This method was taken directly from Reference 26.

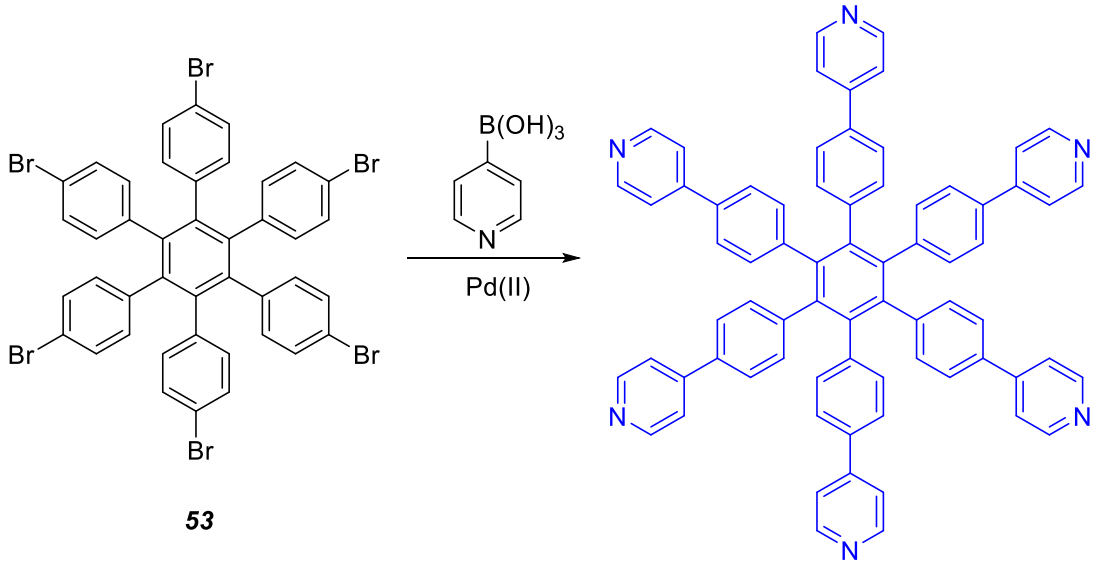

53 **T6**

To a solution of hexa-(4-bromophenyl)benzene (300.0 mg, 297 µmol, 1 eqv) in dimethyleneglycol (9 mL) and THF (21 mL) was added $PdCl_2(PPh_3)_2$ (40.0 mg, 57.0 µmol, 0.19 eqv). After addition of water (12 mL), $NaHCO_3$ (450 mg, 5.36 mmol, 840 eqv) and 4-pyridineboronic acid (882 mg, 7.18 mmol, 24 eqv), the mixture was deoxygenated and stirred at 70 °C for 5 days. Solvents were removed and the crude product was purified by silica column (DCM: MeOH: triethylamine 10: 1: 0.05) to give **T6** as a white solid (87.0 mg, 29%).[26]

^{1}H NMR (400 MHz, $CDCl_3$) **δ** 8.39 (d, J = 5.5 Hz, 12H), 7.31 (d, J = 5.5 Hz, 12H), 7.19 (d, J = 8.5 Hz, 12H), 6.99 (d, J = 8.5 Hz, 12H).

4-Iodobutanesulfonic acid *41*[49]

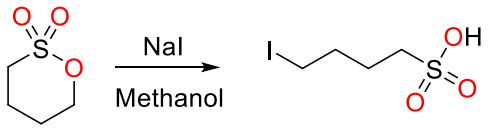

19 ***41***

Butanesultone ***19*** (0.75 mL, 7.34 mmol, 1 eqv) and NaI (1.1 g, 7.34 mmol, 1 eqv) was dissolved in methanol (10 mL). The solution was then heated to 80 °C for 1 hour. The solution was then cooled to 0 °C. The resulting white precipitate was then collected, washed with DCM (5 mL x 3), and then dried under reduced pressure yielding 4-iodobutanesulfonic acid ***41*** (1.50 g, 77%).[49]

^{1}H NMR (400 MHz, D_2O) **δ** 3.31 (t, *J* = 6.6 Hz, 2H), 2.95 (m, 2H), 1.96 (m, 2H), 1.86 (m, 2H).

THS Acetylene

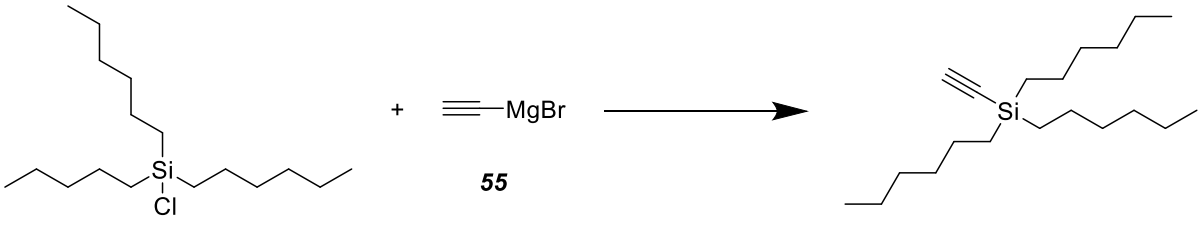

54 ***55*** ***56***

Chlorotrihexylsilane ***54*** (2.30 mL, 6.28 mmol, 1 eqv) was dissolved in THF (4 mL) under argon. Ethynylmagnesium bromide ***55*** (1.0 M, 13.8 mL, 6.91 mmol, 1.1 eqv) was added dropwise over 1 hour. The reaction was then heated to 80 °C and stirred for 20 hours. The reaction was quenched with HCl (1.0 M, 5 mL) and the solution extracted with diethyl ether (10 mL x 3) and dried over Na_2SO_4. The material was purified by silica gel column (petroleum ether 100%). The solvent was then removed under reduced pressure yielding the colourless oil ***56*** (1.37 g, 71%).

^{1}H NMR (400 MHz, $CDCl_3$) **δ** 2.35 (s, 1H), 1.45 – 1.28 (m, 24H), 0.88 (m, 9H), 0.66 – 0.57 (m, 6H).